

FACILITY FORM 802

N65-29148

(ACCESSION NUMBER)

117

(PAGES)

CR 63916

(NASA CR OR TMX OR AD NUMBER)

(THRU)

(CODE)

03

(CATEGORY)

CHARACTERIZATION OF NICKEL-CADMIUM ELECTRODES

BY

W.N. CARSON, JR.
J.A. CONSIGLIO
R.R. NILSON

GPO PRICE \$ _____

CFSTI PRICE(S) \$ _____

Hard copy (HC) *4.00*

Microfiche (MF) *75*

ff 653 July 65



FINAL REPORT

JULY 1, 1963 - DECEMBER 31, 1964

prepared for

GODDARD SPACE FLIGHT CENTER
CONTRACT NAS 5-3477

ADVANCED TECHNOLOGY LABORATORIES

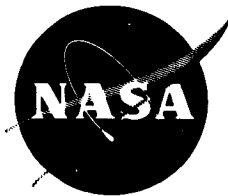
GENERAL  ELECTRIC

Rpt 30859

CHARACTERIZATION
OF
NICKEL-CADMIUM ELECTRODES

BY

W.N. CARSON, JR.
J.A. CONSIGLIO
R.R. NILSON



FINAL REPORT
JULY 1, 1963 - DECEMBER 31, 1964

prepared for

GODDARD SPACE FLIGHT CENTER
CONTRACT NAS 5-3477

ADVANCED TECHNOLOGY LABORATORIES

GENERAL  ELECTRIC

TABLE OF CONTENTS

	<u>Page</u>
List of Tables	ii, iii
List of Figures	iv, v
1.0 INTRODUCTION	1
2.0 CHARACTERIZATION TESTS	3
3.0 SHALLOW DISCHARGE CYCLING TESTS	35
4.0 RANDOM DEPTH OF DISCHARGE CYCLING TESTS	55
5.0 CONSTANT VOLTAGE-CURRENT LIMITED CYCLING TESTS	74
6.0 SUMMARY AND CONCLUSIONS	84
7.0 RECOMMENDED FUTURE WORK	88
APPENDIX I - Control Schematics	I-1 - I-10
APPENDIX II - Plate Weights	II-1- II-8
APPENDIX III - Beta Distribution Derivation	III-1 - III-4

LIST OF TABLES

<u>Number</u>	<u>Title</u>	<u>Page</u>
2.1	Characteristics of Nickel-Cadmium VO Type Plates	4
2.2	Electrode Cleaning Process	5
2.3	Comparison of Characterization Capacities After Two Months Storage	13
2.4	Effect of Excess Charge Conditions on Physical Characteristics of Nickel Electrodes	20
2.5	Positive Electrodes Tested for Gassing Behavior	26
3.1	Shallow Cycling Test Cell Electrodes	38
3.2	X-ray Diffraction Data for Nickel Test Electrodes	44
3.3	X-ray Diffraction Data for Cadmium Test Electrodes	45
3.4	Residual Capacity - Positive Shallow Discharge Cycling Test Electrodes	49
3.5	Residual Capacity - Negative Shallow Discharge Cycling Test Electrodes	50
3.6	Comparison of Characterization and Recharacterization Data for Positive Test Electrodes	51
3.7	Comparison of Characterization and Recharacterization Data for Negative Test Electrodes	52
3.8	Comparison of Graphitic and Nitrate Steps on Positive Shallow Cycling Test Electrodes	53
3.9	Disposition of Shallow Depth of Discharge Test Cell Electrodes in Sealed Test Cells	54

LIST OF TABLES (cont'd)

<u>Number</u>	<u>Title</u>	<u>Page</u>
4.1	Parameters for Random Depth of Discharge Distribution Curves	58
4.2	Revised Random Depth of Discharge Program	58
4.3	Random Depth of Discharge Cycling Test Electrodes	65
4.4	Physical Appearance of Random Depth of Discharge Cycling Positive Test Electrodes	66
4.5	Residual Capacity Measurements of Random Depth of Discharge Cycling Test Cells	67
4.6	Comparison of Characterization and Recharacterization Data for Positive Electrodes	68,69
4.7	Comparison of Characterization and Recharacterization Data for Negative Electrodes	70,71
4.8	Comparison of Graphitic and Nitrate Steps on Positive Shallow Cycling Test Electrodes	72,73
5.1	Constant Voltage, Current Limited Charging Cycling Electrodes	79
5.2	Residual Capacity Measurements of Constant Voltage Current Limited Cycling Test Cells	80
5.3	Comparison of Characterization and Recharacterization Data for Positive Test Electrodes	81
5.4	Comparison of Characterization and Recharacterization Data for Negative Test Electrodes	82
5.5	Comparison of Graphitic and Nitrate Steps on Positive Test Electrodes	83

LIST OF FIGURES

<u>Number</u>	<u>Title</u>	<u>Page</u>
2.1	Basic Cycling Test Circuit	7
2.2	Characterization Test Cell	8
2.3	Typical Characterization Test Curve	10
2.4	Initial Characterization Capacity Distribution	15
2.5	Plate Weight vs. Characterization Capacity	16
2.6	Plate Weight vs. Characterization Capacity	17
2.7	Positive Electrode Blistering	19
2.8	Gas Evolution Measuring Apparatus	23
2.9	Nickel Electrode Gas Rates	28
2.10	Positive Electrode Gassing Tests	29
2.11	Positive Electrode Gassing Tests	30
2.12	Positive Electrode Gassing Tests	31
2.13	Positive Electrode Gassing Tests	32
2.14	Positive Electrode Gassing Tests	33
2.15	Positive Electrode Gassing Tests	34
3.1	Cycling Test Cell Schematic	36
3.2	Photomicrograph - Positive Unformed Electrode	40
3.3	Photomicrograph - Positive Fully Charged Uncycled Electrode	41
3.4	Photomicrograph - Positive Electrode from 40°C Shallow Discharge Cycling Cell	42

LIST OF TABLES (cont'd)

<u>Number</u>	<u>Title</u>	<u>Page</u>
4.1	Random Depth of Discharge Distributions	59
4.2	Random Depth of Discharge Distributions	60
4.3	Random Discharge Cycling Capacity Changes	64
5.1	Electrode P ₅ -29, 40°C, 579 Cycles Photomicrograph	77
5.2	Fully Discharged Negative to Gassing - Photomicrograph	78
6.0	Residual Capacities at Constant Current	87

1.0 INTRODUCTION

This report summarizes the work done under contract NAS5-3477. The objective of the program was to develop a method for the analysis and characterization of the electrodes used in nickel-cadmium spacecraft batteries.

The goal of the program was to develop the relation between the detailed characterization data obtained on single electrodes and the behavior of these electrodes in cells in various modes of cyclic operation. This relation will provide a basis for specifying improved cells for space application and comparing cells from various manufacturers.

The principal characterization data obtained was the complete potential versus time curve for each electrode against a nickel oxide reference electrode for a small number of charge-discharge cycles (6-7) prior to assembling the electrodes into test cells for the cyclic tests. The majority of the characterization tests were made at a constant current of C/10 at room temperature. These curves show the electrode capacity, graphitic and anti-polar capacity, and the effect of impurity levels. In addition a small number of positive electrodes were tested to determine the onset of gassing and gassing rate as a function charging current.

Periodically test cells were removed from the cyclic tests and the individual electrodes were recharacterized and examined for changes in physical properties and comparisons made with the original characterization data.

Some of the electrodes removed from the cyclic tests were examined by x-ray diffraction and photo-micrographs in cross section to determine composition and structural changes. The remainder of the test electrodes, providing they appeared in good mechanical condition by visual inspection, and where time permitted were reassembled into test cells for further cycling.

Test cells fabricated with the characterized electrodes were cycled in three modes of operation, simulating conditions most likely to be encountered in space applications. These modes were as follows:

- (1) Shallow Discharge Cycling to a depth of 21% of the cell capacity at constant current.
- (2) Random Depth of Discharge Cycling averaging 10, 20, 50, and 75% of the cell capacity over a six-day period using random Beta and rectangular distributions for the individual cycle depth of discharge over the six-day period.
- (3) Current Limited Constant Voltage Charging Cycling

The cyclic tests were run concurrently at three temperature levels: 0^o, 25^o(room temperature), and 40^oC.

The plates used in the program were the impregnated sintered plaque type VO made by S.A.F.T. of France and some of the same type made by the General Electric Company at Gainesville, Florida. The latter are designated as KO in this report. The plates had a nominal capacity of 1.2 amp-hrs.

Details of experimental equipment and procedures used as well as relations developed and conclusions for each of the four major program tasks are presented in four separate sections which follow. The breakdown of tasks is:

1. Characterization Tests
2. Shallow Discharge Cycling Tests
3. Random Depth of Discharge Cycling Tests
4. Current Limited Constant Voltage Cycling Tests

2.0 CHARACTERIZATION TESTS

The majority of the plates used in the test program were S.A.F.T. VO type. The general characteristics of the positive and negative plates are given in Table 2.1. The dimensions of the plates are 1-3/4" x 3". The minimum active area per plate is 28.8 cm² which is equivalent to a nominal capacity of 1.20 amp-hr. for the positives and 1.24 for the negatives.

During the course of the characterization of the VO plates, some of the positive plates showed a tendency to develop blisters and pimples when charged at rates of C/5 to C. A short investigation was conducted to determine the conditions leading to the blistering, and whether a bad lot of electrodes had been used inadvertently. The results of the studies on blistering are summarized in Section 2.5.

Plates of the same type made in Gainesville by the General Electric Company, Battery Business Section (KO-15, having a larger active area 41.86 cm²) showed less of a tendency to blister. It was decided to incorporate some of the KO-15 plates, trimmed in dimension to 1-3/4" x 3" into the testing program to determine if these behaved any differently than the S.A.F.T. VO.

2.1 Electrode Preparation

Prior to the initial characterization all plates were electrochemically cleaned, washed, dried, inspected for visual defects and weighed.

The cleaning was done to insure complete activation of active material, supplement the removal of any contaminating ions, establish that there was a proper balance of positive and negative capacity in the selected plates, and bring the plates to the proper state of discharge prior to assembly with cells. The details of the cleaning process are given in Table 2.2.

The final weights of the S.A.F.T. VO plates are tabulated in Appendix II. The average weight of the positive elements after cleaning was 11.150 gms with a standard deviation of 0.290 gms, and for the negative electrodes the average was 10.161 gms with a standard deviation of 0.259 gms. Weight changes for the positive electrodes before and after cleaning averaged ± 0.028 gms; for the negatives the weight decreased an average of 0.273 gms.

Similar data for the trimmed KO type plates are tabulated in Appendix II.

TABLE 2.1

CHARACTERISTICS OF NICKEL-CADMIUM

VO TYPE PLATES

<u>Characteristic</u>	<u>Units</u>	<u>Positive</u>	<u>Negative</u>
Thickness	mm.	0.93 \pm 0.06	0.81 \pm 0.06
Capacity	$\frac{\text{amp.}-\text{hrs.}}{\text{dm}^2}$	4.2 \pm 0.4	4.3 \pm 0.4
Weight of Metal Hydroxide	g/dm ²	16.3 \pm 1.0	16.5 \pm 1.0
Plaque Porosity	%	70 \pm 8	66 \pm 4
Core Thickness	mm.	0.1	0.1

TABLE 2.2

ELECTRODE CLEANING PROCESS

1. The plates are immersed in 25% KOH in separate compartments and allowed to soak for 16 hours.
2. Alternate positive and negative plates are connected in series and discharged through inversion at $C/8$ amps. for 4 to 6 hours. C is the nominal capacity in ampere hours. The individual cell voltages should be greater than 1.50 V at the end of the discharge. If the value is less than this, the inversion is not complete and the discharge must be continued until a value greater than 1.50 V is obtained.
3. The polarity is reversed and the cell charged at $C/8$ amps. for 16 to 20 hours. The voltage must reach 1.5 V.
4. The cells are discharged at approximately $C/2.5$ to zero volts. The cells may be directly shorted with a jumper when the discharge voltage is less than 0.6 V.
5. The individual resistors (or jumpers) are removed and the cells in series are discharged through inversion at $C/12$ for 7 hours.
6. Charged as in 4.
7. Discharge as in 5. The capacity obtained must be at least 125% of C .
8. Individual cells are shorted for a minimum of 1 hour.
9. The cells in series are discharged through inversion at $C/12$ for a maximum of 6 hours.
When a cell reaches minus 1.2 V, it shall be electrically removed from the discharged circuit. The discharge is then continued on the balance of the cells.
- Note: The individual cell voltage after 3 hours of inversion must be between minus 0.1 and minus 1.0 V. If this value is negative in excess of minus 1.0 V, the cell does not contain sufficient excess negative capacity.
10. The separator is removed and the plates washed in de-ionized water until the pH of the final wash water is less than 10.5.
11. The plates are dried in a forced air oven at $100^{\circ}\text{C} \pm 10^{\circ}$ for 2 hours.
12. The plates are removed from the temporary assembly and inspected for defects. Any plate showing evidence of blistering, disintegration or severe pitting is rejected. Any smut or loose active material is removed from the surface by brushing with a dry nylon brush or by wiping with a clean, dry cloth or paper towel.
13. The plates are stored in sealed plastic containers until used.

2.2 Experimental Equipment and Procedures

The primary characterization data obtained for both positive and negative electrodes were complete potential versus time curves for 6 to 7 charge-discharge cycles. To accomplish this each electrode was assembled into a test cell containing two counter electrodes and a reference electrode.

The reference electrode was a nickel oxide electrode, charged fully and then discharged (about 10%) and aged for several weeks. The potential of the electrode remains stable over a period of months if current is not drawn from it. It can be renewed in the test cell if necessary.

The counter electrodes were of the same type used in the test program but were not used in any cyclic tests. For the positives, the counter electrodes used were cadmium plates and conversely for the negatives the counter electrodes were nickel positive plates.

In use, a pair of test cells, one with a cadmium test electrode, the other with a nickel-oxide test electrode are run through the cycling together. Figure 2.1 shows the basic circuit used to obtain the curves. A master timer is used to turn on the charge and discharge power supplies through appropriate relays; the power supplies are constant current units whose terminals must be shorted during "off" periods. The curve pulser relay (K-1) is used to cycle the input to the amplifier between the nickel-reference pair and the cadmium-reference pair at intervals of 1-2 min. The recording gives two curves, one for each electrode. The bias voltage is set to cancel out the reference voltage so that the difference between the curves is the cell voltage that would be observed if the pair of test electrodes were in a cell. The electronic voltmeter is used to avoid current drain on the reference electrode. Alternate recording of the two curves is possible since the Rustrak recorder is a printing type, rather than a continuous curve tracer.

The experimental setup used in the program had a capability for characterizing 10 positives and 10 negatives simultaneously. The detailed circuit schematic and parts list for the characterization control equipment is shown in Appendix I.

The test cells used are shown in Figure 2.2. The electrolyte used was 31% by weight potassium hydroxide in all cases. Fresh electrolyte was used for each electrode characterization.

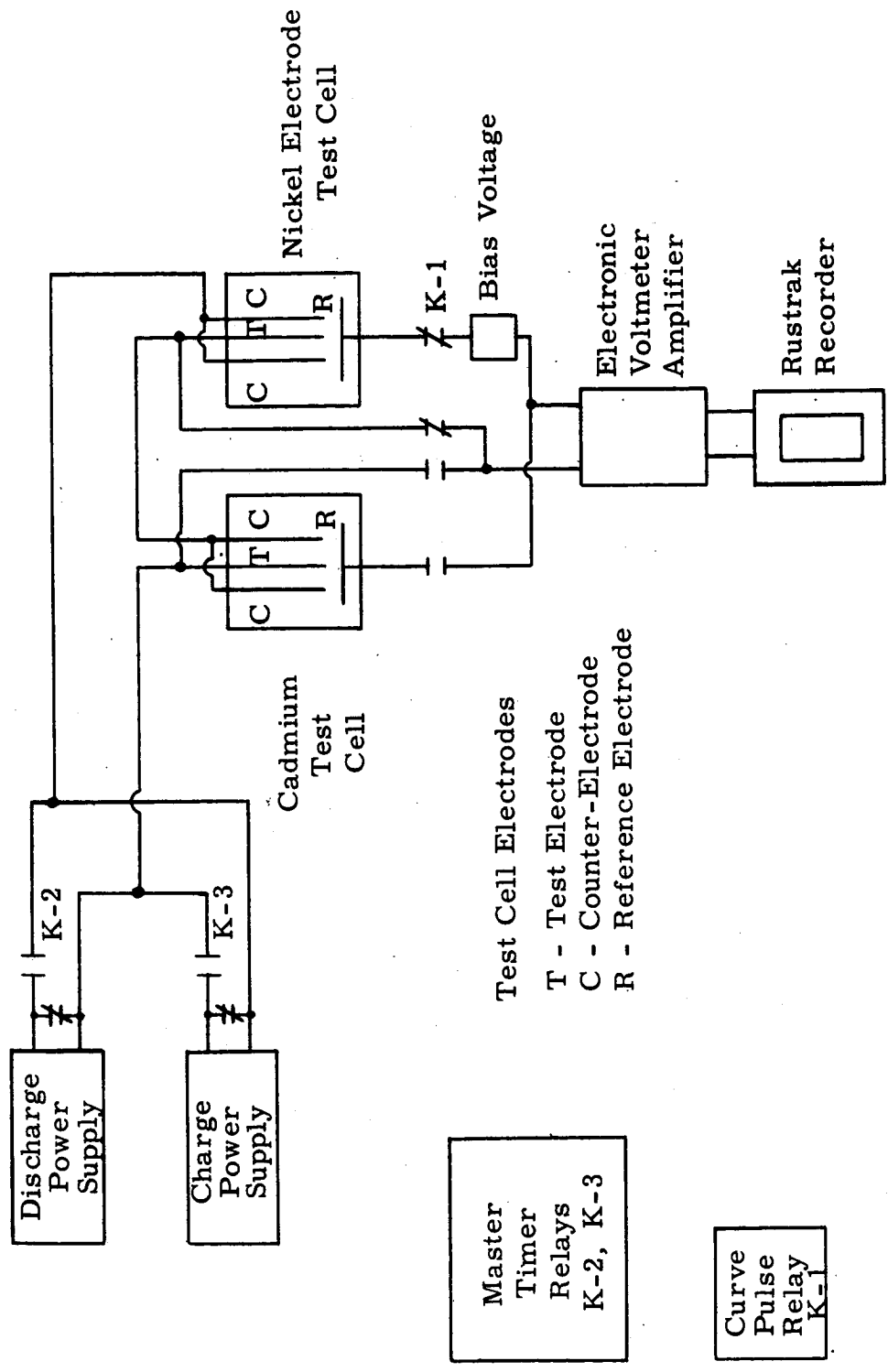


Figure 2.1. Basic Cycling Test Circuit.

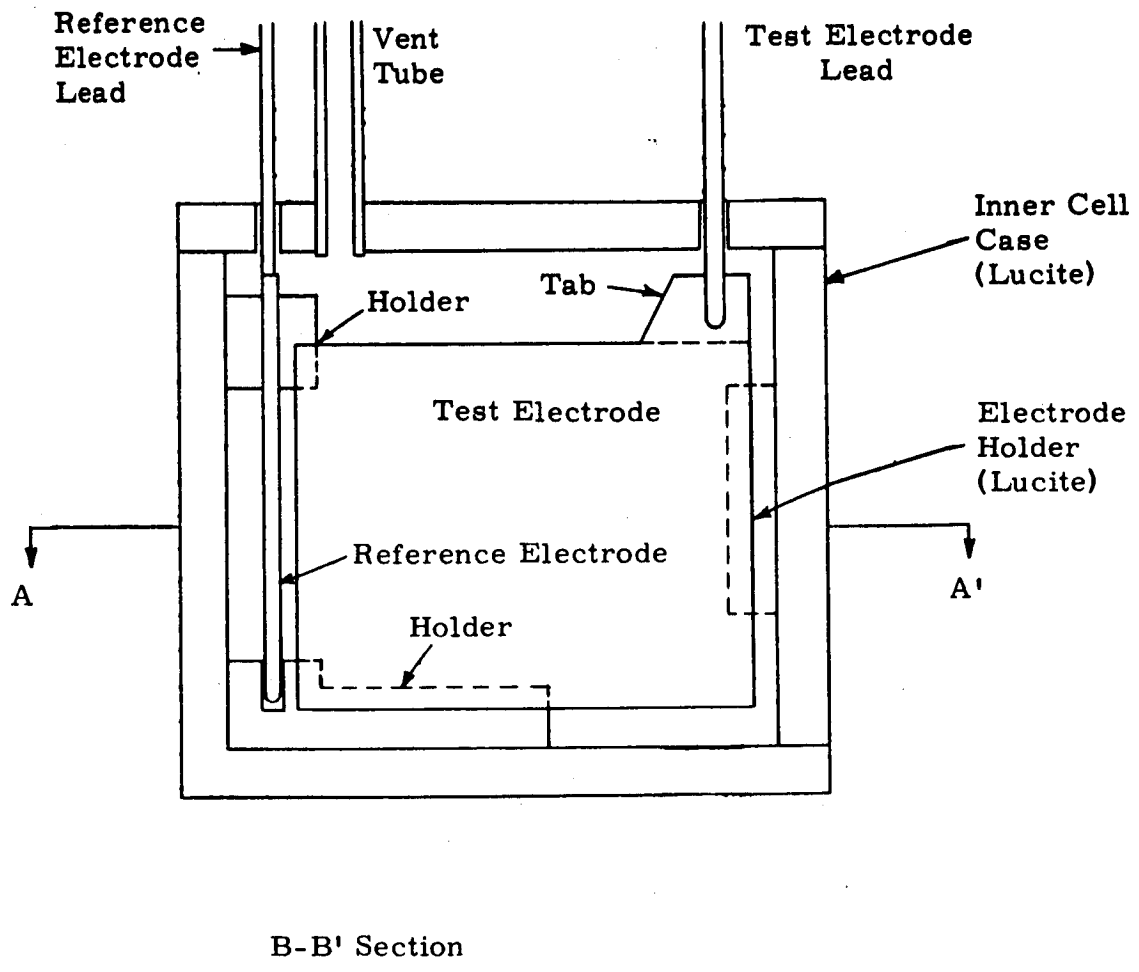
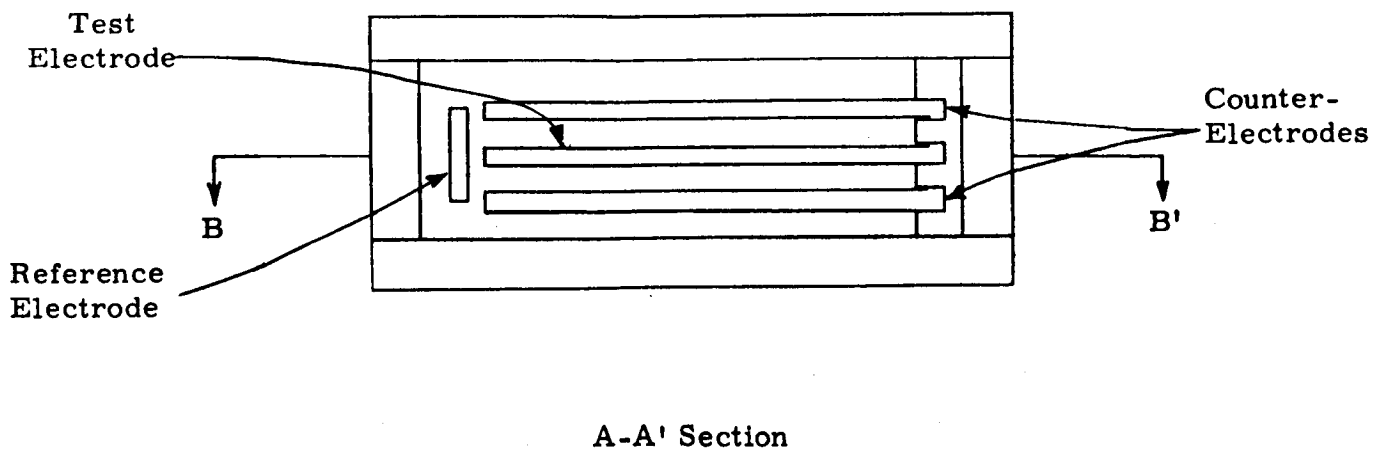


Figure 2.2. Characterization Test Cell.

The original plan called for characterization of plates to be made at three levels of constant-current, charge-discharge rates: C/10, C/5, and C at room temperature. However, in the course of the work, the positives charged at the C/5 and C developed in some cases extensive pimpling and large blisters leading to a loss of active material. In view of these results, it was decided to conduct the characterization test at the C/10 rate. The cycle conditions for the C/10 rate tests were, charge for 720 minutes at 0.140 amp. and discharge for 600 minutes at 0.160 amps, and were conducted at room temperature.

2.3 Characterization Data Interpretation

Figure 2.3 shows a typical set of curves for the potential of cadmium and nickel electrodes during a test cycle. This set of curves was taken using a constant charging and discharging current with a nickel hydroxide electrode for reference. The detail of information is obvious. For the cadmium electrode, the evolution of hydrogen is shown by a small sigmoid rise in the potential with time; no such change in potential is shown by the nickel hydroxide electrode when evolving oxygen. Other regions of interest are the existence of an antipolar capacity in the cadmium electrode (due to the existence of some electrochemically active nickel oxide in the cadmium plates); the graphite capacity shown in the discharge of the nickel electrode and the cadmium antipolarity mass, which is believed due to the absorbed molecular oxygen in the plate; the nitrate reduction region in the nickel plate which occurs whenever a small amount of nitrate as an impurity is present; and the carbonate region of the cadmium electrode. This curve is the only non-destructive test known for these impurities in electrodes, and quantitative estimates of the amount can be made from the area under the curve.

The importance of measuring the nitrate impurity is that the presence of nitrate promotes self-discharge in sealed nickel-cadmium cells. Nitrate is reduced to ammonia at the cadmium electrode, and the ammonia is re-oxidized at the nickel electrode to nitrate or nitrite. Only a few parts per million of nitrate suffice to give a high rate of self-discharge. Nitrate in small to moderate amounts markedly lowers the capacity of the nickel hydroxide electrode. The mechanism is not clearly understood at present, but may involve a second type of self-discharge.

The effect of carbonate ion appears to be dependent upon the hydroxyl ion concentration in the electrolyte. The cadmium electrode potential is governed by the Nernst equation:

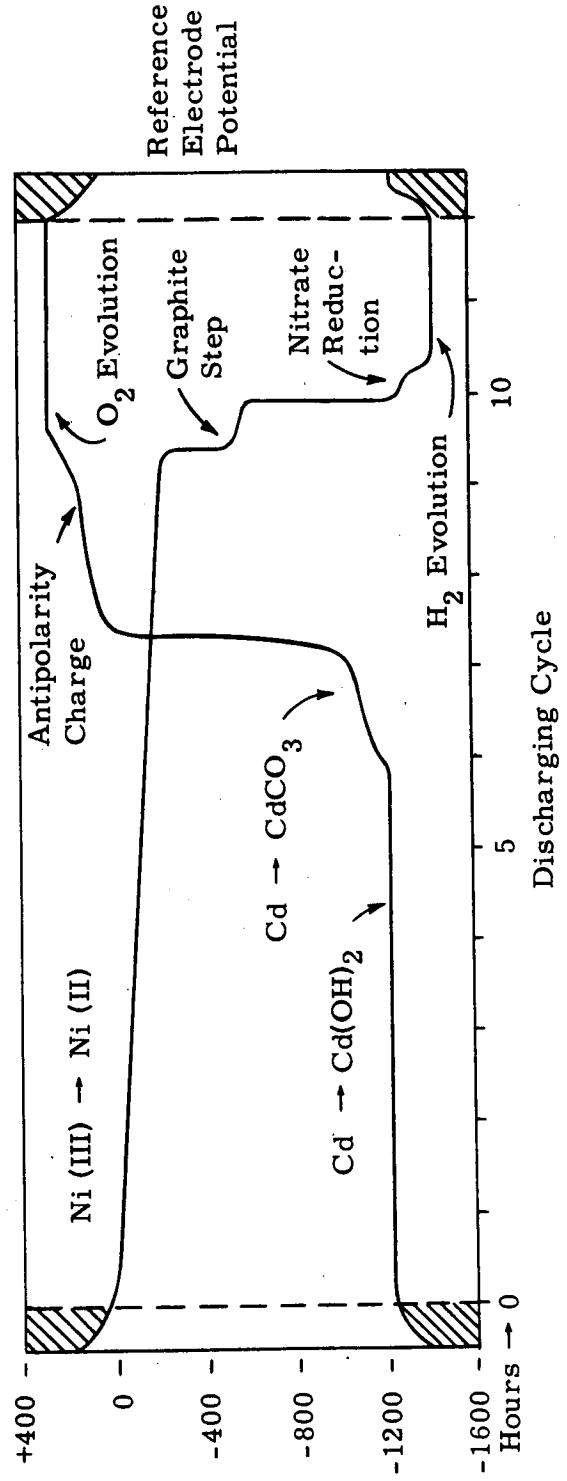
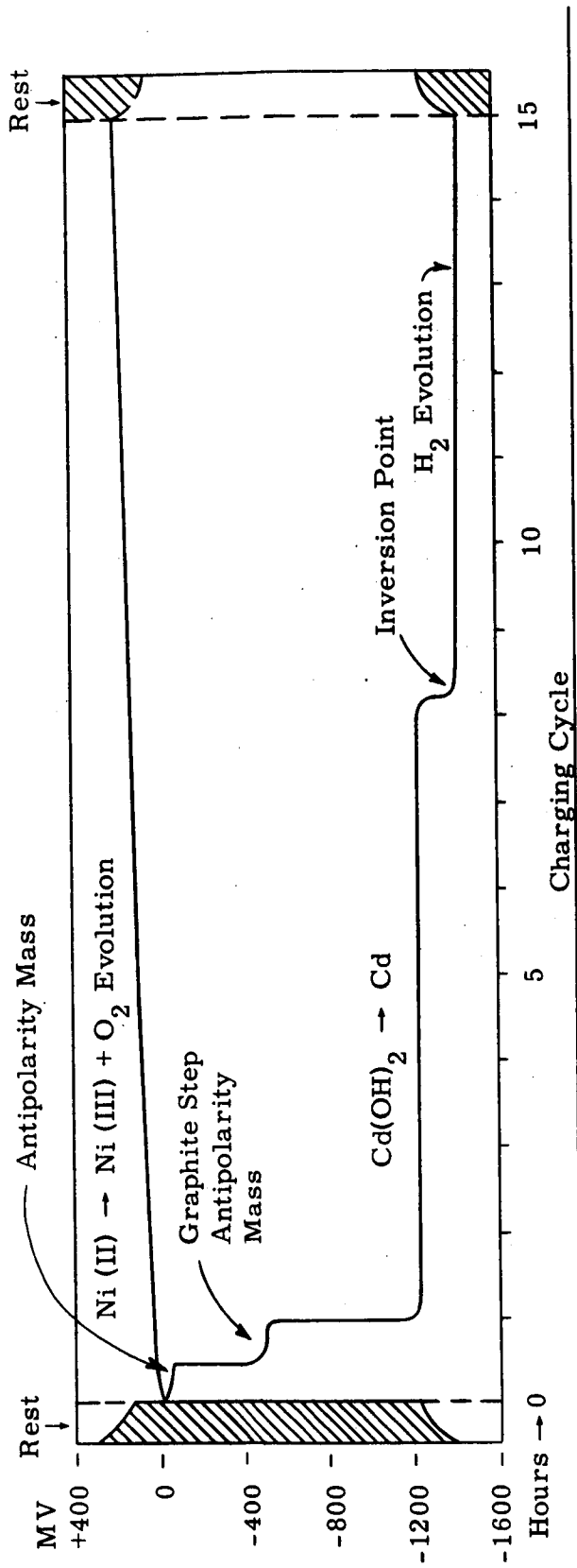


Figure 2.3. Typical Characterization Test Curves.

$$E = E^{\circ} - \frac{RT}{2F} \ln \frac{(Cd^{++})}{(Cd)}$$

where

- E is the EMF of the electrode against hydrogen
 E° is the standard electrode potential against hydrogen in basic solution
 R Gas Constant
 T Absolute Temperature
 F Faraday's Constant
 (Cd) Concentration of cadmium metal = unity
 (Cd⁺⁺) Concentration of cadmium ion in solution

The concentration of cadmium ion is controlled by the solubility product of any possible insoluble compound; thus for the hydroxide:

$$K_{sp} = (Cd^{++}) (OH^{-})^2$$

from which we have the derivation for the cadmium electrode potential

$$\begin{aligned} E &= E^{\circ}_B - \frac{RT}{2F} \ln \frac{K_{sp}}{(OH)^2} \\ &= E^{\circ}_B - \frac{RT}{2F} \ln K_{sp} + \frac{RT}{F} \ln(OH) \\ &= E^{\circ}' + \frac{RT}{F} \ln(OH) \end{aligned}$$

If sufficient hydroxyl ion is present in the electrolyte, large amounts of carbonate have little or no effect on the potential since cadmium hydroxide is much less soluble than cadmium carbonate, and the potential is governed by the hydroxyl ion concentration. In the case where insufficient hydroxide is present, then the solubility product of cadmium carbonate enters into the reaction governing for the cadmium ion concentration and thus alters the value of the potential of the electrode.

These conclusions are borne out in experiments. If carbonate is added to the 30% KOH without decreasing the KOH concentration, amounts in the range of 40-50 g/L have no effect on the potential, and show no carbonate plateau in the discharge curve. If various amounts of carbonate solution are used to replace the 30% KOH then the effect is related to the amount added. The cell loses no discharge capacity in terms of ampere-hours with an almost pure carbonate electrolyte, but the cell voltage drops by 0.1 to 0.2 volt giving a loss in watt-hour capacity.

The importance of a non-destructive test for impurities such as nitrate and carbonate is that they can be used to check the cell prior to sealing and assure that the cleanup of the electrodes and electrolyte is complete without requiring destruction of samples of the cleaned electrodes.

In characterization test, additional data on all behavior can be obtained by adding separators to the test cells. The changes in behavior due to their presence can be made explicit in comparison to the cell with the separator. Also, the effect of additives such as surfactants, cellulose decomposition products, etc., can be checked quantitatively.

A valuable adjunct to the characterization tests is the fact that comparison of the electrode voltage curves taken in the first test cycles can be made with those taken in later cycles. This comparison often shows minor changes in the performance which ordinarily are obscured by other major changes. Thus, the growth of antipolar capacity on the cadmium electrode shows a rate of corrosion of the nickel substrate of this electrode; a growth of antipolar capacity on the nickel electrode would show migration of cadmium and so on. The long term behavior of the electrode is often indicated in the earliest test cycles, and the onset of degradation of the electrode is easily detected over a period of a few cycles. It is this feature of detecting trends in performance during cell operation that makes feasible the possibility of developing a short term acceptance test.

2.4 Initial Characterization Test Results

The characteristics determined from the potential time curves of the initial characterization tests were the capacities of the positives and negatives, and the graphitic capacity and nitrate reduction capacities for the positives. Time did not permit an evaluation of the negative plates for the extent of the carbonate and antipolarity charge capacities.

The distribution of the average capacity of the positives and negatives for the six characterization cycles for the majority of the plates used in the cycling tests are shown in Figure 2.4. It should be noted that the capacity spread for the positive plates is greater for the VO plates than the KO plates. The spread of the negative capacities is significantly greater than for the positive plate capacities. The maximum to minimum capacity ratio for the negatives is approximately 1.7; for the KO positives 1.2; and for the VO positives 1.4.

TABLE 2.3
COMPARISON OF CHARACTERIZATION CAPACITIES AFTER TWO-MONTHS STORAGE

Electrode Number	In Air at 40°C - Discharge State						Average ma.hrs.	Per cent Change of Original
	1	2	3	4	5	6		
P-121	*1020	1050	1060	1070	1060	1060	1055	-2.5
	**1040	1020	1040	1030	1020	1020	1028	
P-122	1000	1020	1020	1040	1020	1020	1020	+5.3
	1060	1070	1080	1070	1060	1070	1072	
P-123	940	970	960	980	970	970	965	+1.8
	980	980	990	980	980	980	982	
P-124	990	1010	1010	1040	1020	1020	1015	+3.8
	1060	1060	1070	1060	1040	1060	1053	
P-125	1010	1020	1040	1040	1060	1060	1038	-0.3
	1040	1020	1040	1040	1020	1020	1035	
N-121	1340	1330	1350	1290	1340	1330	1330	-7.5
	1280	1270	1240	1210	1210	1200	1235	
N-122	1370	1380	1360	1380	1330	1320	1357	-5.8
	1340	1320	1280	1250	1250	1230	1278	
N-123	1360	1350	1340	1360	1330	1320	1343	-9.9
	1280	1250	1230	1170	1170	1160	1210	
N-124	1310	1330	1350	1380	1330	1310	1335	-7.5
	1250	1260	1240	1210	1220	1220	1235	

POSITIVES

NEGATIVES

Notes: (1) Δ% = Difference between maximum and minimum capacity as % of the minimum capacity.
* Before storage
** After storage
Charge rate - C/10

The average plate capacity for both positives and negatives is essentially independent of the total discharged plate weight determined after the electrochemical cleaning of the plates. These results are shown in Figure 2.5 and 2.6. This lack of correlation is to be expected since the capacity is largely a function of the plaque sinter porosity, thickness, and the fraction of this void volume impregnated with active material. The porosity tolerance limits as shown in Table 2.1 could well account for the observed variation in capacities.

The graphitic capacities ranged from 50 to 300 ma. hrs. and the nitrate step from 0 to 30 ma. hrs. There was no detectable relation between either of these and the plate capacity. Similarly there was no detectable relation between the graphitic capacity and the nitrate step.

In addition to the above characteristics, a two-months storage test was conducted on a few positive and negative electrodes to determine if the electrodes changed capacity on storage in air in the discharged state at 40°C. The capacity changes noted for these electrodes are summarized in Table 2.3. The trends indicate a slight capacity gain for the positives on the average and a capacity loss for the negatives on the average. The variation of capacities on successive cycles noted in the table is typical for most of the electrodes characterized.

The initial characterization data for the electrodes used in cycling tests is presented in the following sections of the report dealing with the results of each of the cycling tests. The results of X-ray and photomicrographic examinations are presented in the same manner.

2.5 Positive Electrode Blistering Problem

The positive VO electrodes were observed to develop blisters and pimples when characterized at the 1C rate (1200 ma) in the characterization tests. This phenomena was also encountered with some of the electrodes during the electrochemical cleaning procedure prior to the initial characterization tests.

A short investigation was conducted to determine during what portion of the cycle the blistering occurred, under what conditions, and whether the particular lot of electrodes being used in the program was more susceptible than other lots.

INITIAL CHARACTERIZATION CAPACITY DISTRIBUTION

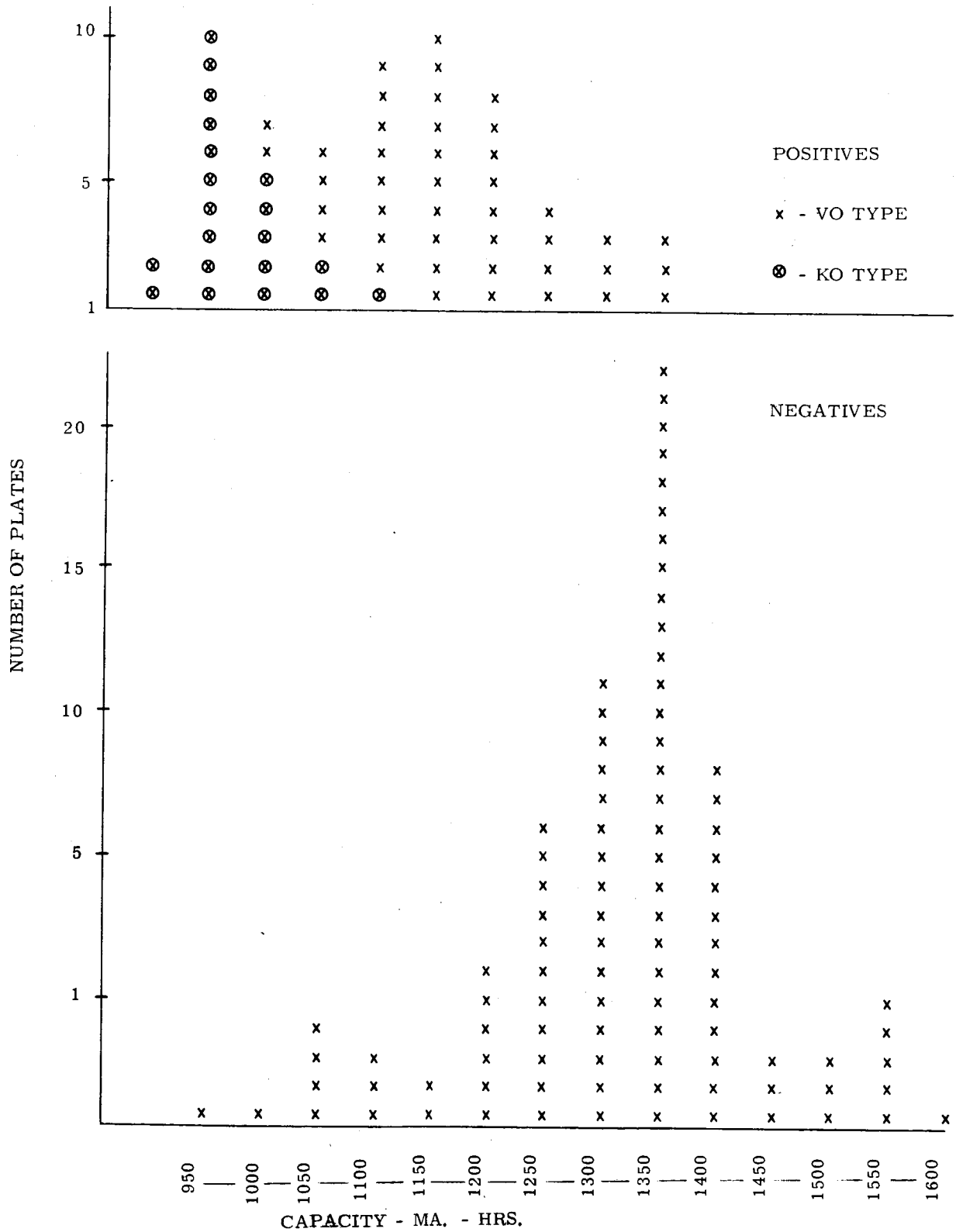
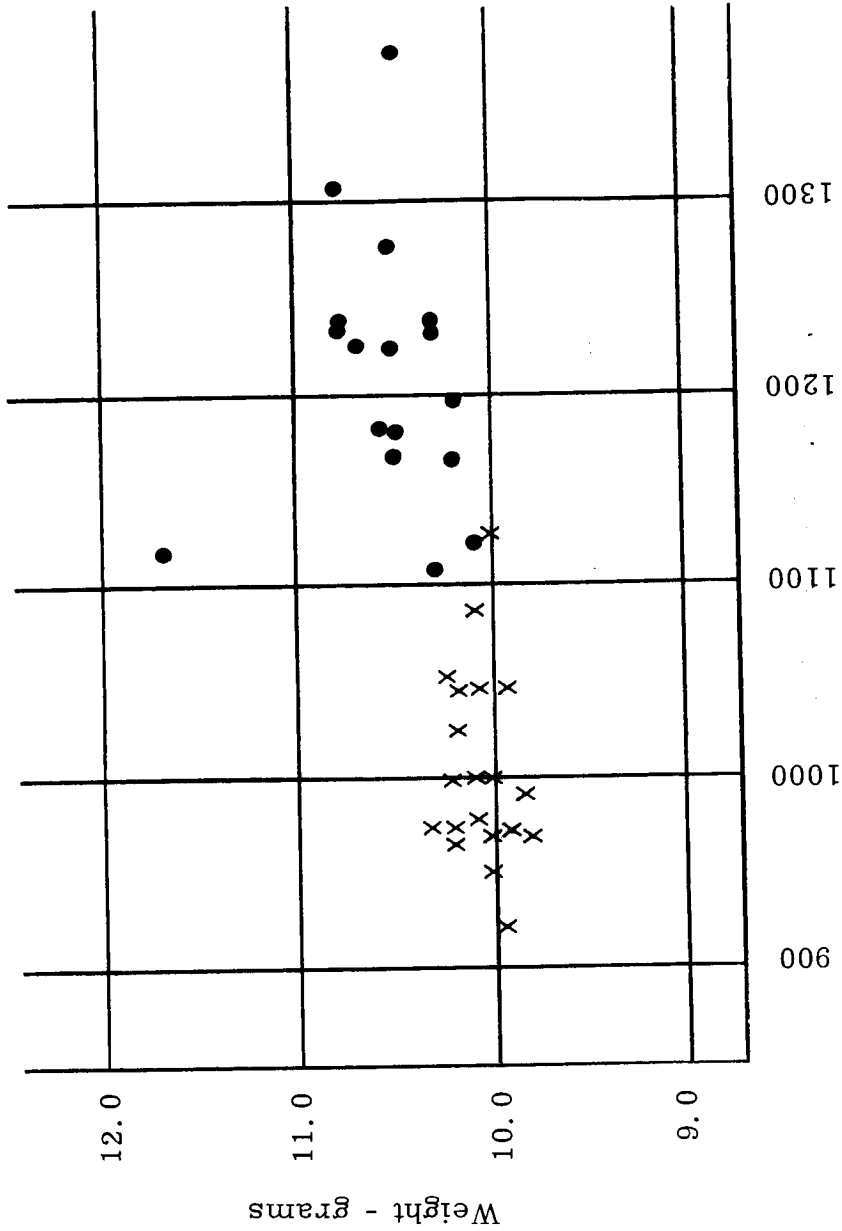


Figure 2.4

PLATE WEIGHT VS CHARACTERIZATION CAPACITY

Positives ● - VO-TYPE
 x - KO-TYPE



Average Capacity - MA. - HRS.

Figure 2.5

PLATE WEIGHT VS CHARACTERIZATION CAPACITY
 NEGATIVES - VO TYPE

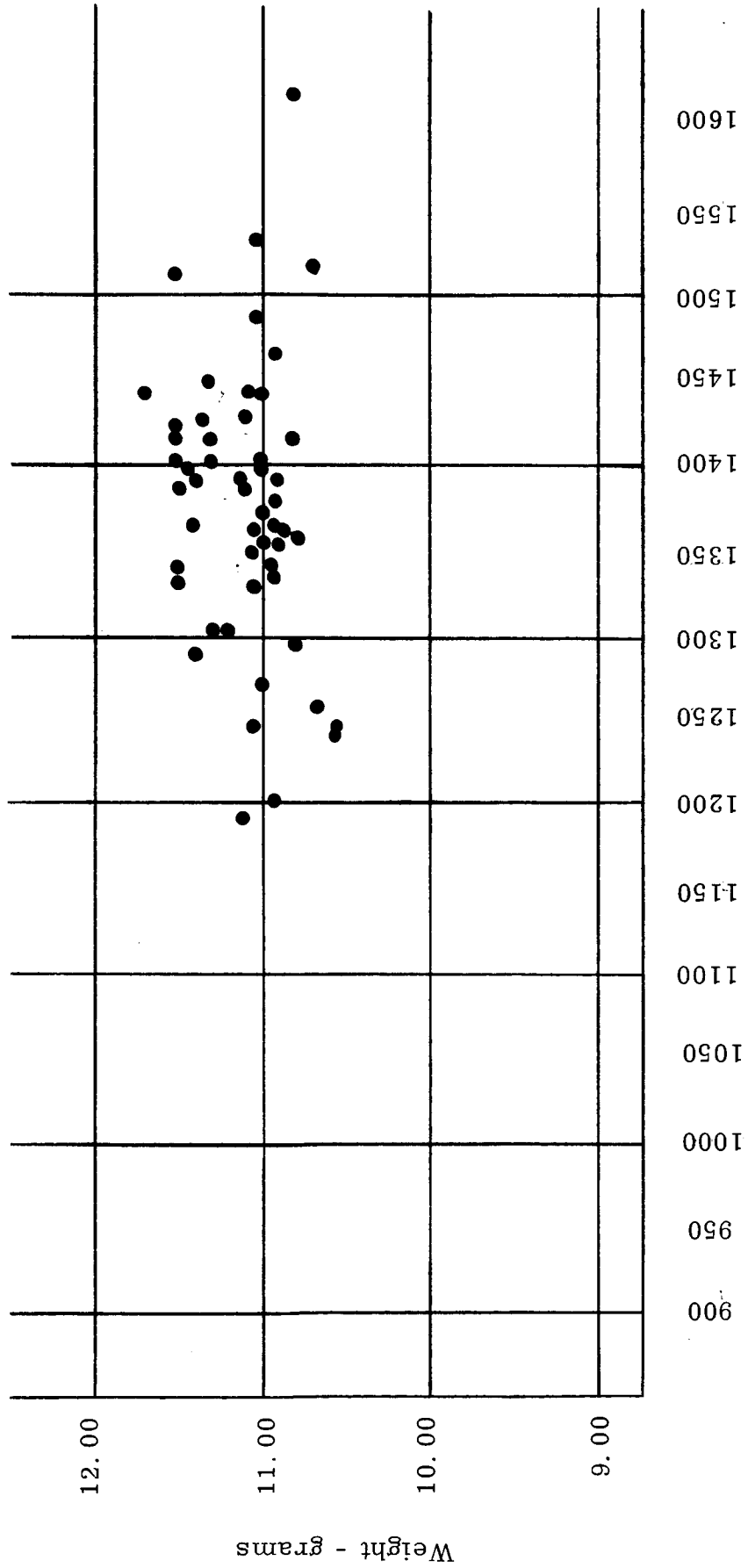


Figure 2.6

The blisters developed on both surfaces of the plate and in many cases the sintered nickel matrix physically separated from the nickel-plated sheet of the electrode. Examples of blistered electrodes are shown in Figure 2.7. The size of the blisters ranged from 1/8 to 1/2 inch in diameter. For the purpose of classification, pimples were arbitrarily defined as being less than 1/8 inch in diameter.

There was no history of manufacturing problems at the time the plaques were made. No electrodes of the lot used in our test have been used in production cells and, therefore, there is no comparative information on our electrodes and their performance in cells.

Reproducibility of the phenomena was confirmed by testing additional electrodes from the same lot being used in the program and another lot. Plates removed from commercial, vented-type cells employing the same type of plates also developed blisters when characterized at the 1C rate. Pre-treatments such as forming the plates at low charge and discharge rates (C/20 to C/10) prior to testing at 1C showed some reduction in the extent of blistering with respect to both number and size of blisters per plate.

Examination of electrodes during various stages of charge and overcharge established that the electrodes developed pimples during the overcharge portion and occasionally mild blistering compared to those encountered during the characterization tests at the 1C rate. It is believed that these pimples may be further enlarged to blisters in the inversion period of 15 minutes duration used in the initial characterization cycle.

Finally a group of positive electrodes of the VO type made at the General Electric Company Battery Business Section facility at Gainesville were put on a test along with some of the VO plates being used in the program. The plates made at Gainesville are designated as KO. The test consisted of operating cells containing two positive electrodes at varying charge rates, at two electrolyte concentration levels of 25 and 31% for varying periods of time to note behavior during excessive overcharge. In this test, one of the electrodes in each cell is continuously overcharged, and the other is continuously overdischarged. The results of these tests with respect to pimple and blister formation are listed in Table 2.4.

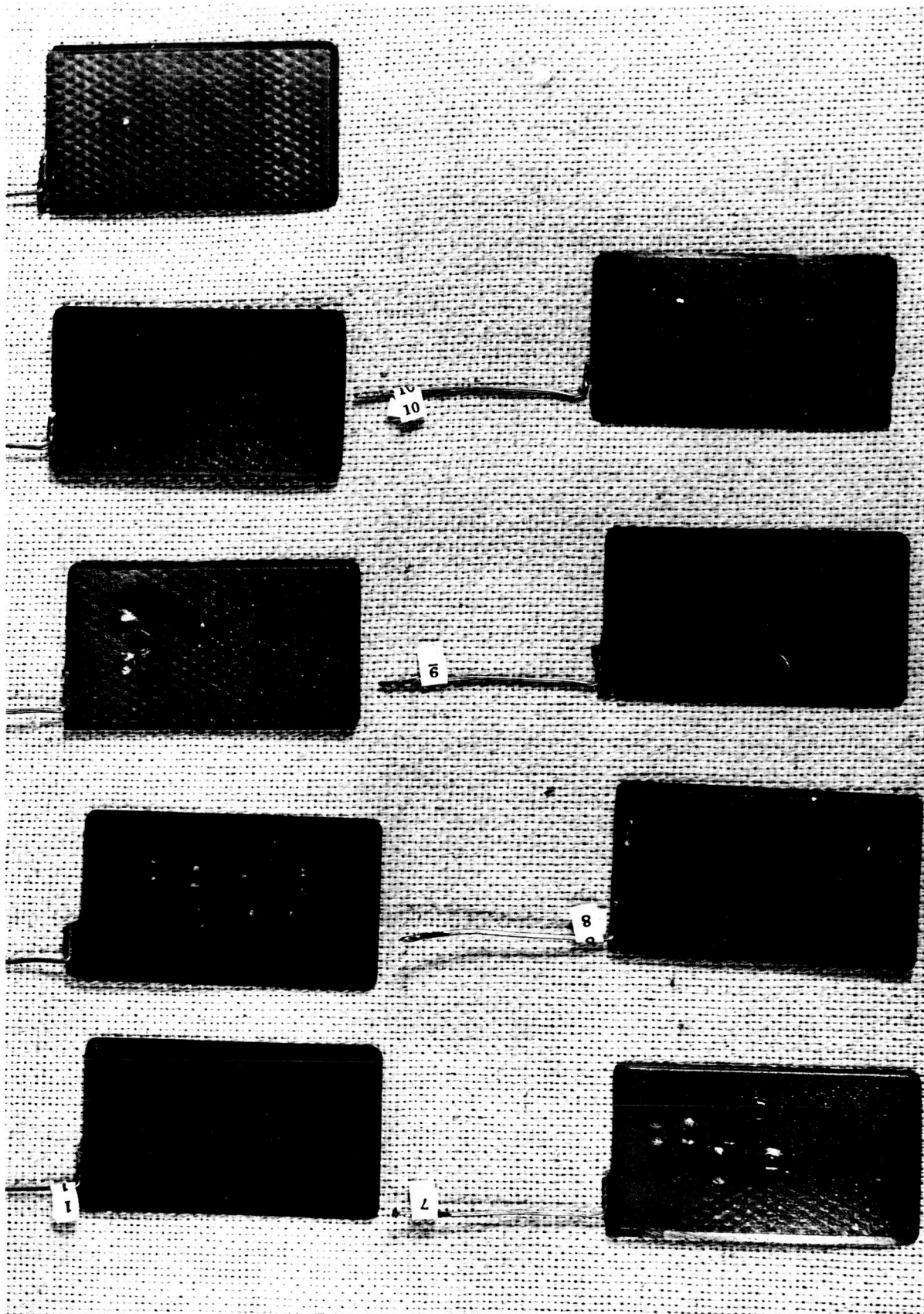


Figure 2.7. Positive Electrode Blistering - Nominal Plate Capacity 1.0 Amp-Hr. Conditions - Charge 101 min; Discharge - 84 min @ 1.0 Amp - 25°C.

TABLE 2.4

EFFECT OF EXCESS CHARGE CONDITIONS ON PHYSICAL CHARACTERISTICS
OF NICKEL ELECTRODES AT ROOM TEMPERATURE IN 25% AND 31% KOH ELECTROLYTE

	<u>GE</u>	<u>SAFT</u>
KO-15	1.4 amp. hr. Nominal Capacity	VO 1.2 amp. hr. Nominal Capacity
	25% KOH - One Plate	25% KOH --- Three Plates
	C/10 - C/7 - C/1.4 --- 535-675-500% Excess	C/7 - C/5 - C/1 --- 960-950-700% Excess
	No Effect	No Effect
		C/7 - C/1 --- 340-700% Excess
		No Effect
		C/5 -----410% Excess
		Blisters
	31% KOH --- One Plate	31% KOH -----Two Plates
	C/10 - C/7 - C/1.4 -----535-675-500% Excess	C/7 -----260% Excess
	No Effect	Pimples
		C/7 -----110% Excess
		Pimples

The conclusions drawn are that the VO plates being used in the program are more susceptible to the blistering phenomena than the KO plates. The electrolyte concentration appears to be a contributing factor since for the VO plates, the plates in the 31% KOH electrolyte showed pimples at lower percentage overcharge and lower charge rates. None of the counter electrodes which were on continuous over-discharge showed any pimples.

The pimples, therefore, appear to start during overcharge at higher charge rates, at higher concentrations of electrolyte and may develop into larger blisters during overdischarge.

On the basis of these results, it was decided to insert KO plates into the test program for comparison purposes and to restrict the initial characterization and recharacterization tests to the C/10 rate.

It was not possible to devote more attention to this phenomena during the course of the program. However, it is recommended that it be investigated further in any future programs.

2.6 Oxygen Evolution Tests

As part of the initial characterization data, the start of oxygen evolution and the rate of oxygen evolution as a function of charging rate was determined for a limited number of positive electrodes. The objective of these tests was to determine if this tool could be used to ascertain the quality of electrodes and also to note if gassing characteristics of electrodes changed under different modes of cyclic operation.

2.6.1 Experimental Equipment & Procedure

The apparatus for measuring the rate of oxygen evolution consisted of a sealed flooded test cell containing counter-electrodes and a reference electrode in separate compartments from the test electrode. The gas evolved from the test electrode was collected in a small calibrated volume which was vented to the environment at a pre-set pressure differential. A schematic diagram of the apparatus and test cell is shown in Figure 2.8.

The test cell (made of Lucite) has three compartments and contains six electrodes in the following arrangement:

<u>Compartment I</u>	Positive reference electrode	R ₁
	Negative cadmium counter-electrode	C ₁
<u>Compartment II</u>	Nickel screen auxiliary electrode	A ₂
	Positive test electrode	T ₂
<u>Compartment III</u>	Nickel screen auxiliary electrode	A ₃
	Negative cadmium counter-electrode	C ₃

The compartments are separated from each other by baffled walls and the electrodes are completely submerged in an excess of 31% by weight potassium hydroxide electrolyte. The cell is covered by a lid which was screwed to the cell container. The gas tight seal between lid and container consists of a neoprene gasket. A gas outlet tube, located at the center of the lid, leads to the gas measuring device.

The two auxiliary electrodes A_2 and A_3 respectively, are omitted in this drawing.

In operation as gas is evolved from the test electrode the pressure within the closed system begins to rise until the pressure reaches a pre-set value at which point the capacitive switch on the manometer operates. The normally closed solenoid valve then opens and the accumulated gas escapes. The pressure in the system then returns to its initial value and the solenoid valve closes.

Each activation of the valve releases a constant volume of gas and concurrently changes the polarity of the latching relay. The contacts of this relay are wired so that the potential of the test electrode vs. the reference electrode or of the negative counter electrodes vs. the reference electrode are alternatively fed into the amplifier. By means of the selector switch, a recorder with an appropriate speed of paper transport can be connected to the amplifier. After the first release of gas, the resulting recorder charts show two distinctive broken lines, one representing the potential vs. time curves of the test electrode and the other representing the potential of the counter electrodes.

For evaluating the data from these charts, either the distance between two subsequent events is measured or the number of events per unit of time are counted. As each event represents a constant amount of gas evolved and released, the gasing rate in milliliters per unit of time can easily be calculated.

The system is calibrated before starting runs with each new electrode. This procedure is as follows: A constant direct current is passed between the auxiliary electrode A_2 and the two counter electrodes C_1 and C_3 so that oxygen is evolved from A_2 . The currents applied represent charge rates of $C/10$, $C/5$, $C/2$ and $1C$, respectively, based on the known capacities of the test electrodes. After a full gasing of the auxiliary electrode is accomplished, the times elapsed between two subsequent activations of the solenoid valve are measured by means of an electric stop watch and an average value for Δt is calculated for each current using between 20 and 30 individual gas release.

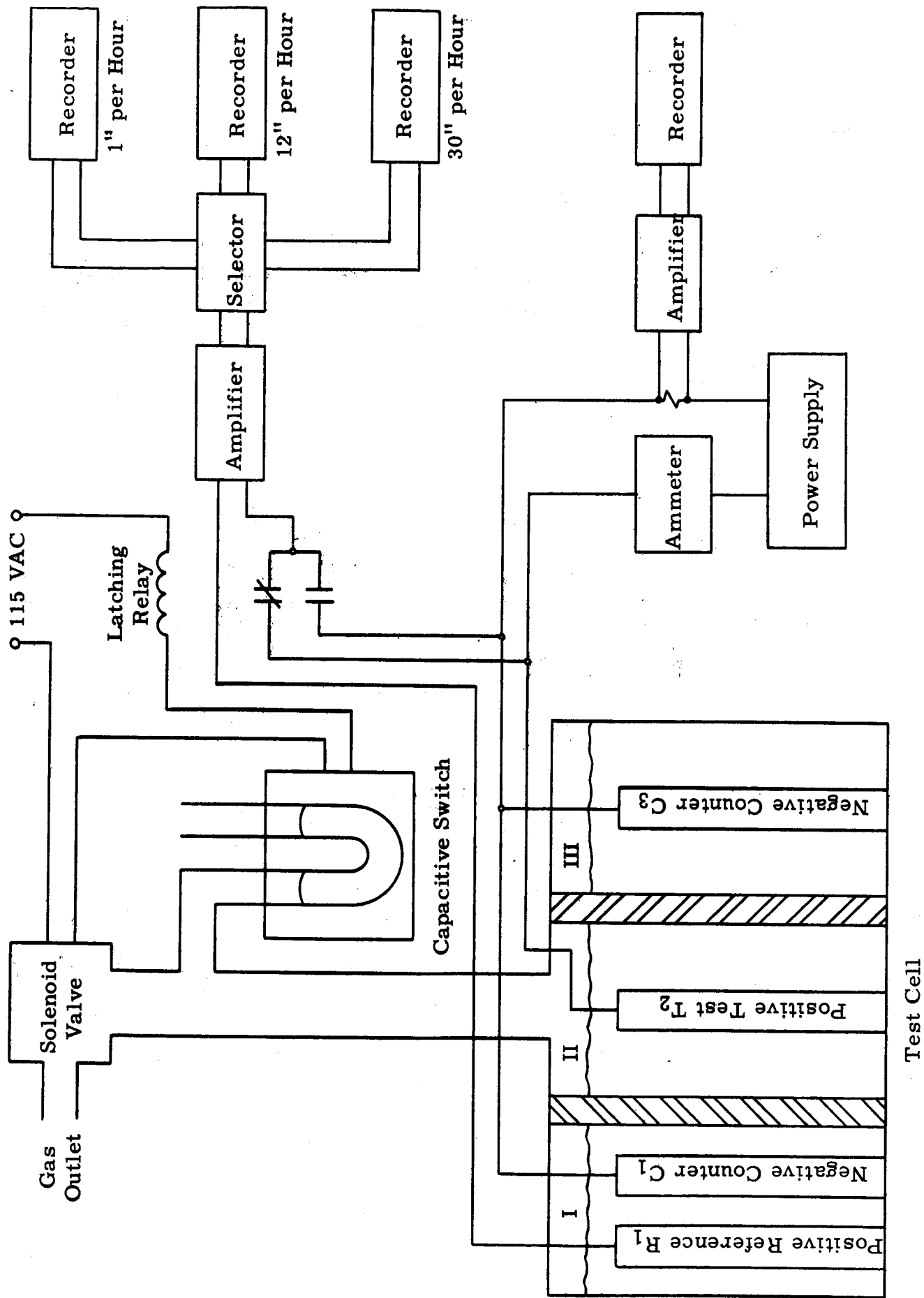


Figure 2.8. Gas Evolution Measuring Apparatus.

The volume, V_r , released per activation of the solenoid is the product of two constants, namely,

V_o = the total volume of the system and,

f = the ratio between the activation pressure differential to actuate the capacitive switch and one atmosphere standard pressure.

and it can be calculated from,

$$V_r = V_o \times f = \text{const.} = n_{th} \times \Delta t$$

where,

n_{th} = theoretical gas evolution rate in ml. sec.⁻¹

Δt = the average length of time between two subsequent activations.

The reproducibility of V_r for the currents used was good, and a numerical value of about one milliliter was observed for different experimental setups.

Each experimental run at a given charge current started with a checking of the constancy of V_r by evolving oxygen from A_2 and measuring the time between subsequent activations of the solenoid valve. Immediately after this test calibration, the test electrode T_2 was charged against the two counters C_1 and C_2 respectively, while the onset of oxygen gasing from T_2 and the increase of the gasing rate were recorded on one of the vent recorders.

Regardless of the charge rate applied, a total of 2,000 ma-hrs. per run was passed through the cell before the test electrode was put on rest. The rest period varied from 10 minutes to two hours, depending on the timing of the program. The test electrode then was discharged against the cadmium counter electrodes at the C/2 rate, and the capacity discharged, C_d , was calculated from the breaking point of the potential vs. time curve of the test electrode.

As soon as the potential of the test electrode reached the region of hydrogen evolution, the discharge of T_2 was terminated. The discharge of the counter electrodes was then continued against the auxiliary electrode, A_2 , in order to prepare the counter electrodes for the next experiment.

The results of these measurements are conveniently presented in the form of curves showing the percentage of current going into oxygen evolution at any time versus a normalized state of charge factor for the test electrode up to the same time. The normalized state of charge factor, X , is defined as follows:

$$X = \frac{C_t - C_g}{C_d} \quad (100)$$

where C_t = total amp-hr input to the cell up to time t .

C_g = total amp-hr consumed in oxygen evolution up to time t .

C_d = amp-hr capacity of test plate determined by discharge measurement to break point in potential-time discharge curve.

2.6.2 Results

Preliminary tests with formed and unformed VO electrodes showed that the start of gas evolution and rate of gas evolution varied from run to run and was dependent on the previous history of the electrodes. With unformed electrodes the initial run showed early gassing and poor charge acceptance at C/5 rates of charge. Progressive increases in charge rate from run to run going to the C rate showed progressive delays in the start of gassing except for the run at the C rate. See Figure 2.9.

Subsequent to these preliminary experiments a short program was planned to explore the gassing behavior of electrodes with different histories. The emphasis was primarily on electrodes which had developed pimples or blisters during the initial characterization or during the electrochemical cleaning procedure. Two electrodes removed from cyclic tests at constant voltage-current limited charging were also tested to provide some insight on the effects of cycling if any. The electrodes tested included both KO and VO types. The electrodes used in this phase of the work along with their histories are listed in Table 2.5.

The results of these tests are plotted in Figures 2.10, 2.11, 2.12, and 2.13. These plots show the total amount of oxygen evolved after various levels of total charge input had been returned to the test cell. These figures also show the charge rate used on succeeding cycles and the electrode capacity determined at a discharge rate of 600 ma after each charge cycle.

Generally, the rate of oxygen evolution for all the electrodes examined was found to be measurable when the electrodes had accepted 50 to 60% of their rated capacity.

TABLE 2.5

POSITIVE ELECTRODES TESTED FOR GASSING BEHAVIOR

<u>Type</u>	<u>Number</u>	<u>History</u>	<u>Charge Rates, ma.</u>
(1) VO	P ₀ -70 P ₁ -42	Characterized) Uncharacterized) Pimples	120,240,600 and 1200
(2) VO	P ₇ -3 P ₇ -4	Uncharacterized) Uncharacterized) Blisters	20,120,240,600 and 1200
(3) KO VO	P-126 none	Characterized) Uncharacterized) No Pimples	120 and 1200
(4) KO VO	P-54 P ₅ -23	100 Cycles- 0°C) 579 Cycles-40°C)	Constant voltage current limited charging tests
			120,600, and 1200

With increasing state of charge, the portion of the charge current used for oxygen evolution increases non-linearly and on the average, at a state of charge factor value of 100 per cent, about 40 per cent of the charge current goes into oxygen gassing. In almost all cases, at a state of charge factory value of 120 to 140% results in a total conversion of the charge current into oxygen evolution. These observations are illustrated by the results for VO type electrodes plotted in Figures 2.14 and 2.15.

For the two VO type electrodes with pimples (Figure 2.10) the gassing behavior is significantly different and appears to be related to the differences in charge rate sequence used for testing the two electrodes. A charge sequence of alternately low to high charge rate from cycle to cycle yielded a lower level of gassing than the charge rate sequence of progressively increasing from low to a high value.

For the two VO electrodes (Figure 2.11) with blisters subjected to a charge rate sequence of progressive increases to a maximum value and then progressive decreases, the extent of gassing at a given total charge input level is significantly lower than the corresponding electrode (P₁-42, Figure 2.10) with pimples. Further testing is required to confirm if this difference is reproducible.

For the two electrodes without pimples or blisters (Figure 2.12) one a KO and the other a VO, there was no significant difference of gassing at all levels of charge input. One point deserves comment, on successive cycles at a constant charge rate, one of the electrodes (P₀-126) showed a progressive increase in the amount of gassing. This type of behavior was noted for three other electrodes P₁-42, P₇-3 and P₇-4.

For the two electrodes which had been cycled, one at 0°C and the other at 40°C for different number of cycles (Figure 2.13), there was no difference in gassing behavior. The gassing behavior compared to the similar uncycled electrodes (Figure 2.12) is not significantly different.

Nickel Electrode Gas Rates
 SAFT VO Type - Unformed
 Nominal Capacity - 1.0 amp. hr.
 Tests at room temperature

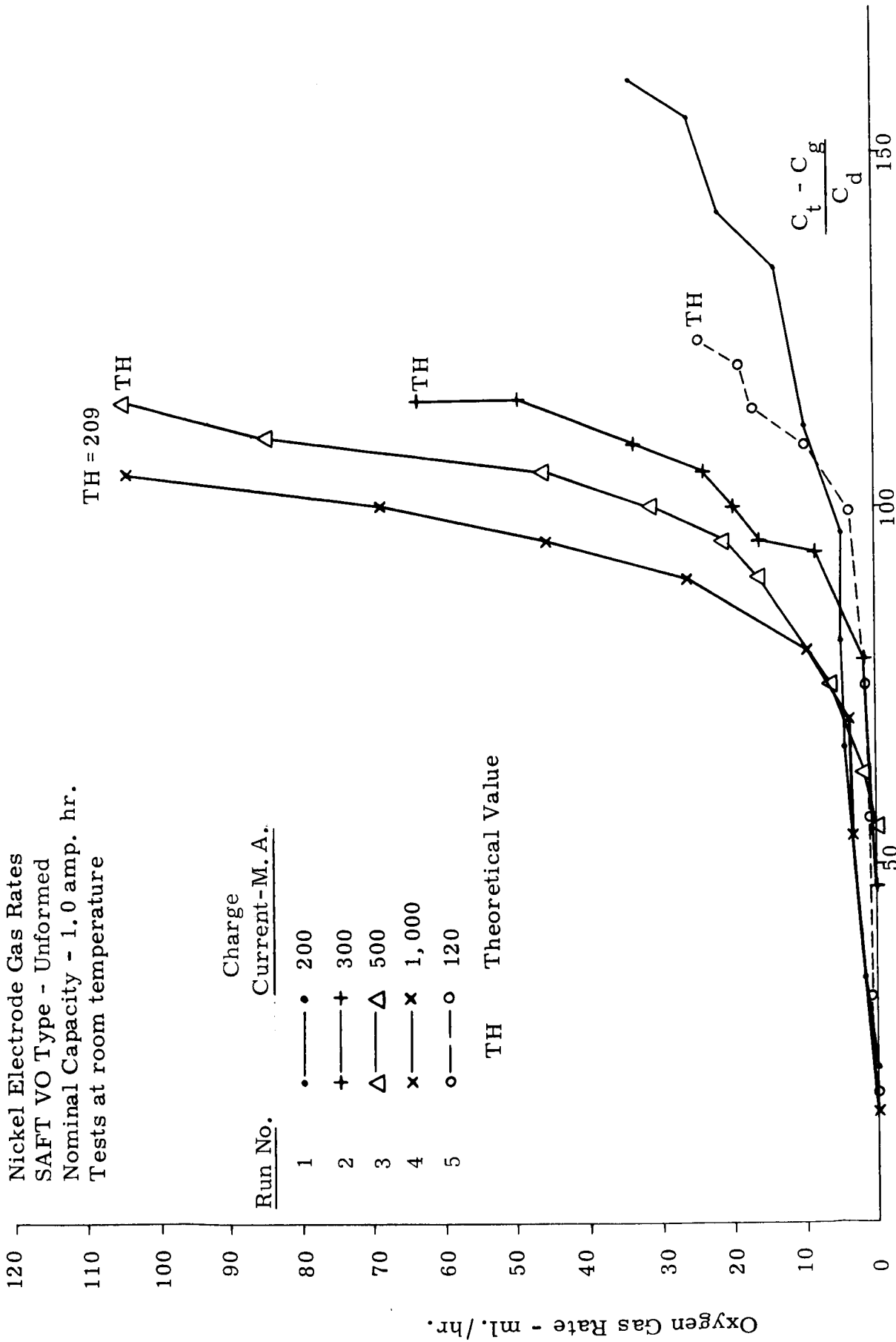


Figure 2.9. State of Charge - Percent.

POSITIVE ELECTRODE GASSING TESTS

Electrode Type - VO

VO

No. - P₀ - 70

P₁ - 42

Pimpled

Pimpled

Electrochemically

Electrochemically

Cleaned

Cleaned

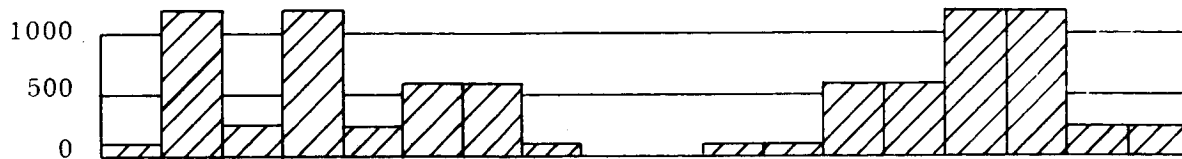
6 Cycles of

0 Cycles of

Characterization

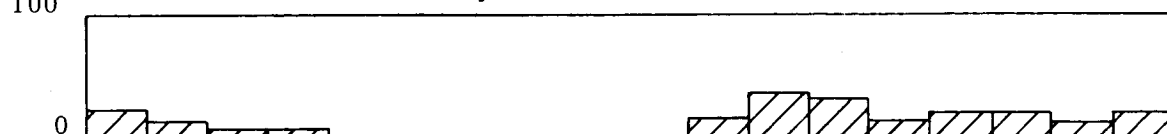
Characterization

Charge Rate - MA.

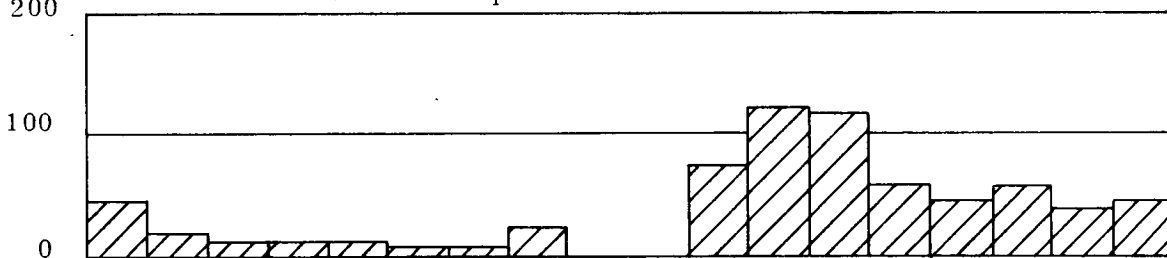


800 MA. HRS. Total Input

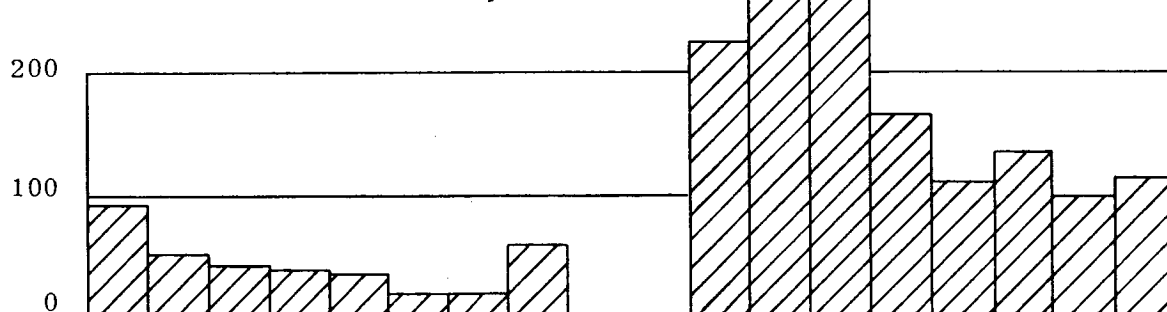
Total Oxygen Evolved - MA. Hrs. Equiv.



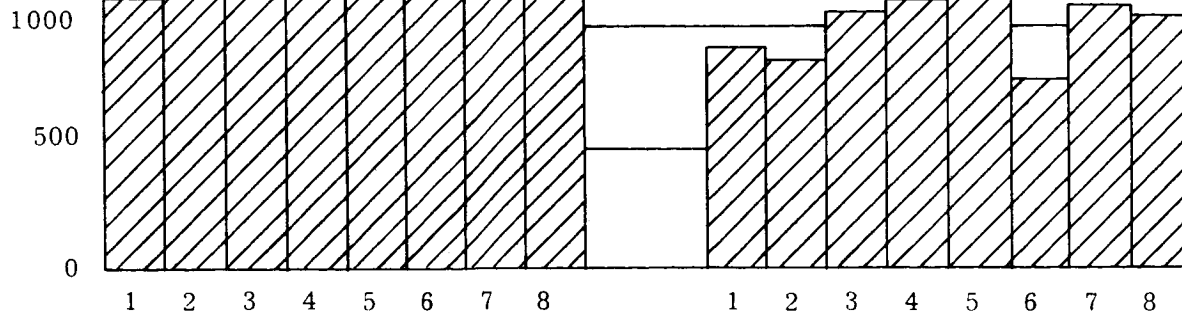
1000 MA HRS. Total Input



1200 MA. HRS. Total Input



Discharge Capacity
MA. HRS.



CYCLE NUMBER

Figure 2. 10

POSITIVE ELECTRODE GAS EVOLUTION TESTS
Electrochemically Cleaned Only

Electrode Type VO
No. P7-3
Blistered

VO
P7-4
Blistered

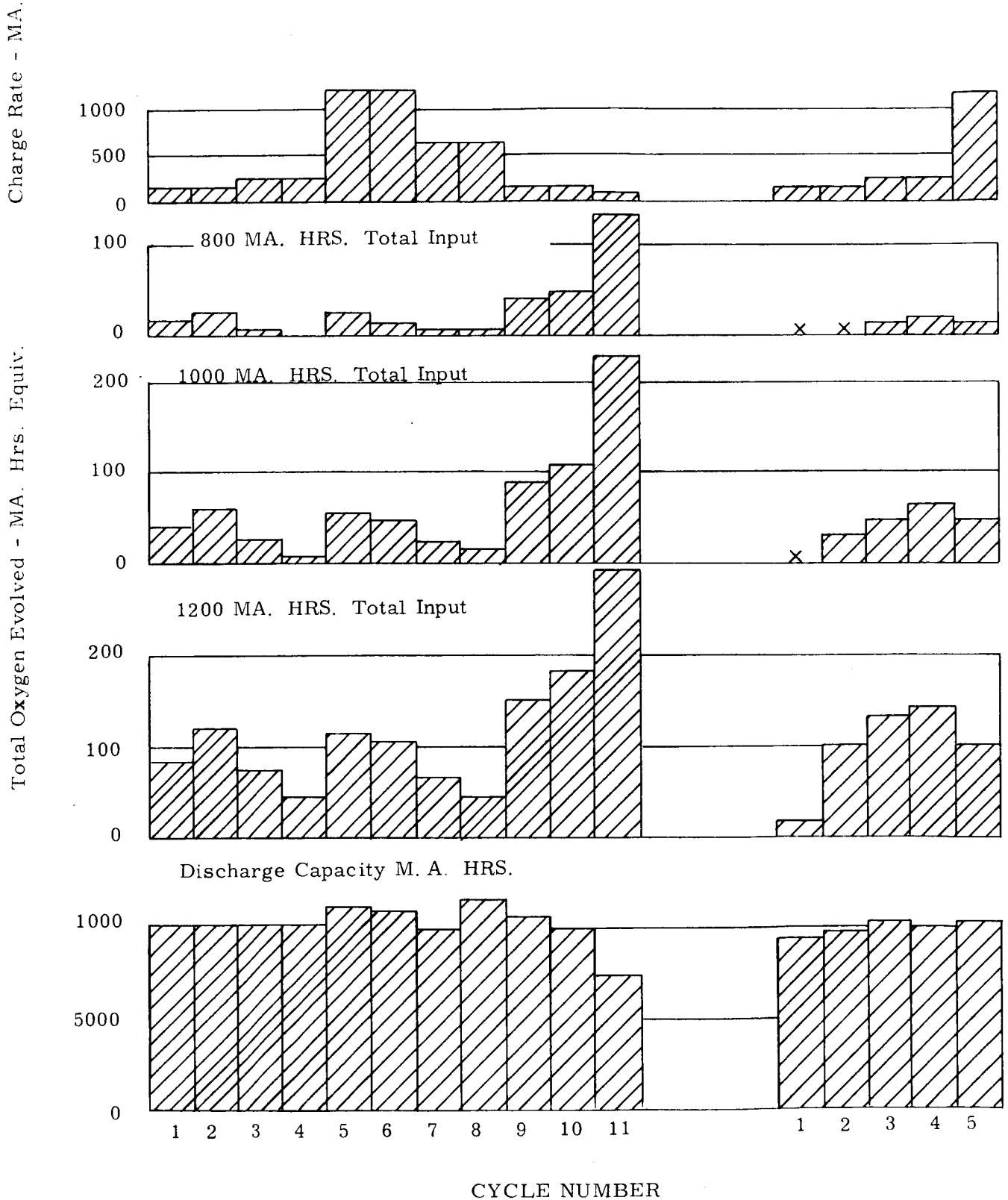
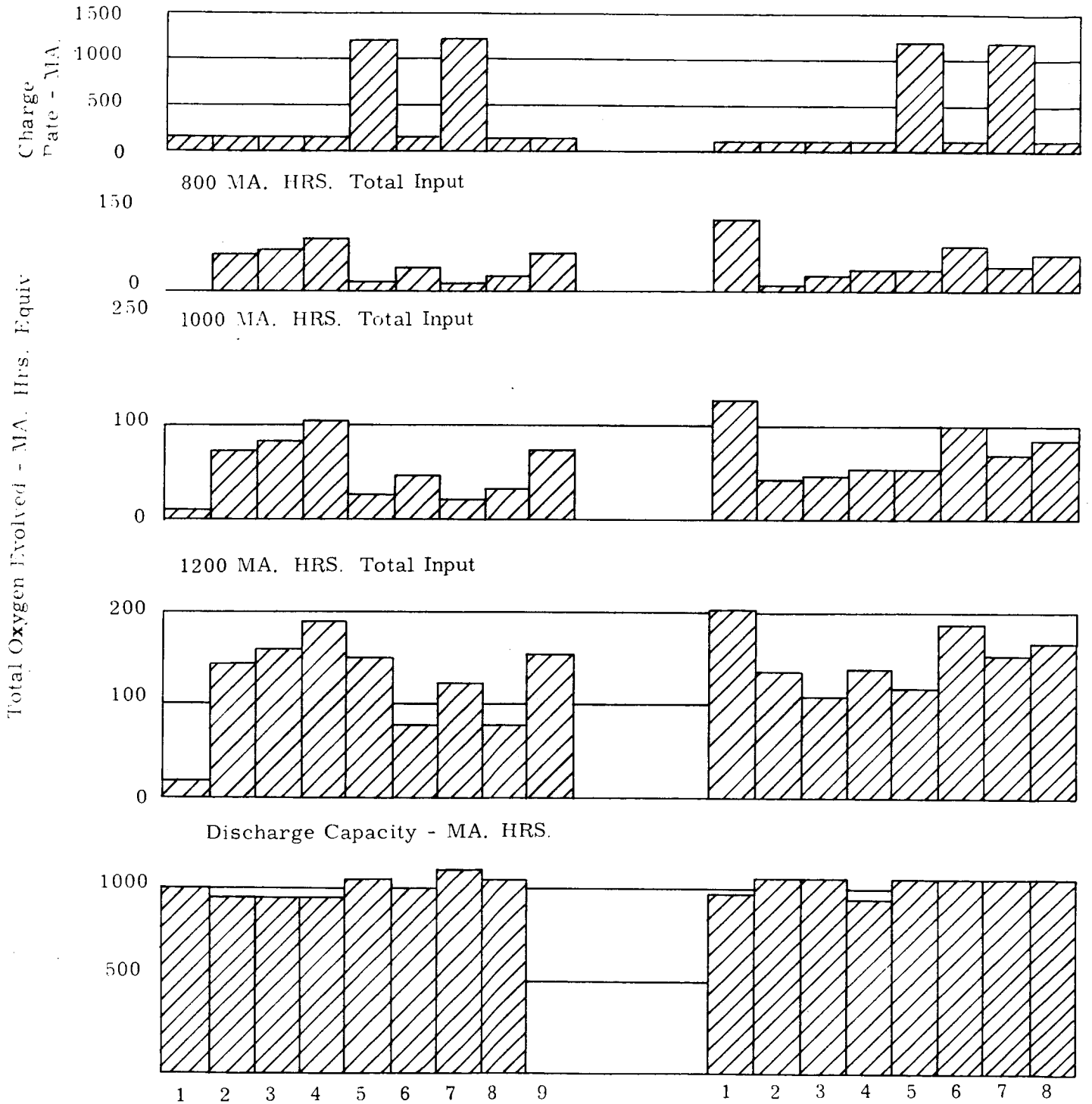


Figure 2. 11
-30-

POSITIVE ELECTRODE GAS EVOLUTION TESTS

Electrode Type - KO
 No. - P-126
 Electrochemically
 Cleaned
 6 Cycles of
 Characterization

VO
 None
 Electrochemically
 Cleaned
 0 Cycles of
 Characterization



CYCLE NUMBER

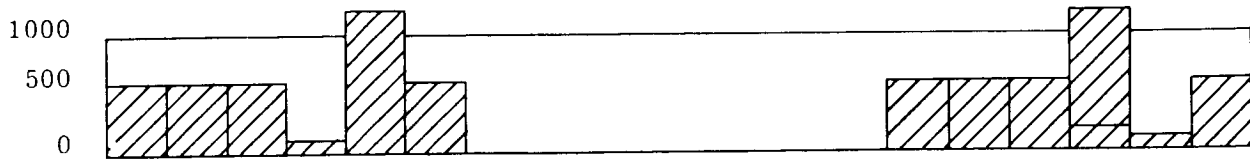
Figure 2.12

POSITIVE ELECTRODE GAS EVOLUTION TESTS
After
Constant Voltage - Current Limited Charging Cycling Tests

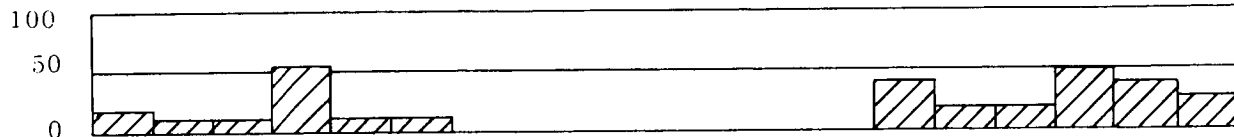
Electrode Type KO
No. P-54
100 Cycles @ 0°C

VO
P5-23
579 Cycles @ 40°C

Charge Rate - MA. Hrs.

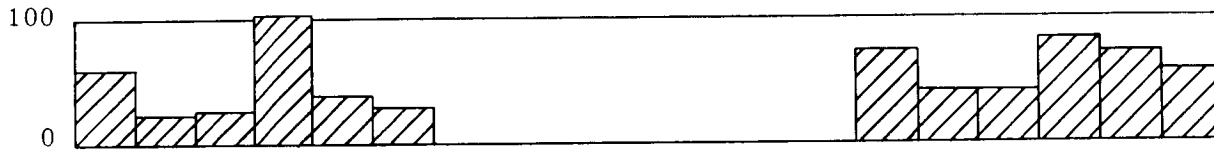


300 MA. HRS. Total Input

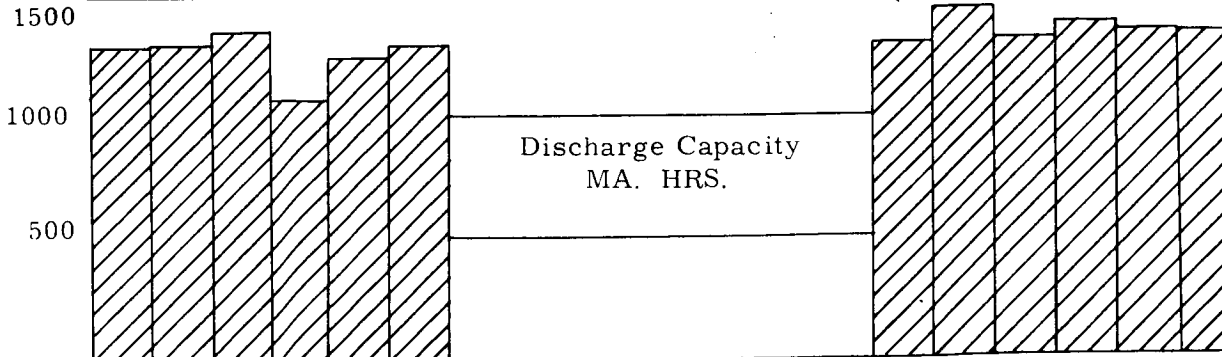
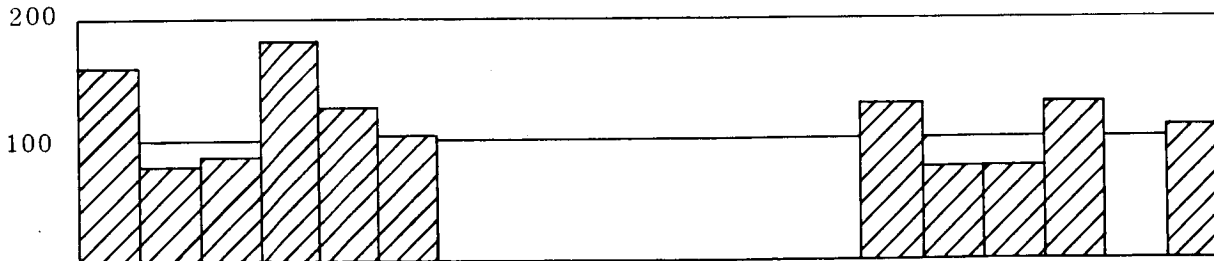


1000 MA. HRS. Total Input

Total Oxygen Evolved - MA. Hrs. Equiv.



1200 MA. HRS. Total Input



1 2 3 4 5 6 1 2 3 4 5 6

CYCLE NUMBER

Figure 2.13

Figure 2. 14. Gassing Behavior of Positive Electrode
SAFT-VO Type. Electrode No. P7-3.

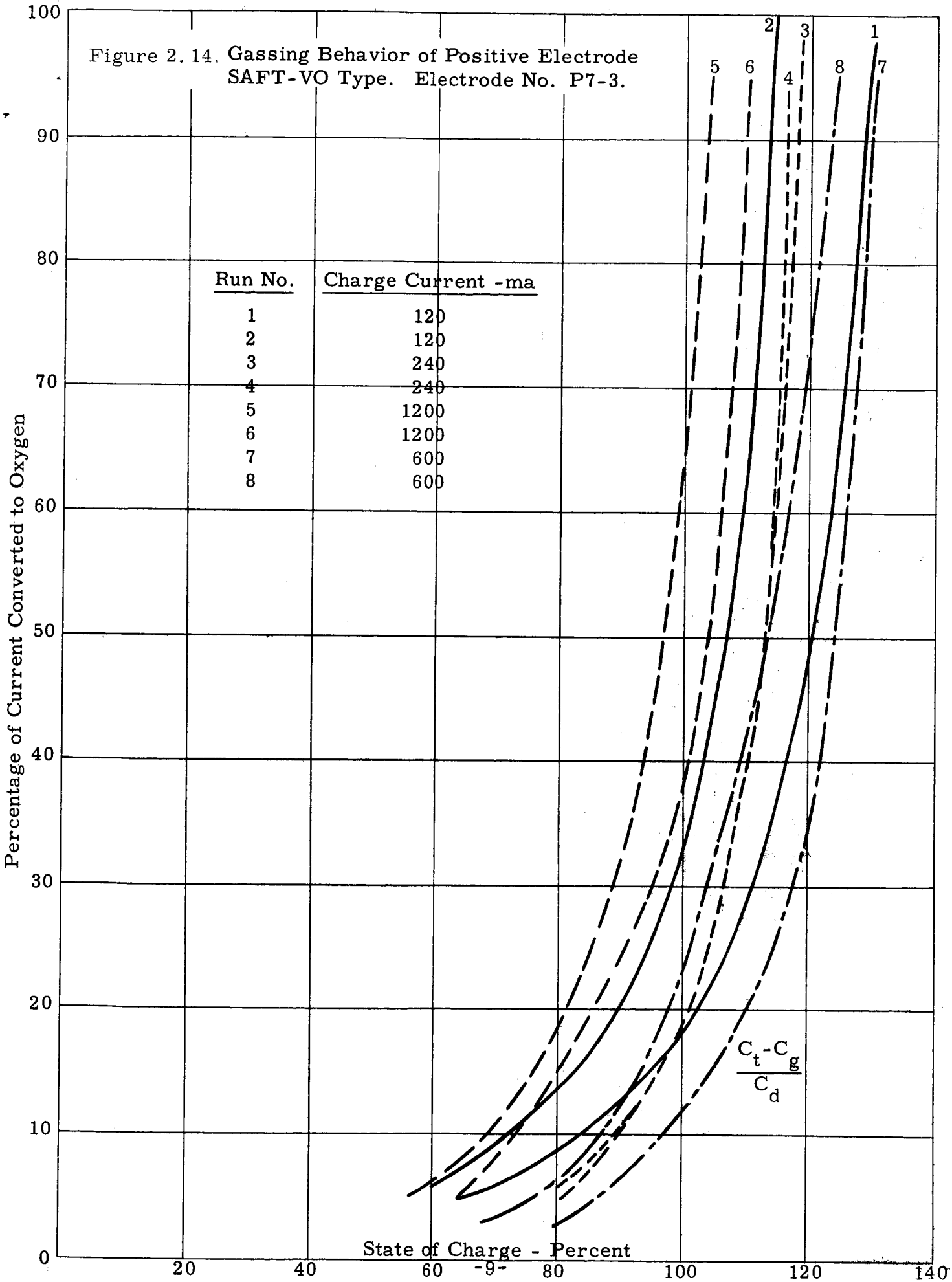
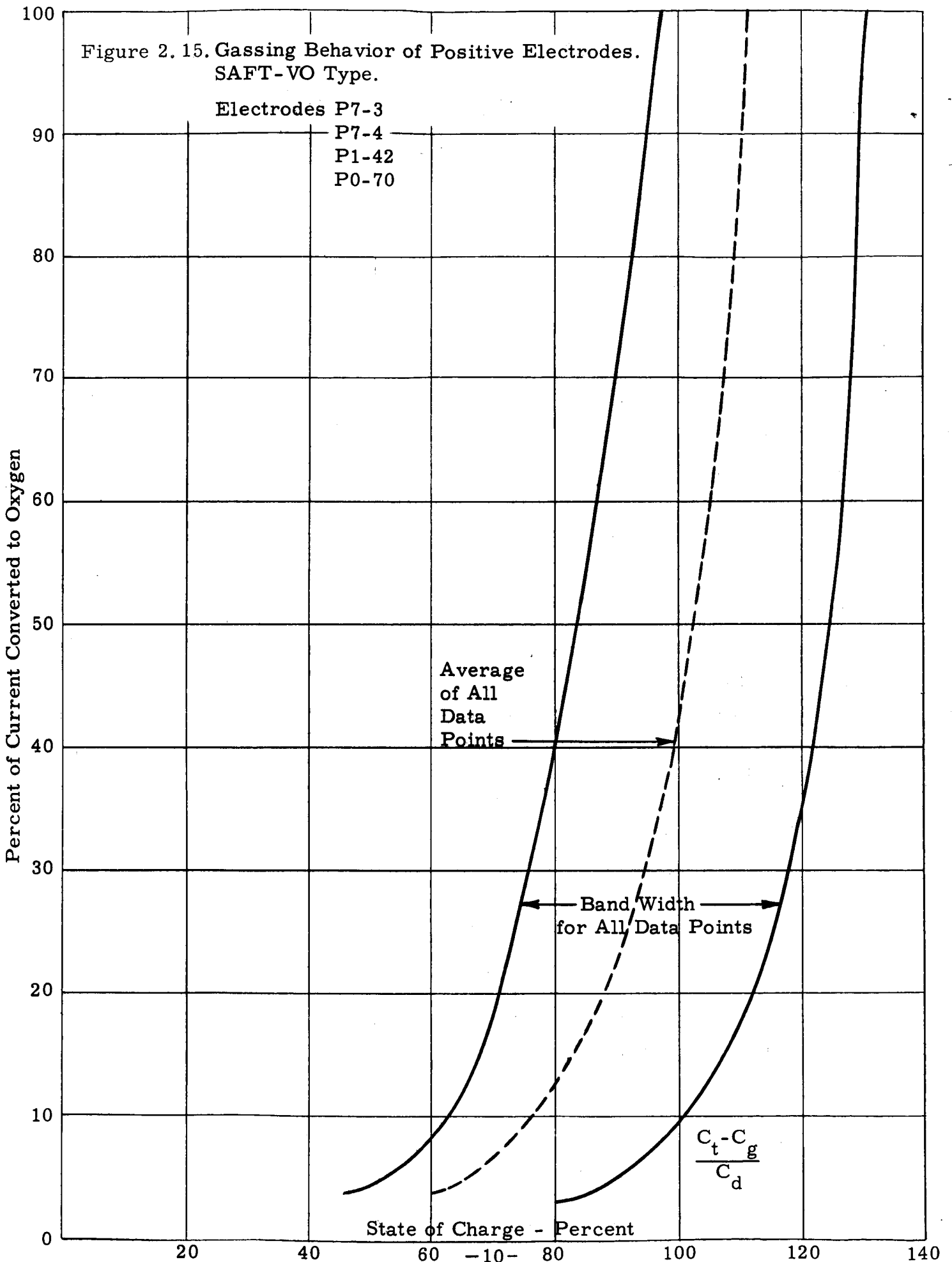


Figure 2. 15. Gassing Behavior of Positive Electrodes.
SAFT-VO Type.

Electrodes P7-3
P7-4
P1-42
P0-70



3.0 SHALLOW DISCHARGE CYCLING TESTS

These tests were designed to determine the onset and severity of memory effects. This phenomena has been observed in nickel-cadmium cells operating in repetitive discharge-charge cycles in which a constant fraction of the total cell capacity is used in each cycle. The end effect is that after a period of operation in this mode, a complete discharge of the cell usually yields a residual capacity equal to or only slightly greater than the capacity being used in the cycling mode. The amount of capacity recovered is dependent on the discharge rate used. The cell can be returned to rated capacity by one or two complete charge-discharge cycles.

3.1 Experimental Equipment and Procedures

The test cells consisted of four nickel and five cadmium electrodes assembled as shown in Figure 3.1. The separator material was one layer of unwoven felted nylon, whose nominal compressed thickness was 6-10 mils. The cell plates were loaded with a $6\frac{1}{2}$ lb. weight while the end face plate seal was made. This assured equal compression of the separators in spite of variations in plate thicknesses. The cells were vented to the atmosphere through a small hole at the top of the cell pack.

The electrolyte was 31% by weight reagent grade potassium hydroxide in distilled water. Each cell was initially filled with 11 cc. of electrolyte. Makeup water was added to a fixed meniscus point on a weekly basis.

A total of nine cells were constructed, with three cells being used at each temperature level; 0°C, 25°C (room temperature) and 40°C. The 0°C test cells were kept at temperature in a Tenney Eng. Inc., Model #TMUF 100240 Environmental Test Chamber and the 40°C test cells were kept at temperature in a Blue M Elect. Co.; Stabiltherm Lab Oven, Model #0V490A-1.

The cycling conditions used simulated a 90-minute orbit, with 35 minutes for discharge and 55 minutes for charge. The current during the discharge period was 1.7 amperes and for the charge period 1.3 amperes.

The capacity removed per cycle was 1.0 amp-hr and the amount returned on charge was 1.20 amp-hr. Based on a nominal positive plate capacity of 1.2 amp-hr this corresponds to a depth of discharge of approximately 21%.

The cycle control equipment schematic diagram for these tests is in Appendix II.

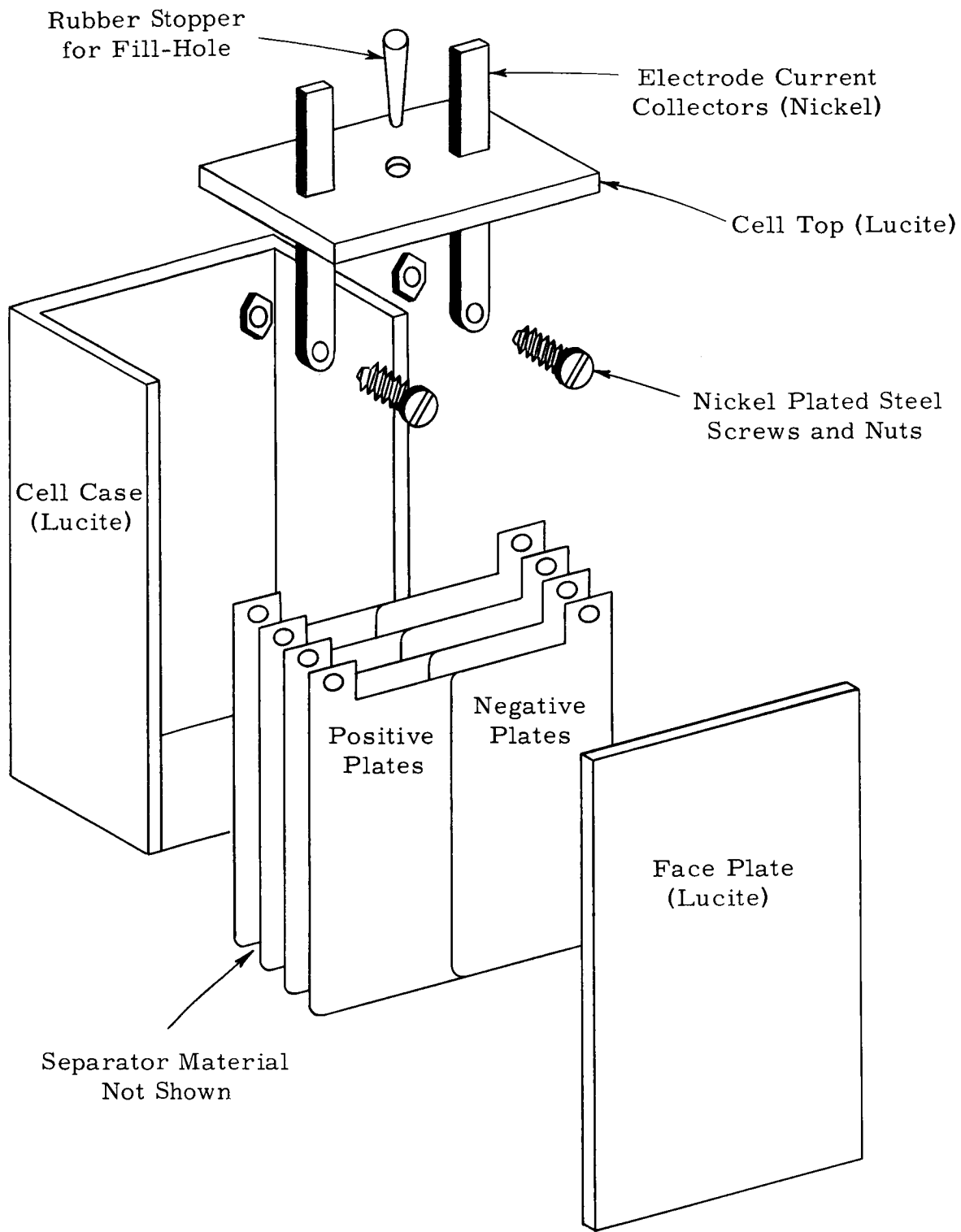


Figure 3.1. Cycling Test Cell Schematic.

Test cells were removed from the cycling tests after various intervals of cycling, and a pair of electrodes (a positive and negative) were individually tested for residual capacity, using fully charged counter electrodes. The discharge was conducted in two parts, first at a constant current of 500 ma. to a cell voltage of 0.6 volts, then through a constant resistance load of 10 ohms to 0.1 volts.

Some of the electrodes were returned to the cycling test but in sealed cells designed to vent at 50 psi. Electrodes removed for testing or because of bad surface conditions were replaced with fresh, uncycled electrodes. The intent here was to simulate more closely the intended use conditions and to provide a basis of comparison with the vented test cells.

Residual plates were recharacterized as described in Section 2.0 and comparisons of the potential versus time curves were made with the original characterization curves. In addition, test plates were removed from the cells without discharging them and examined by X-ray diffraction and photomicrographs to note composition and structural changes.

3.2 Shallow Discharge Cycling Test Results

Of the nine original cells put on test, three failed in service. The characterization condition, test temperature, number of test cycles, electrode identification and comments on visual appearance of the electrodes after the test cycling are outlined in Table 3.1. One of the 0°C test cells developed electrolyte leaks and was removed early in the program and is not included in the table.

3.2.1 Visual Examination of Test Electrodes and Separator Material

One positive electrode was taken from each test cell except #5 and examined microscopically. The photographs which follow illustrate all of the effects observed in the examination of positive plates. The samples were vacuum impregnated with clear Bakelite ERL2795* epoxy resin and mounted at a slight incline. They were then sectioned and polished obliquely to broaden the sinter structure and nickel plates steel core. All samples were etched with 2% Nital to reveal the nickel plate steel boundary of the core plate and photographed at 100 x. Comparison samples of unformed, fully charged and fully discharged electrodes were also photographed.

*A special resin which hardens without exotherm.

TABLE 3.1

SHALLOW DISCHARGE CYCLING TEST ELECTRODES

CC# (#cycles)	Charact'n Condition	Test Temp.	Cadmium Electrodes	Nickel Electrodes	Comments	Electrode Condition
4 (2078)	C/10	0°C	N ₁ -26,27,28 29,30	P ₁ -25,26 27,28		P-Extensively pimples, active mat'l spalling off N-Good, black scum on surface
6 (2078)	C/5	0°C	N ₁ -51,52,53, 54,55	P ₁ -53,54 57,61	Test cell found to be shorted out.	Cell not disassembled- external appearance is good except for short circuit area.
5 (2579)	C/1	25°C	N ₁ -41,42,43, 44,45	P ₁ -43,45, 46,49		P - No change. N - No change.
3 (2660)	C/10	25°C	N ₁ -21,22,23, 24,25	P ₁ -21,22, 23,24		P-All pimples, P ₁ - 23 has large blister. N ₁ - No change.
1 (2660)	C/5	25°C	N ₁ -1,2,3,4,5	P ₁ -1,2,3,4	Test cell found to be shorted out. No obvious reason.	P - Pimples - two short circuits. N - No change.
7 (849)	C/10	40°C	N ₁ -46,47,48, 49,50	P ₁ -90,91, 92,94		P - No change. N - No change.
9 (849)	C/3	40°C	N ₁ -71,72,73, 74,75	P ₁ -73,74, 75,77		P - Blisters & pimples, some spalling of active material. N - Good, some black scum.
2 (849)	C/5	40°C	N ₁ -6,7,8, 9,10	P ₁ -5,6, 7,8.		P - Badly blistered, much loose black material. N - Good, black scum.

Figure 3.2 shows an unformed positive electrode. The features of interest are the regular distribution of sinter structure (white areas), active material (light gray), porosity (black or dark gray), and thickness of the nickel plate on the steel core plate (approximately 0.4 mils). Also apparent is a small hole near the electrode surface which may be a precursor to a pimple or blister. Only one was seen on this sample.

Finally, there is a crack or discontinuity in the sinter structure. It is termed an "incipient crack" to differentiate it from the type of cracks seen on cycled or a simply fully charged plate also examined.

Figure 3.3 is a photomicrograph of a positive plate which was cleaned, characterized and fully charged (average characterization capacity = 1158 ma. hrs.). There was no macroscopic peculiarity prior to preparation for microscopic examination.

The characterization cycling was not enough to enlarge the porosity but it did succeed in opening up cracks within the electrode. Moreover, some attack on the nickel plate of the skeleton can be seen. The large black areas were not fully impregnated and sinter structure was probably removed during polishing.

Figure 3.4 is a photomicrograph of a positive plate cycled at 40°C. The nickel plate thickness in the punched part of the steel core was fairly typical of all electrodes examined.

However, the plate thickness adjacent to the sinter structure on the 40°C plates was considerably reduced in thickness to 0.1 mil. Loss of physical contact with the sinter structure can also be seen on these plates in contrast to the others. Generally, there is an increase of porosity with some portions completely lacking sinter structure. Two pimples can be seen. One is the section through the pimple and one is the top of an adjacent protrusion. The difference in density of sinter structure of these pimples with that seen in the positive uncycled plate, Figure 3.2, is quite striking and suggest corrosion of the structure as the pimple enlarged. The oxidation of sinter structure may contribute to the recharacterization capacity in some cycled plates even though in some cases there was a significant loss of active material during disassembly of the test cells.

3.2.1.2 X-ray Examination of Shallow Discharge Cycle Test Electrodes

X-ray diffraction patterns from 4-45°, 2θ using CuKα radiation (Zr filter) with a G. E. Model XRD-3 were taken of one each of the positive and negative plates from each cell. These electrodes were kept in the cells until just prior to the examination. To prevent artifact formation, all samples were sealed wet and unwashed in 0.5 mil Profax* film envelopes during analysis.

*Biaxially oriented polypropylene film, Hercules Powder Company.

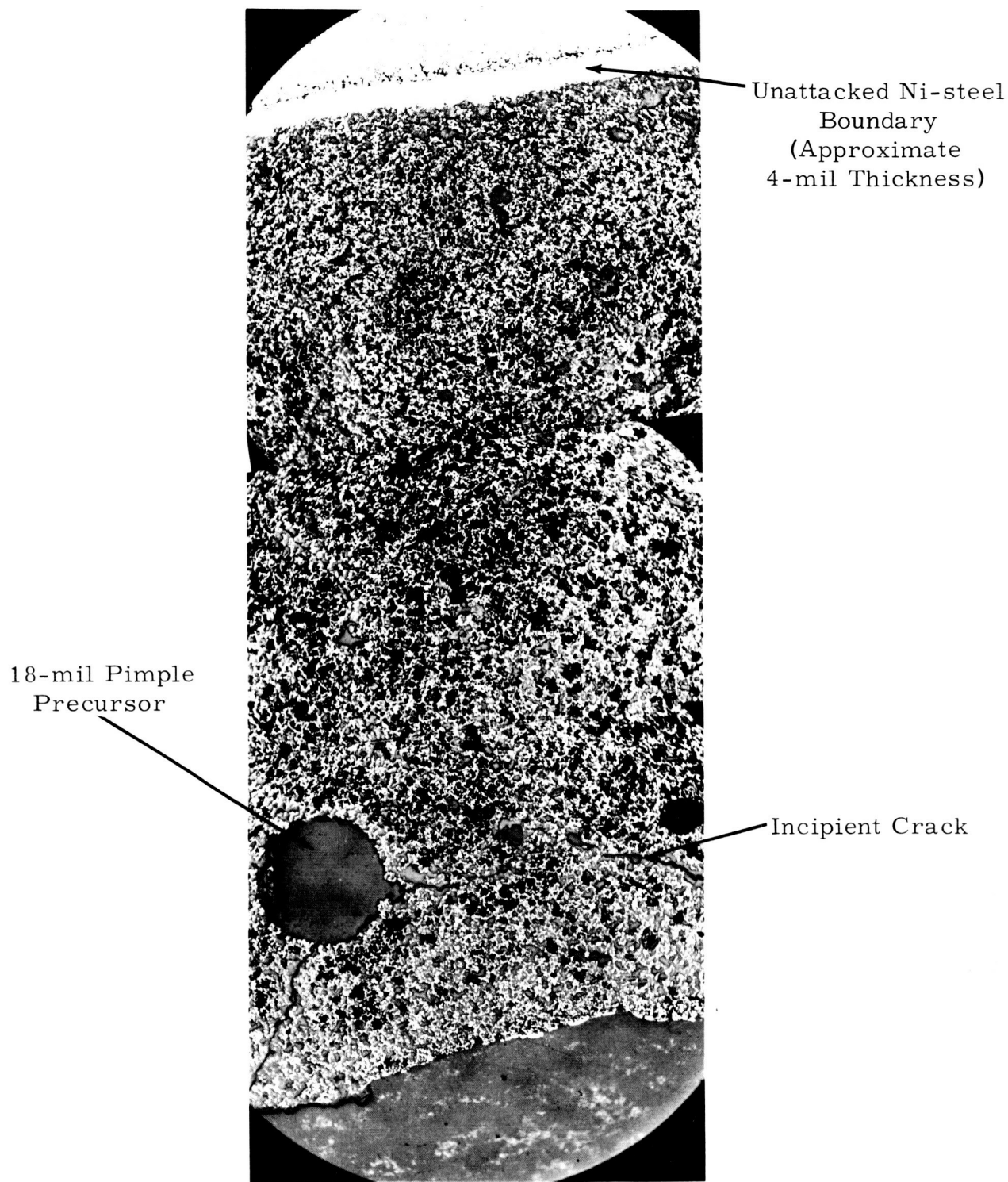


Figure 3. 2. Photomicrograph - Positive Unformed Nickel Electrode - 45X, 2% Nital Etchant.

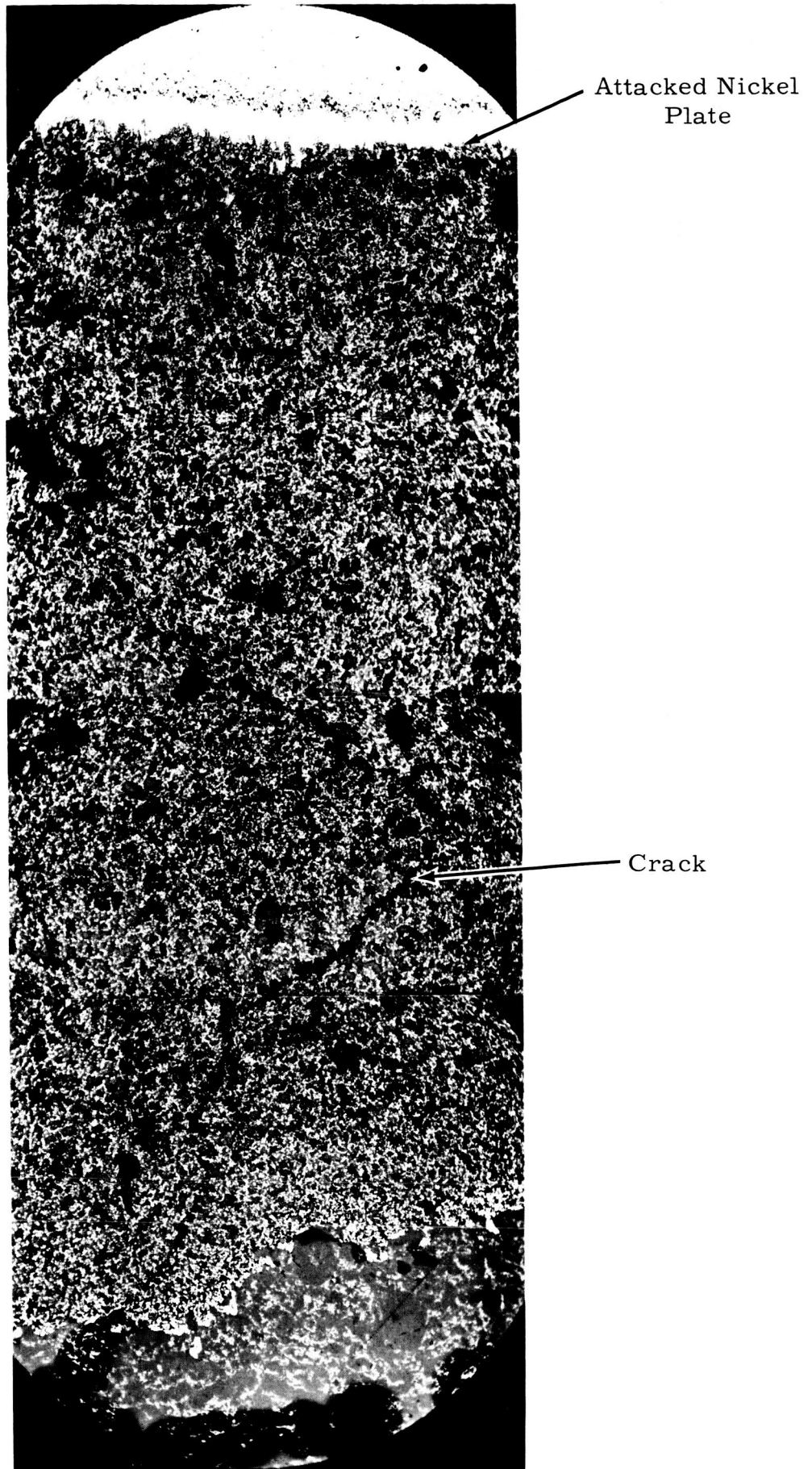


Figure 3.3. Photomicrograph - Positive Fully Charged Uncycled Electrode - 45X, 2% Nital Etchant.

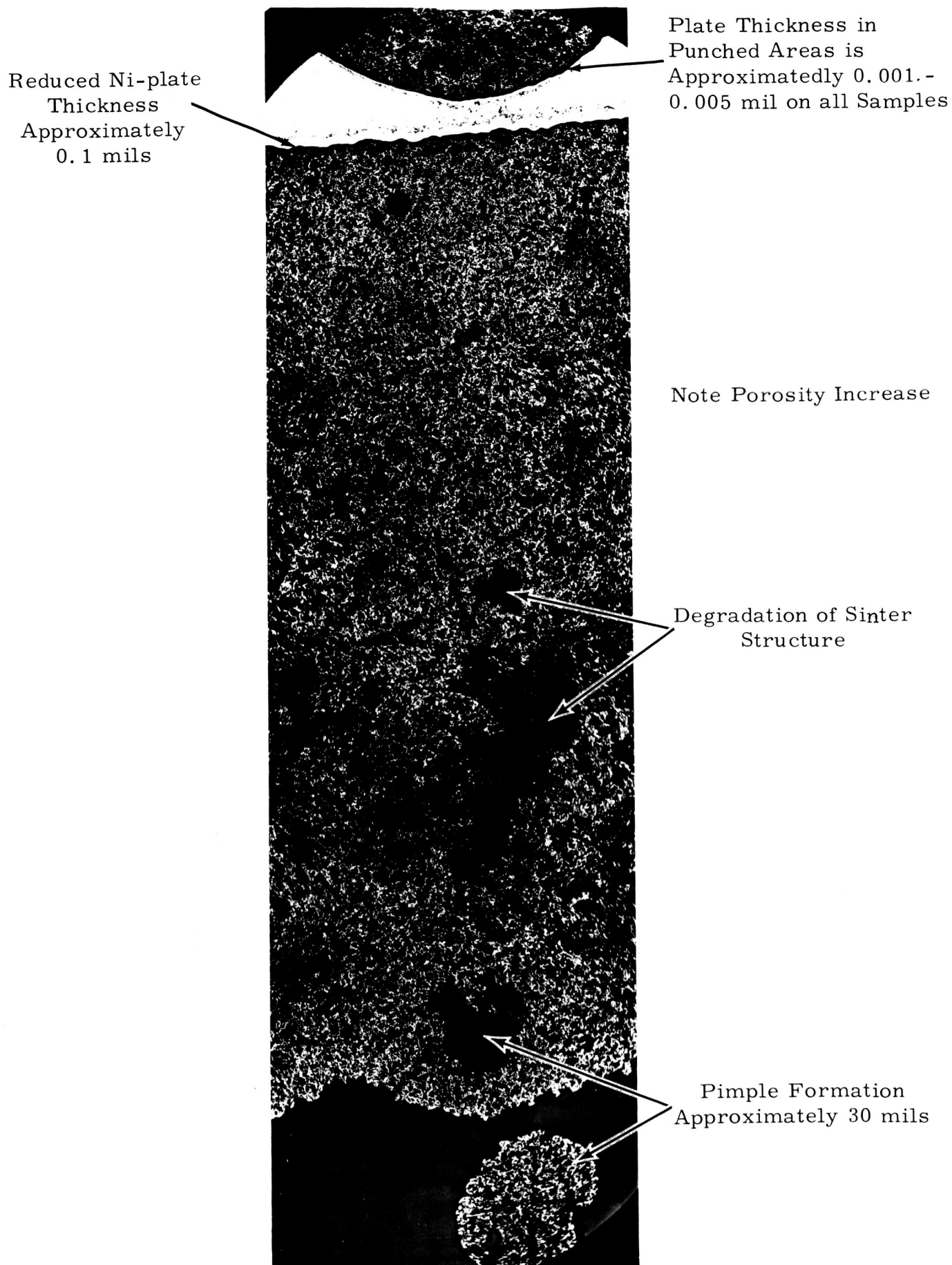


Figure 3.4. Photomicrograph - Positive Electrode from 40°C Shallow Discharge Cycling Cell - 45X, 2% Nital Etchant.

Peak heights of specific angles of interest were measured and recorded in Table 3.2 for the positive test electrodes. The peak heights of a fully charged and a fully discharged positive electrode are also shown for reference. Those shown are of one pair of plates and are typical of but not identical to those of other plates in the same charge condition. Relative values are proportional to the surface composition of the area examined. They vary from sample to sample and, to a lesser degree from one area to another on the same plate.

No unusual peaks (other than NiOOH , $\text{Ni}(\text{OH})_2$, Ni) were found in any of the plates examined. It was possible to make only a rough estimate of state of charge from the X-ray data. No orientation of substrate or active material was unequivocally established.

Peak heights of interest in the negative test electrodes are recorded in Table 3.3 together with those of a fully charged and a fully discharged plate. No unusual peaks or orientation of materials were observed. There was no correlation of peak height ratios with state of charge nor did the $\text{Ni}/\text{Cd}(\text{OH})_2$ peak height ratios suggest extrusion of active material over the cycling history of the electrodes.

3.2.1.3 X-ray Examination of Shallow Discharge Cycling Test Separator Material Results

The felted nylon separator material suffered some degradation in that some of the fibers adhered to the electrodes and tore the separator on pulling the electrode and separator apart. There seemed to be no correlation between the 0° and 25°C test conditions and degree of degradation. The extent of this type of degradation was greater in two of the 40°C test cells in spite of the shorter testing time involved. In these cells, the separator was extensively torn in the disassembly of the cell. In two cells (CC#'s 1 and 6), the separator was burned through in the short circuit areas. The separator material showed little or no signs of degradation in the other cells.

Separator material samples from each cell were also examined on the positive and negative electrode sides by X-ray diffraction. Cadmium hydroxide deposits were found on both sides of each sample although the diffraction intensity varied considerably from area to area. This finding was true on all samples tested and not restricted to the shorted out cells. The beam intensity was held at a minimum to reduce penetration of the beam into the nylon separator material.

TABLE 3.2 - X-RAY DIFFRACTION DATA FOR NICKEL-TEST ELECTRODES

Nickel Electrode	Peak Heights - Inches from Peak to Background										Residual* Capacity (ma hrs)
	Angle(°2θ)	20.0°	23.1°	15.2°	17.6°	29.3°	Peak Height Ratios				
	d-Space(A°)	2.04	1.77	2.69	2.40	1.40	23.1°	20°	17.6		
Cmpd	Nickel	Metal	Nickel Hydroxide	B-NiOOH	17.6°	23°	15.2				
Plane(hkl)	(111)	(200)	(100)	(101)	(110)						
Fully Charged	6.5	3.5	-	0.3	0.25	11.7	1.87	-			1200
Fully Discharged	6.5	3.75	0.5	1.5	-	2.5	1.74	3.0			0
#4- 0°C/2078 cycles P ₁ -27	5.4	3.0	0.2	0.5	-	6.0	1.80	2.5			188
#3- 25° C/2660 cycles P ₁ -22	3.6	2.15	-	0.30	0.20	7.15	1.68	-			1138
#5- 25°C/2660 cycles P ₁ -45	7.05	3.50	0.15	0.70	-	5.0	2.02	4.7			230,317,263
#9- 40°C/849 cycles P ₁ -75	7.4	4.25	0.40	1.10	-	3.86	1.74	2.75			0
#7- 40°C/849 cycles P ₁ -91	8.1	4.0	0.2	0.50	-	8.0	2.03	2.5			363
#2- 40°C/849 cycles P ₁ -7	4.9	3.2	0.35	0.80	-	4.0	1.53	2.3			0

*Capacity of companion plate

TABLE 3.3 - X-RAY DIFFRACTION DATA FOR CADMIUM TEST ELECTRODES

Cadmium Electrode	Peak Heights - Inches from Peak to Background										*Residual Capacity (ma hrs)		
	Angle 2θ	Nickel Metal					Cadmium Hydroxide						
		d-Spacing (Å)	(111)	(200)	(101)	(002)	(100)	(101)	(159°)	(101)		(101)	Peak Height Ratios
Fully Charged	20.0°	23.1°	17.3°	14.5°	13.4°	1.1	2.1	2.1	1.89	3.16	1.9	0.268	1300
Fully Discharged	2.04	1.77	2.35	2.81	3.03	1.5	2.8	1.88	1.0	1.87	7.5	0	
#4 - 0°C/2078 cycles N ₁ -27	6.0	3.4	1.9	0.7	3.0	5.0	1.77	4.28	1.67	1.58	781		
#3 - 25°C/2660 cycles N ₁ -23	2.45	1.45	5.7	1.7	1.2	2.0	1.69	3.35	1.67	0.21	1373,1383		
#5 - 25°C/2660 cycles N ₁ -45	6.1	3.45	1.8	0.7	3.6	4.5	1.77	2.58	1.73	2.0	289,312		
#9 - 40°C/849 cycles N ₁ -71	6.4	3.5	2.45	0.25	3.9	5.9	1.84	10	1.51	1.59	763		
#7 - 40°C/849 cycles N ₁ -49	4.8	3.2	1.1	0.3	2.8	5.8	1.50	3.66	2.07	2.54	583		
#2 - 40°C/849 cycles N ₁ -9	2.8	3.15	1.45	0.6	4.3	6.9	1.13	2.43	1.6	2.97	538		
After Storage in N ₂	4.3	3.6	2.1	0.9	5.7	>10	1.20	2.33	<1.76	2.71	538		

*Capacity of companion plate

In addition to the unsuspected cadmium hydroxide on the separator material, there was considerable black magnetic residue on the positive side of several pieces. The black residue had strong nickel and nickel hydroxide peaks. Very little black material was visible on the cadmium side of the material.

3.2.2 Electrochemical Test Results

Electrochemical tests performed on the shallow discharge tests consisted of determining the residual capacities of the plates as described in Section 3.1 and recharacterizing the test electrodes at the C/10 rate and comparing the results with the original characterization as discussed in Section 2.0. Residual capacity and recharacterization tests were made only on electrodes from unshorted cells.

3.2.2.1 Residual Capacity Test Results

The residual discharge capacities of the positive and negative shallow discharge cycling test electrodes respectively are listed in Tables 3.4 and 3.5. One 25°C test cell (#3) received an extra charge before removal from cycling test program.

Except for that cell, the constant current positive electrode capacities (expressed as per cent of characterization capacity) tended to be higher at 25°C than at 0°C with approximately the same number of cycles. One test electrode at 40°C had the same residual capacity as the 25°C electrodes but also the fewest number of cycles. However, three out of four electrodes at 40°C showed zero capacity.

The negative electrodes had a higher residual capacity at 0°C than at 25°C while the 40°C test electrodes were about the same as the 0°C test electrodes although with fewer cycles.

In general, the negative electrode residual capacities were as high or higher than the positive electrodes tested. There was no evident relation of residual capacity with shallow discharge cycling test temperatures. There is insufficient data to draw any conclusions with respect to the effect of the number of cycles.

3.2.2.2 Comparison of Characterization and Recharacterization Capacities

The characterization and recharacterization data for the positive shallow discharge cycling test electrodes are listed in Table 3.6. The range of change between the average characterization and recharacterization capacities was from -23.4% to +13.7% of original capacity with no correlation with temperature

or number of test cycles. The % spread* of high to low values for any one electrode ranged from 0-13% on characterization to 9-25% on recharacterization with no temperature or number of test cycles correlation. The characterization capacities were relatively constant through six cycles but the recharacterization values tended to decrease with successive cycles and also showed more scatter than the characterization data.

The characterization and recharacterization data for the negative shallow discharge cycling test electrodes are listed in Table 3.7. The range of change between the average characterization and recharacterization capacities was from -16.6 to +32.5% with no correlation with temperature or number of test cycles. The % spread of high/low values for any one electrode ranged from 0-41% on characterization to 7-34% on recharacterization with no correlation with temperature or number of test cycles. Most characterization capacities tended to remain constant through six cycles but the recharacterization values tended to decrease with successive cycles.

3.2.2.3 Comparison of Graphitic and Nitrate Steps on Characterization and Recharacterization

The origin and significance of the graphitic and nitrate reduction steps were discussed in Section 2.3. A compilation of these capacities for the positive shallow cycling test electrodes is shown in Table 3.8.

On characterization the spread of graphitic capacities over six cycles ranged from a low of 50-80 ma-hrs. to a high of 238-254 ma-hrs. Most individual electrodes showed a trend to higher graphitic capacities on successive cycles. On recharacterization, the spread was from a low of 24-76 to a high of 99-153 ma-hrs. The trend was toward a higher capacity on successive cycles. In most cases, the graphitic capacities decreased after cycling tests. There was no correlation of graphitic capacities or changes of graphitic capacity with characterization capacities or changes of characterization capacities after cycling. The nitrate steps behaved in a similar fashion. Low to high ranges on characterization were from 0-0 to 14-17 ma-hrs. On recharacterization, the values ranged from a low of 0-2 to a high of 0-12 ma-hrs. In general, the initial characterization capacities were higher than the recharacterization capacities. The trend in both was toward higher values with successive cycles. There was no correlation of changes in graphitic or nitrate reduction steps with temperature or number of cycles.

*% spread refers to the difference between the high and low values of any given characterization run divided by the low value.

3.2.2.4 Disposition of Test Plates

Most of the positive plates exhibited extensive pimpling and were not returned to the shallow discharge cycling test as originally planned. These were replaced by KO-15 plates for reasons discussed in Section 2.6. Some of the SAFT positive plates were in "satisfactory" condition and were returned to the testing program.

None of the negative plates suffered obvious physical degradation and with a few exceptions, all were returned to testing program. Exceptions were those plates which were damaged in disassembly and those which were cut apart for x-ray examination.

The new shallow cycle test cells were mounted in sealed cells fitted with pressure gauges and relief valves designed to vent excess pressure at 50 psi \pm 5%. The disposition of electrodes in these cells compared with those in the unvented cells is given in Table 3.9.

No provision was made in these cells to replenish water consumed in electrolysis. It was expected that they would evolve oxygen until some maximum pressure was reached at which point the rate of gas evolution would be equaled by the rate of recombination with the cadmium plates. In the event of cell failure, by-pass switches were included that would permit any number or combination of cells to be removed from the circuit without affecting the others. This also would permit cells to be removed and to be examined periodically rather than all at the same time.

After the cells had been cycling for a few weeks, however, the cells started to dry out one by one. By the end of four weeks in the sealed cases, all the cells had dried out completely. Some showed burn marks visible from the outside of the case. The 0°C cells dried out first but there was no order at 25° and 40°C. Because of the degree of uncertainties associated with these cells, no further examination of these electrodes was made. The water apparently was lost by venting of the cell during cycling.

TABLE 3.4

Residual Capacity-Positive Shallow Discharge Cycling Test Electrodes

<u>Temp.</u> <u>°C</u>	<u>Cell</u>	<u>Electrode</u> <u>No.</u>	<u># cycles</u>	<u>Resid. Cap.</u> <u>Const. Cur.</u>	<u>Const. Load</u>	<u>%* of Char. Cap.</u> <u>(Rechar)</u>
0	#4	P ₁ -28	2078	163	25	13.8 (14.3)
25	#3	P ₁ -23**	2660	1100	38	
	#5	P ₁ -43	2579	230	--	
	#5	P ₁ -46	2579	256	61	23.7 (21.8)
	#5	P ₁ -49	2579	263	87	23.2 (22.7)
40	#9	P ₁ -77	849	0	0	
	#7	P ₁ -92	849	300	63	21.6 (27.9)
	#2	P ₁ -6	849	0	0	
	#2	P ₁ -8	849	0	0	

*Residual Capacity at constant current as per cent of characterization or recharacterization capacity.

**Electrodes from Cell #3 received an extra charge before being removed from the Shallow Discharge Cycling test program.

Table 3.5

Residual Capacities-Negative Shallow Discharge Cycling Test Electrodes

<u>Temp.</u> <u>°C</u>	<u>Cell</u>	<u>Electrode</u> <u>No.</u>	<u>#cycles</u>	<u>Resid. Cap.</u> <u>Const. Cur.</u>	<u>Const. Load</u>	<u>%* of Charc. Cap.</u> <u>(Rechar.)</u>
0	#4	N ₁ -26	2078	730	51	52.5 (51%)
25	#3	N ₁ -24**	2660	1347	26	
	#3	N ₁ -25**	2660	1338	45	
	#5	N ₁ -42	2579	244	45	23.0 (18.8)
	#5	N ₁ -43	2579	271	41	28.2 (21.2)
	#5	N ₁ -44	2579	200	--	
40	#9	N ₁ -72	849	730	33	57.4 (59)
	#7	N ₁ -50	849	524	59	47.3 (40.4)
	#2	N ₁ -10	849	528	16	43.5 (43.0)

*Same as Table 3.4

**Electrodes from Cell #3 received an extra charge before being removed from the Shallow Discharge Cycling test program.

TABLE 3.6

COMPARISON OF CHARACTERIZATION AND RECHARACTERIZATION DATA FOR POSITIVE TEST ELECTRODES

Electrode Number	Cycles	Test Temp.	Cycle No.						Average Ma. Hrs.	Per cent(1) Change	
			1	2	3	4	5	6			
P ₁ -28	2078	0°C	* 1190 **(1170)	1170	1180	1180	1180	1180	1180	1182 1139)	-3.5%
P ₁ -23	2660	25°C	1140 (1035)	1130	1140	1140	1140	1140	1140	1138 1033)	-9.0%
P ₁ -24	2660	25°C	1050 (1075)	1050	1050	1040	1040	1050	1050	1048 1042	-0.5%
P ₁ -43	2579	25°C	1060 (1150)	1060	1060	1060	1060	1060	1060	1060 1143)	+9.0%
P ₁ -46	2579	25°C	1190 (1170)	1060	1060	1060	1060	1060	1060	1082 1173)	+8.8%
P ₁ -49	2579	25°C	1060 (1220)	1125	1125	1125	1125	1190	1190	1133 1160)	+2.5%
P ₁ -77	849	40°C	1230 (1170)	1140	1260	1260	1260	1290	1230	1235 1123)	-9.0%
P ₁ -90	849	40°C	1270 (1270)	1300	1220	1220	1290	1290	--	1274 1215	-4.7%
P ₁ -92	849	40°C	1375 (1100)	1395	1320	1320	1385	1415	1475	1394 1067)	-23.4%
P ₁ -6	849	40°C	1155 (1250)	1155	1158	1158	1158	1155	1155	1155 1313)	+14.3%
P ₁ -8	849	40°C	1210 (1030)	1190	1190	1190	1210	1190	1225	1203 1060)	-11.7%

(1) % Change is difference between the average characterization and recharacterization capacities divided by the average characterization capacity expressed in per cent.

*Characterization capacity.

**Recharacterization capacity.

TABLE 3.7

COMPARISON OF CHARACTERIZATION AND RECHARACTERIZATION DATA FOR NEGATIVE TEST ELECTRODES

Electrode Number	Cycles	Test Temp.	Cycle No.						Average Ma. Hrs.	Per cent(1) Change
			1	2	3	4	5	6		
N ₁ -26	2078	0°C	* 1400 **(1490)	1390	1400	1390	1390	1390	1393 1433)	+2.8%
N ₁ -21	2660	25°C	1400 (1300)	1400	1390	1290	1290	1390	1393 1203)	-13.6%
N ₁ -22	2660	25°C	1390 (1190)	1390	1375	1390	1385	1355	1381 1152)	-16.6%
N ₁ -24	2660	25°C	1390 (1410)	1390	1385	1390	1390	1350	1383 1298)	-6.1%
N ₁ -25	2660	25°C	1390 (1480)	1390	1385	1385	1320	1390	1377 1378)	+0.1%
N ₁ -41	2579	25°C	1060 (1150)	1060	1060	1060	1060	1060	1060 1345)	+26.9%
N ₁ -42	2579	25°C	1060 (1400)	1125	1060	1060	1060	1000	1061 1300)	+22.5%
N ₁ -43	2579	25°C	750 (1320)	1060	1000	940	1000	1000	962 1275)	+32.5%
N ₁ -44	2579	25°C	810 (1320)	1060	1060	1060	1060	1000	1008 1297)	+28.7%
N ₁ -72	849	40°C	1405 (1300)	1345	1170	1170	--	--	1273 1238)	-2.7%
N ₁ -50	849	40°C	1060 (1410)	1090	1090	1125	1125	1125	1103 1298)	+17.7%
N ₁ -10	849	40°C	1315 (1320)	1275	1245	1190	1140	1140	1218 1230)	+1.0%

(1) % Change is the difference between the average characterization and recharacterization capacity.
 *Characterization capacity.
 **Recharacterization value.

TABLE 3.8

COMPARISON OF GRAPHITIC AND NITRATE STEPS ON POSITIVE SHALLOW CYCLING TEST ELECTRODES

Electrode Number	Cycles	Test Temp.	Graphitic Step			Ma. Hrs.			Nitrate Reduction Step - Ma.Hrs.***					
			1	2	3	4	5	6	1	2	3	4	5	6
P ₁ -28	2078	0°C	* 48 **(32)	112 67	112 80	110 84	112 80	105 88)	14 (0	14 2	14 4	14 2	17 2	17 2)
P ₁ -23	2660	25°C	63 (24	66 58	73 67	80 72	87 75	87 76)	11 (0	14 4	14 7	14 10	14 10	17 10)
P ₁ -24	2660	25°C	91 (40	98 96	102 114	105 127	112 120	116 131)	7 (0	10 2	7 2	7 4	7 7	7 7)
P ₁ -43	2579	25°C	50 (72	75 115	70 122	75 126	50 129	80 129)	- (0	10 4	10 4	5 4	5 4	5 4)
P ₁ -46	2579	25°C	- (28	50 67	75 70	75 73	100 87	100 92)	- (-	- -	- 4	5 7	5 7	5 4)
P ₁ -49	2579	25°C	120 (99	200 131	200 140	180 147	200 153	200 147)	- (0	- -	- 4	- 7	- 4	- 7)
P ₁ -77	849	40°C	130 (91	130 104	135 112	144 116	139 126	126 120)	- (0	- -	- 4	- 7	- 4	- 4)
P ₁ -90	849	40°C	110 (91	132 112	132 126	147 140	158 150	172 154)	14 (0	15 4	16 4	16 7	15 7	15 7)
P ₁ -92	849	40°C	110 (19	133 27	131 33	144 40	150 47	150 56)	10 (0	- 8	10 8	- 8	0 10	0 8)
P ₁ -6	849	40°C	238 (16	252 37	242 53	244 59	252 59	254 63)	14 (0	14 8	20 8	14 8	20 11	- 12)
P ₁ -8	849	40°C	106 (11	126 21	126 24	131 32	140 35	140 37)	14 (0	14 8	14 8	14 8	14 8	14 12)

*Characterization Capacity ** Recharacterization Capacity
 ***"0" - No indication of nitrate reduction step
 "-"- - Visible but not measurable indication

TABLE 3.9

DISPOSITION OF SHALLOW-DISCHARGE TEST ELECTRODES
IN SEALED TEST CELLS

Test	Temp.	Vented Cells		Sealed Cells	
		Cadmium	Nickel	Cadmium	Nickel
#4	0°C	N ₁ -26,27 28,29,30	P ₁ -25,26 27,28	N ₁ -26,28,29 30; N-71	P-61,62 79,80
#6	0°C	N ₁ -51,52,53 54,55	P ₁ -53,54 57,61	N ₁ -61,62,63 64,65	P ₁ -63,64 65,66
#8	0°C	(Electrolyte leaked cell not examined)		N-86,87,88 89,90	P-86,87 89,90
#5	25°C	N ₁ -41,42,43 44,45	P ₁ -43,45 46,49	N ₁ -41,42,43 44; N-81	P-81,82, 83,84
#3	25°C	N ₁ -21,22,23 24,25	P ₁ -21,22 23,24	N ₁ -21,22,24 25; N-72	P-63,64 65,66
#1	25°C	N ₁ -1,2,3, 4,5	P ₁ -1,2, 3,4,	N-73,74,75 76,77	P-67,68 69,70
#7	40°C	N ₁ -46,47,48 49,50	P ₁ -90,91 92,94	N ₁ -46,47,48 N-82	P ₁ -90,92,94 P-8
#9	40°C	N ₁ -71,72,73 74,75	P ₁ -73,74 75,77	N ₁ -72,73,74 75; N-85	P ₁ -73,74,77 P-88
#2	40°C	N ₁ -6,7,8 9,10	P ₁ -5,6 7,8	N ₁ -6,7,10 N-83,84	P-75,76 77,78

4.0 RANDOM DEPTH OF DISCHARGE CYCLING TESTS

These tests were designed to determine the effect of cell operation in which the average or mean depth of discharge for all cycles over a period of a week was fixed at pre-determined levels of 10, 25, 50, and 75%. At each level, the depth of discharge for a given cycle was selected on a random basis. Two types of distribution for the depth of discharge of individual cycles over the period of a week were used: one based on a Beta distribution and the other a rectangular distribution.

The use of random cycling was an attempt to simulate more closely the actual operation of secondary cells in practical applications in contrast to the more artificial operation in regular charge and discharge cycles. It was also felt that the onset of memory would be delayed or avoided by this type of cycling. Any correlation of properties with the depth of discharge would be based on the average depth of discharge in this type of cycling. In order to establish a reliable analysis of the effect of depth of discharge and number of cycles on the operation of the cells and electrodes, the spread and distribution of the depths of discharge should be controlled, and the sequence of the tests randomized over a substantial time period. This control of the randomization of the cycling was performed by arranging the experiments on a known statistical basis.

It was apparent at the beginning that two general distributions should be studied since these correspond to actual use situations in applying cells. Thus, the cells are often used in a manner that suggests that the frequency of a given depth of discharge falls off rapidly as the deviation of the depth of discharge from the average increases; e.g. the chance of having a large deviation of depth of discharge is much smaller than a small deviation, but that a large deviation does occur with some finite probability. This type of distribution is closely simulated by the Beta distribution about the average. The skewness arises from the fact that there are absolute limits on the depth of discharge e.g. zero and 100%, hence any average depth of discharge cannot have a normal distribution about the average.

The rectangular distribution is based on the fact that applications occur in which the cells are discharged within prescribed limits, but the probability of any depth of discharge within these limits is the same as for any other depth of discharge occurring. Thus a cell may be discharged an average depth of discharge of 50% within the limits of 35% to 65% depths of discharge. The name rectangular arises from the plot of frequency vs. depth of discharge.

The generation of the distributions for these functions was done by the statistical group in the laboratory. The Beta distribution is defined by:

$$f(x) = \frac{\Gamma(p+q)}{\Gamma(p)\Gamma(q)} (1-x)^{p-1} x^{q-1} \quad 0 \leq x \leq 1$$

whose shape is determined by the parameters p and q . The parameters can be uniquely specified from a knowledge of the desired mean and standard deviation (a measure of dispersion about the mean) as follows:

$$\bar{x} = \frac{q}{p+q}$$

$$\sigma^2 = \frac{pq}{(p+q+1)(p+q)^2}$$

where \bar{x} is the mean depth of discharge we wish to simulate and σ^2 is the square of the standard deviation which measures the variability of the individual depth of discharge about the mean.

The mean depth of discharges are assumed; hence only the standard deviations need be determined. It was reasoned that the spread about the mean would be directly proportional to the mean, i.e., the higher the depth of discharge, the higher the dispersion about the mean depth of discharge. It was further assumed that this relationship, expressed in terms of the coefficient of variation σ/\bar{x} , would be a constant, c . The value of $c = 1/4$ was chosen. Table 4.1 shows the mean, variance, p and q of the four depth of discharges. Due to the method of generating the Beta variables, $2p$ and $2q$ were required to be integers. This caused a small deviation from the desired values of σ and is shown in Table 4.1.

There is no simple, direct method for generating random variables from a Beta distribution since the integral,

$$\int_0^a (1-x)^{p-1} x^{q-1} dx \quad 0 \leq a \leq 1$$

cannot be evaluated by elementary methods. However, it is known from statistical theory that the variable

$$z = \frac{\sum_{i=1}^n w_i^2}{\sum_{i=1}^n w_i^2 + \sum_{i=1}^{n+m} w_i^2}$$

where w_i ($i=1,2,\dots,m+n$) are independent variables each generated from a normal distribution with mean zero and variance one, has a Beta distribution with parameters $p = \frac{m}{2}$ and $q = \frac{n}{2}$. (See Appendix III for derivation). The w_i can be obtained from standard random normal deviate tables, or as in this case generated on a digital computer.

The generated sets of z 's (200 for $\mu = .10$, 100 for $\mu = .25$, 50 for $\mu = .50$, and 25 for $\mu = .75$) can be used to simulate random depth of discharges based on the Beta distribution model.

The random discharge distributions for the Beta function and the rectangular function are shown in Figures 4.1, 4.2 for the mean values of 10 to 75%.

4.1 Experimental Equipment and Procedure

The cycling control equipment schematic for this series of test is shown in Appendix I. The individual charge and discharge of each group of cells to be operated at the desired average depth was controlled by means of a tape programmed with the distributions shown in Figures 4.1 and 4.2 with slight modifications.

The modification arose from changes made in the control equipment. The original stepping-relays proved to be short-lived in use and were replaced with double pole double throw relays. This modification made it impossible to retain the originally programmed rest periods between charge and discharge. In effect this led to a larger number of events per week than originally anticipated. The revised program is compared with the original in Table 4.2. The revised program tape cycle was six days and 18 hours rather than the originally planned 7-day cycle.

The test cells for these tests contained one positive and two negative electrodes. One cell was used at each average depth of discharge temperature level.

The cycle conditions for these tests were to charge at 100 ma ($\sim c/10$ rate) and to discharge at 200 ma ($\sim c/5$ rate). The amount of overcharge varied from 20 to 50% of the previous discharge depending on the average depth of discharge. These values are given in Table 4.3.

The cells were cycled for a period of approximately five weeks, after which the cells were removed from the cycling in the charged condition. The cells were checked for no load potential and then disassembled for visual inspection.

TABLE 4.1

PARAMETERS FOR RANDOM DEPTH OF DISCHARGE DISTRIBUTION CURVES

Average Depth Discharge	Standard Deviations					
\bar{x}	σ^*	σ^{**}	p	q	m	n
.10	.0250	.0253	126	14	252	28
.25	.0625	.0619	36	12	72	24
.50	.1250	.1213	8	8	16	16
.75	.1875	.1936	1	3	2	6

*nominal value of

**actual value of

TABLE 4.2

REVISED RANDOM DEPTH OF DISCHARGE PROGRAM

	10%	25%	25%	50%	50%	75%
	β	β	Rect.	Rect.	β	β Dis.
#Event-Cycles Original	67	29	29	15	15	11
Av. Depth Dis. Original	9.76%	26.2%	25.6%	51.3%	50.7%	75.4%
#Event-Cycles Revised	95	36	34	19	19	13
Av. Depth Dis. Revised	9.8%	25.9%	26.7%	29.3%	51.2%	71.5%

Random Discharge Distributions

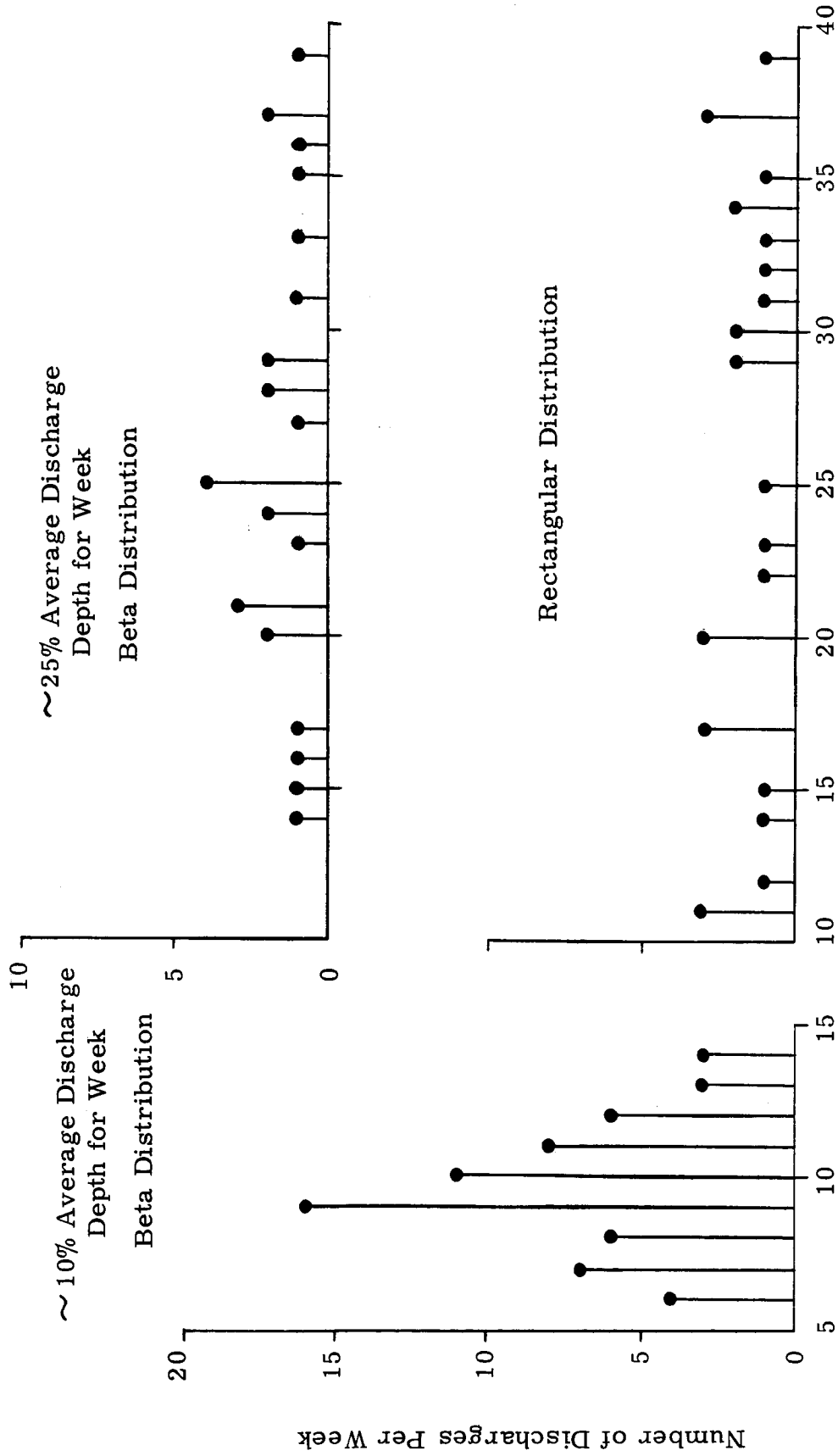


Figure 4. 1.

Percent Depth of Discharge - Individual Cycle

Random Discharge Distributions

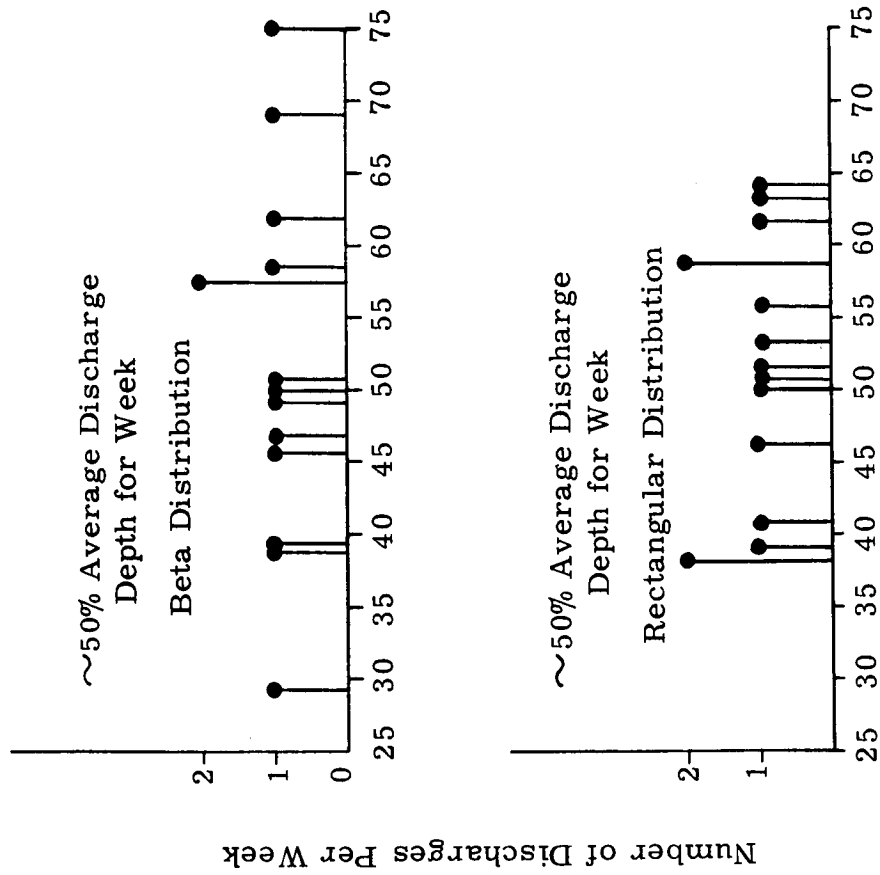


Figure 4.2.

Percent Depth of Discharge - Individual Cycle

The residual capacity of one positive and one negative electrode from each cell was measured by discharging the electrode in a cell containing a fully charged electrode of opposite polarity. The discharge was conducted in two parts, the first at a constant current of 460 ma down to a cell potential of 0.6 V and the second at a constant resistance load of 10 ohms to a cutoff voltage of 0.1 V.

These electrodes were then recharacterized and the curves compared with the original characterization curves to note changes in capacity, graphitic capacity and nitrate reduction steps.

None of the electrodes from these tests were examined by x-ray diffraction since the results from the previous studies in Section 3.0 showed this technique to be of limited analytical value.

None of the electrodes were examined by photomicrography because of the lack of time.

4.2.0 Results

The data on electrodes used in these tests at the various temperature and discharge levels are summarized in Table 4.3. There were a total of seven cell failures by shorting, three of these were at 0°C and four at 25°C. In this section as all others, a shorted cell is defined as one having no measurable potential upon removal from the cycling tests after the last charge interval. The cause of these shorts has not been identified. The plates were never dried out by loss of water, however, concentration changes cannot be ruled out as a contributing factor since water makeup was done on a weekly basis. There was no detectable correlation of failures with either depth of discharge or number of cycles. The lack of cell failures at 40°C is noted but unexplainable.

4.2.1 Visual Examination

The appearance of the electrodes after cycling is summarized in Table 4.4. Generally the positive electrodes at 0° and 25°C were free of pimples, and the majority of the electrodes at 40°C showed moderate extent of pimples. All of the negative electrodes, except three, showed no change from the uncycled condition. The three electrodes had a dull black surface in contrast to the dull gray color of uncycled plaques.

The degree of separator degradation compared to that observed in the shallow discharge cycling tests was markedly less.

4.2.2 Electrochemical Test Results

4.2.2.1 Residual Capacity Test Results

The residual capacity measurements for positive and negative electrodes are summarized in Table 4.5.

All of the positive electrodes showed residual capacities, even in those cells which showed no potential upon removal from the cycling tests after the last charge interval. In these shorted cells the negatives had zero residual capacity. All other negative electrodes showed residual constant current capacities that tended to be greater than the positive electrodes. Since many of the cells had shorts, no significance is attached to trends in residual capacity versus depth discharge.

The constant load residual capacities of the positive electrodes are of the same order of magnitude as the graphite capacities determined during recharacterization.

There was no detectable dependence of residual capacities on original characterization capacities.

4.2.2.2 Comparison of Characterization and Recharacterization Capacities

The characterization and recharacterization data for the positive random depth of discharge cycling test electrodes is listed in Table 4.6. The range of change between the average characterization and recharacterization capacities was from -22.7% to +9.4% of original capacity with no correlation with depth of discharge. The change in capacity expressed as a percentage of the original average characterization capacities was dependent on the temperature. These trends are shown for both positive and negative electrodes in Figure 4.3. Note that the number of cycles decreases with increasing depth of discharge.

Table 4.7 is a compilation of characterization and recharacterization data for the negative random depth of discharge cycling test electrodes. The range of change between the average characterization and recharacterization capacities was from -17.6 to +3.5% with no correlation with the depth of discharge. The dependency of the change in capacities as a percentage of the original average characterization capacities with temperature is shown in Figure 4.3.

The positive electrodes at 0° and 25°C used in these tests were of the KO type. There was no noticeable difference in capacity changes for these compared to the VO positives. It is also noted that all shorted cells were ones containing KO plates. No comment can be made with respect to the significance of this observation.

4.2.2.3 Comparison of Graphitic and Nitrate Steps on Characterization and Recharacterization

The origin and significance of the graphitic and nitrate reduction steps were discussed in Section 2.3. A compilation of these capacities for the positive test electrodes is listed in Table 4.8.

On characterization, the spread of graphitic capacities over six cycles ranged from a low of 69-107 ma-hrs. to a high of 258-290 ma-hrs. Most individual electrodes showed a trend to higher capacities on successive characterization cycles. On recharacterization, the spread was from a low of 13-101 to a high of 139-209 ma-hrs. The trend was toward a higher capacity on successive cycles. In all cases, the graphitic capacities decreased after the cycling tests. There was no correlation with temperature or depth of discharge.

The nitrate steps behaved in a similar fashion. Low to high ranges on characterization were from 0-7 to 13-25 ma-hrs. On recharacterization, the values ranged from a low of 0-13 to a high of 21-30 ma-hrs. In general, the nitrate steps after cycling were not significantly different from the original characterization values. There was no correlation with temperature or depth of discharge.

RANDOM DISCHARGE CYCLING
CAPACITY CHANGES
RECHARACTERIZATION
VS
CHARACTERIZATION

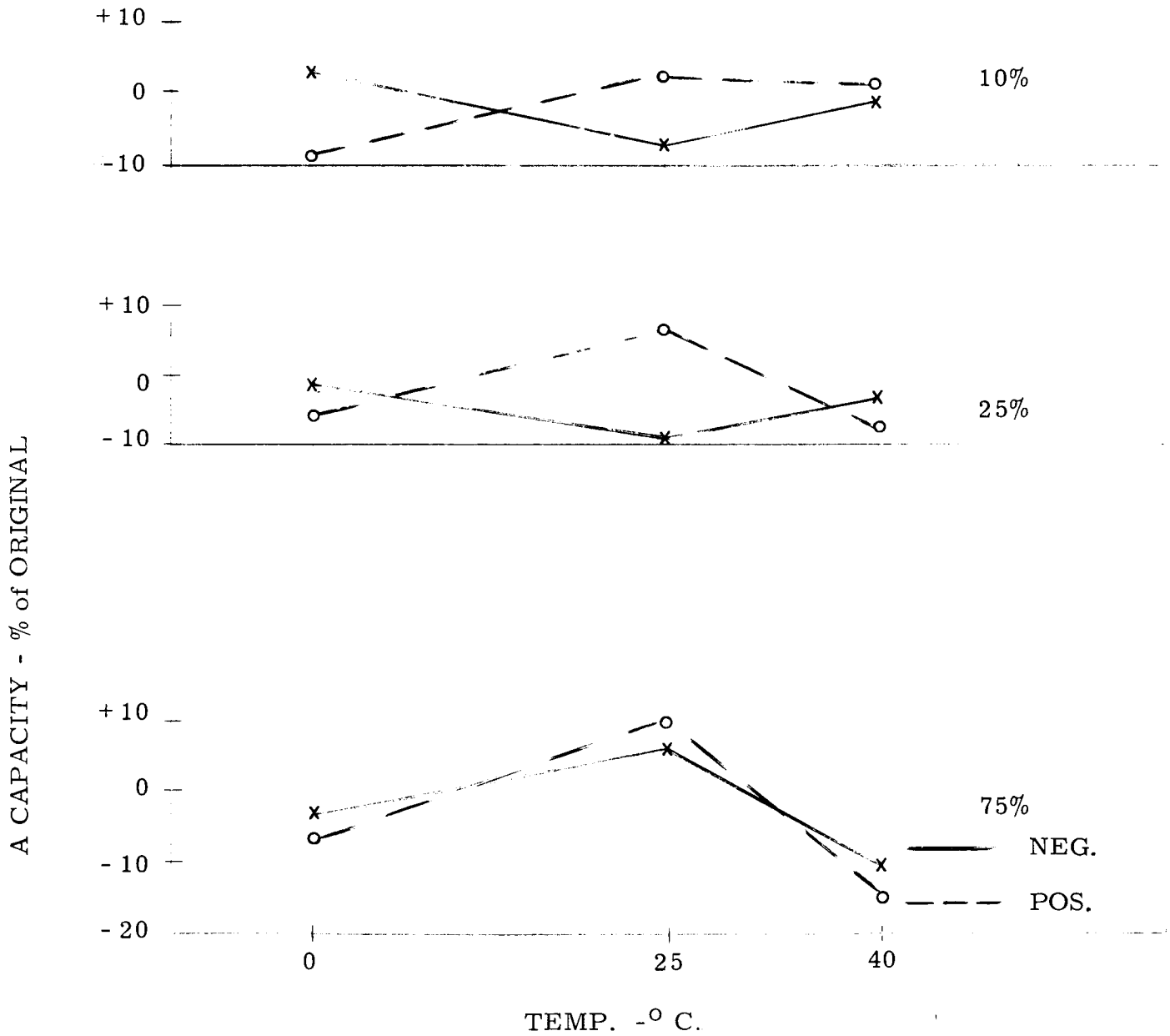


Figure 4.3

TABLE 4.3

RANDOM DEPTH OF DISCHARGE CYCLING TEST ELECTRODES

Timer #	1	2	3	4	5	6
% Average Dis.	10% β	25% Rect.	25% β	50% Rect.	50% β	75% β
0°C	N ₀ -69 N ₀ -70 P-99	N ₀ -64 N ₀ -66 P-100	N ₃ -16* N ₃ -17 P-71	N-9 N-11 P-72	N ₃ -21* N ₃ -22 P-73	N ₃ -18* N ₃ -19 P-74
25°C	N-5* N-6 P-55	N ₃ -5* N ₃ -6 P-56	N ₃ -3* N ₃ -4 P-57	N-96 N-4 P-58	N ₀ -58 N ₀ -59 P-59	N ₃ -9* N ₃ -10 P-60
40°C	N ₃ -11 N ₃ -15 P ₃ -9	N ₀ -61 N ₀ -63 P ₀ -68	N ₀ -67 N ₀ -68 P ₀ -71	N-7 N-8 P-8	N-1 N-2 P ₁ -95	N ₁ -98 N ₀ -60 P ₃ -25
Number of Cycles	475	170	180	95	95	65
% Overcharge	20	40	35	55	21	22

* Denotes short cell on the basis of no potential measurable upon removal from cycling test in the charged condition.

TABLE 4.4

PHYSICAL APPEARANCE OF RANDOM DEPTH OF DISCHARGE CYCLING POSITIVE TEST ELECTRODES

Timer#	1	2	3	4	5	6
% Average Dis.	10% β	25% Rect.	25% β	50% Rect.	50% β	75% β
0°C	Good	Good	Good	*Good	Small Pimples	Good
25°C	*Good	Good	Good	Good	Good	Good
40°C	Good	*Pimples Small Blisters	1 Blister	Pimples	Small Pimples 1 Blister	Small Pimples
Number of Cycles	475	170	180	95	95	65
% Overcharge	20	40	35	55	21	22

* There was no change in Negative Electrodes except those in the cells with asterisks. These were very dark but otherwise similar to uncycled electrodes.

TABLE 4.5
RESIDUAL CAPACITY MEASUREMENTS OF RANDOM DEPTH OF DISCHARGE CYCLING TEST CELLS

Positive Electrodes	Depth of Discharge	No. Cycles	RESIDUAL CAPACITY		(Ma-Hrs)	VO 40°C
			KO 0°C	KO 25°C		
Constant Current	10% β	475	1020	495*		1150
	25% β	180	742*	456*		333
	25% Rect.	170	700	662*		910
	50% β	95	653*	316		908
	50% Rect.	95	815	425		850
	75% β	65	472*	195*		417
Constant Load	10% β	475	205	188*		268
	25% β	180	184*	203*		92
	25% Rect.	170	175	151*		112
	50% β	95	96*	101		96
	50% Rect.	95	225	113		118
	75% β	65	135*	69*		113
Negative Electrodes	Depth of Discharge	No. Cycles	RESIDUAL CAPACITY		(Ma-Hrs)	VO 40°C
			VO 0°C	VO 25°C		
Constant Current	10% β	475	1250	0*		933
	25% β	180	0*	0*		985
	25% Rect.	170	675	0*		1000
	50% β	95	0*	18		563
	50% Rect.	95	1175	922		865
	75% β	65	0*	0*		1140
Constant Load	10% β	475	32	0*		73
	25% β	180	3*	1*		38
	25% Rect.	170	23	7*		30
	50% β	95	1*	4		27
	50% Rect.	95	16	43		58
	75% β	65	1*	1*		90

*Shorted Cells

TABLE 4.6

COMPARISON OF CHARACTERIZATION AND RECHARACTERIZATION DATA FOR POSITIVE TEST ELECTRODES

Electrode Number	Cycles	Depth of Discharge	Test Temp.	Cycle No. -						Average Charge	Per Cent(1) Change
				1	2	3	4	5	6		
P-99	475	10% β	0°	* 1000 ** (930	1030	1050	1060	1070	1060	1045 954)	-8.7
P-55	475	10% β	25°	(910 (970	930	950	960	960	1000	945 969)	+1.5
P ₃ -9	475	10% β	40°	1190 (1318	1220	1230	1280	1300	1200	1237 1253)	+1.5
P-100	180	25% Rect.	0°	1120 (1000	1130	1130	1120	1130	1120	1125 977)	-13.2
P-56	180	25% Rect.	25°	940 (1000	970	980	1000	980	1000	972 1021)	+5.0
P ₀ -68	180	25% Rect.	40°	1120 (1110	1120	1080	1100	1100	1120	1107 1072)	-3.0
P-71	170	25% β	0°	(990 (960	1021	1021	1030	1040	1050	1025 966)	-5.8
P-57	170	25% β	25°	(890 (960	900	920	930	940	950	920 980)	+6.5
P ₀ -71	170	25% β	40°	1170 (1110	1170	1150	1170	1160	1160	1163 1094)	-6.0

(1) % Change is the difference between the average characterization and recharacterization capacities, expressed in percentage of characterization value.

* Characterization capacity.

** Recharacterization capacity.

(cont'd next page)

TABLE 4.6 (Cont'd)

Electrode Number	Cycles	Depth of Discharge	Test Temp.	Cycle No. - Ma.-Hrs.						Average Charge	Per Cent(1) Change
				1	2	3	4	5	6		
P-72	95	50% Rect.	0°	941 (1021)	960 1021	960 1050	970 1040	981 1050	1000 1050	969 1039)	+7.2
P-58	95	50% Rect.	25°	950 (1021)	980 1000	980 1040	1041 1040	1021 1050	1000 1070	995 1037)	+4.0
P-8	95	50% Rect.	40°	1100 (1061)	1100 1050	1110 1040	1120 1050	1120 1050	1140 1050	1115 1050)	-5.7
P-73	95	50% β	0°	960 (970	990 941	1000 941	1010 960	1020 981	1040 1000	1003 966)	-3.7
P-59	95	50% β	25°	940 (1021	960 981	980 1021	980 1030	980 1050	980 1070	970 1029)	+6.2
P ₁ -95	95	50% β	40°	1310 (1070	1340 1030	1270 1021	1340 1030	1370 1040	1445 1040	1346 1039)	-22.7
P-74	65	75% β	0°	1090 (1021	1080 1000	1080 1000	1090 1010	1080 1030	- 1030	1084 1015)	-6.6
P-60	65	75% β	25°	930 (1050	960 1030	980 1061	990 1061	990 1090	1000 1101	975 1066)	+9.4
P ₃ -25	65	75% β	40°	1075 (950	1050 950	1165 941	1125 950	1145 960	1155 960	1119 952)	-15.0

(1) % Change is the difference between the average characterization and recharacterization capacities, expressed in percentage of characterization value.

* Characterization capacity.
** Recharacterization capacity.

TABLE 4.7

COMPARISON OF CHARACTERIZATION AND RECHARACTERIZATION DATA FOR NEGATIVE TEST ELECTRODES

Electrode Number	RA#	°C Temp.	Cycle No.						Average Charge	Per cent (1) Change
			1	2	3	4	5	6		
N ₀ -70	10% β	0°	* 1400	1330	1270	1260	1250	1280	1298	+3.5
			** (1430	1381	1330	1320	1300	1300	1344)	
N-5	10% β	25°	1350	1320	1300	1280	1290	1270	1302	-6.4
			(1261	1210	1221	1200	1221	1200	1219)	
N ₃ -15	10% β	40°	1360	1335	1435	1370	1320	1380	1367	-1.2
			(1510	1380	1350	1318	1275	1275	1351)	
N ₀ -64	25% Rect.	0°	1460	1390	1310	1320	1300	1320	1350	-3.6
			(1381	1350	1300	1280	1250	1250	1302)	
N ₃ -5	25% Rect.	25°	1430	1410	1380	1440	1440	1290	1398	-6.1
			(1320	1310	1320	1310	1310	1310	1313)	
N ₀ -61	25% Rect.	40°	1440	1360	1300	1320	1300	1320	1340	-4.9
			(1341	1280	1280	1249	1261	1230	1274)	
N ₃ -16	25% β	0°	1240	1190	1300	1275	1200	1265	1245	-1.5
			(1290	1270	1230	1200	1190	1181	1227)	
N ₃ -4	25% β	25°	1440	1400	1370	1410	1410	1250	1380	-8.7
			(1290	1261	1270	1250	1261	1230	1260)	
N ₀ -68	25% β	40°	1420	1370	1310	1320	1300	1320	1340	-5.8
			(1320	1261	1270	1240	1240	1240	1262)	

(1) % Change is the difference between average characterization and recharacterization capacities expressed as a percentage of the characterization value.

* Characterization capacity.

** Recharacterization capacity.

(cont'd next page)

TABLE 4.7 (Cont'd)

Electrode Number	RA #	°C Temp.	Cycle No.						Average Charge	Per Cent (1) Change
			1	2	3	4	5	6		
N-9	50% Rect.	0°	1280	1260	1260	1250	1270	1260	1163	-9.4
			(1181)	1170	1170	1120	1101	1120	1144)	
N-96	50% Rect.	25°	1287	1243	1225	1182	1190	1190	1220	-3.9
			(1310)	1280	1280	1250	1261	1230	1269)	
N-8	50% Rect.	40°	1400	1390	1380	1370	1380	1380	1383	-13.7
			(1250)	1200	1210	1170	1160	1170	1193)	
N ₃ -22	50% β	0°	1390	1550	1460	1540	1340	1395	1446	-9.5
			(1370)	1360	1310	1300	1280	1280	1309)	
N ₀ -58	50% β	25°	1530	1400	1410	1370	1340	1330	1397	-9.9
			(1280)	1250	1261	1250	1261	1250	1259)	
N-2	50% β	40°	1240	1240	1240	1240	1240	1240	1243	-17.6
			(1101)	1050	1000	1000	990	1000	1024)	
N ₃ -18	75% β	0°	1340	1305	1405	1330	1290	1350	1337	-3.2
			(1360)	1341	1300	1261	1250	1250	1294)	
N ₃ -9	75% β	25°	1310	1280	1240	1290	1280	1240	1273	+6.1
			(1381)	1350	1360	1341	1341	1330	1351)	
N ₀ -60	75% β	40°	1460	1380	1300	1300	1280	1250	1328	-9.9
			(1310)	1240	1181	1160	1150	1141	1197)	

(1) % Change is the difference between average characterization and recharacterization capacities expressed as a percentage of the characterization value.

* Characterization capacity.

** Recharacterization capacity.

TABLE 4.8

COMPARISON OF GRAPHITIC AND NITRATE STEPS ON POSITIVE SHALLOW CYCLING TEST ELECTRODES

Electrode Number	Cycles	Depth of Discharge	Test Temp.	Cycle No.-Graphitic Step-Ma.Hrs.						Cycle No.-Nitrate Step Ma.Hr.							
				1	2	3	4	5	6	1	2	3	4	5	6		
P-99	475	10% β	0°C	*265 (139)	227	246	246	252	252	252	252	25	19	19	13	13	13
				**	183	189	195	208	202	202	202	--	13	7	7	7	7)
P-55	475	10% β	25°C	195 (57)	208	220	237	252	239	239	170	13	13	13	13	13	13)
P ₃ -9	*475	10% β	40°C	183 (126)	195	202	227	220	202	202	151	7	7	13	7	7	7)
P-100	180	25% Rect.	0°C	126 (44)	139	157	170	183	195	145	145	13	13	19	19	13	13)
P-56	180	25% Rect.	25°C	170 (44)	101	132	145	157	220	164	164	19	13	13	13	13	13)
P ₀ -68	180	25% Rect.	40°C	69 (13)	88	94	101	94	107	101	101	13	7	7	7	7	7)
P-71	170	25% β	0°C	252 (88)	239	239	246	252	252	170	170	13	13	13	13	13	13)
P-57	170	25% β	25°C	220 (44)	233	252	271	258	246	183	183	13	13	13	13	7	13)
P ₀ -71	170	25% β	40°C	132 (44)	157	151	145	151	151	145	145	7	7	7	7	7	7)
P-72	95	50% Rect.	0°C	233 (110)	220	220	227	233	233	170	170	13	13	13	13	13	13)

*Characterization Capacity.

** Recharacterization Capacity.

(Cont'd next page)

Table 4.8 (Cont'd)

Electrode Number	Cycles	Depth of Discharge	Test Temp.	Cycle No.-Graphitic Step-Ma.Hrs.						Cycle No.-Nitrate Step-Ma.Hr.								
				1	2	3	4	5	6	1	2	3	4	5	6			
P-58	95	50% Rect.	25°C	227 (94	214	283	265	265	252	252	13	13	13	13	7	7	7	7
P-8	95	50% Rect.	40°C	88 (94	139	157	157	170	176	176	--	7	7	7	7	7	7	7
P-73	95	50% β	0°C	290 (151	271	265	258	265	258	258	13	7	7	13	7	7	7	7
P-59	95	50% β	25°C	220 (94	220	239	252	252	239	239	13	7	7	7	7	7	7	7
P ₁ -95	95	50% β	40°C	69 (31	88	88	101	120	126	126	7	7	13	7	7	7	--	7
P-74	65	75% β	0°C	132 (88	164	183	202	214	214	214	13	13	13	13	7	13	7	13
P-60	65	75% β	25°C	258 (145	246	277	283	283	258	258	13	7	7	13	7	7	7	7
P ₃ -25	65	75% β	40°C	139 (44	176	195	208	214	208	208	--	7	7	7	7	7	7	7

5.0 CONSTANT VOLTAGE-CURRENT LIMITED CYCLING TESTS

These tests were designed to determine the effect of cyclic operation under constant voltage, current limited charging conditions. In contrast to the previous test in which only a part of the cell capacity was removed in each discharge, these cells were discharged to 0.9 V cell voltage cutoff.

5.1 Experimental Equipment and Procedures

The cycling control equipment for this series of test is described in Appendix I.

The test cells consisted of four positive and five negative electrodes. The electrodes inserted into this test group were type VO initially. However, during the course of the cycling test, the compressor motor on the refrigeration chamber failed necessitating a shutdown. In the subsequent checkout of the system, the 0°C cells were accidentally exposed to a temperature of -90°C for a short time to replace the positive electrodes with KO electrodes since visual inspection of the electrodes showed them to be severely blistered. One of these refabricated cells subsequently failed to pass a leak check and was replaced with a cell containing type KO positives and negatives.

The charging potentials for the cells were 1.50, 1.47, and 1.42V respectively at 0°, 25°, and 40°C. The current was limited to 800 ma. (\sim C/5 rate) during the charging portion of the cycle which lasted for 7-3/4 hours. The discharge was made at a constant current of 2000 ma. (\sim C/2 rate) to a cell voltage cutoff of 0.9 V followed by a rest period for a total of 10-3/4 hours per cycle.

Following the completion of cycling, the test cells were removed in the charged condition, checked for residual capacity, and disassembled for inspection. One positive and one negative electrode from each cell was then recharacterized for comparison with the original characterization.

5.2.0 Results

The data on the electrodes used in the cells for these tests and the number of cycles completed at the three temperature levels are listed in Table 5.1. One cell at each temperature level developed a short during the course of the cycling.

5.2.1 Visual and Photographic Examinations

One positive and one negative electrode was taken from an unshorted cell, one set of electrodes was examined from each temperature level. The electrodes were potted and photographed just as the electrodes described in Section 3.0.

The positive electrodes showed a tendency towards more extensive pimpling and blistering with increasing temperature as indicated in Table 5.1. Figure 5.1 is typical of all electrode photomicrographs which were very similar in spite of the difference in external appearance. Comparing this figure with Figure 3.3, two outstanding differences were noticed. In these cells there was no sign of corrosive attack of the nickel plate (0.45 mils) on the core plate nor on the adjacent sinter structure. The active material, on the other hand, was clustered very densely in certain areas while almost totally absent in others. The presence of sintered nickel structure in the latter pockets makes it seem unlikely that the active material was merely dislodged during the polishing procedure. The pimples seen here are similar to those previously noted in the other cycling tests.

As for other cycling tests, the negative electrodes showed no distinctive peculiarities. Figure 5.2 shows a fully discharged cadmium plate. In all electrodes examined microscopically, the nickel plate was approximately 0.45 mils thick. All had a very uniform distribution of materials and none were attacked at the junction of the sinter with the core.

5.2.2 Electrochemical Test Results

5.2.2.1 Residual Capacity Test Results

The results of the residual discharge capacity measurements for the positive and negative test electrodes are listed in Table 5.2. The highest residual capacity was found for electrodes in the 0°C tests which also had received the lowest number of cycles. At 25 and 40°C, the negative electrodes show significantly lower values of residual capacity than the positive electrode. These results are partly confounded by the electrodes having different numbers of cycle histories. The trend is lower capacities with increasing number of cycles for both positives and negatives at 0 and 40°C.

5.2.2.2 Comparison of Characterization and Recharacterization Capacities

The characterization and recharacterization data for the positive test electrodes are listed in Table 5.3. The range of change between the average characterization and recharacterization capacities was from -22.6% to +12.6% of original capacity. Generally the positive electrodes showed increases in capacities after cycling ranging from 1 to 12.6% with no detectable trends with temperature.

The characterization and recharacterization data for the negative electrodes is listed in Table 5.4. The range of change between the average characterization and recharacterization capacities was from -1.2% to -9.2% with no detectable trends with temperature.

5.2.2.3 Comparison of Graphitic and Nitrate Steps on Characterization and Recharacterization

The graphitic and nitrate steps before and after cycling for the positive electrodes are listed in Table 5.5. On characterization, the spread of graphitic capacities over six cycles ranged from a low of 82-139 ma-hrs. to a high of 252-277 ma-hrs. Most individual electrodes showed a trend to higher capacity on successive recharacterization cycles. In most cases, the graphitic capacities decreased after the cycling tests. There was no detectable trend with temperature or cycle number.

The nitrate steps behaved in a similar fashion. Low to high ranges on characterization were from 0-13 to 13-25 ma-hrs. On recharacterization, the values ranged from a low of 0-6 to a high of 0-18 ma-hrs. In general, the initial characterization capacities were higher than the recharacterization capacities. The trend in both characterization and recharacterization was toward higher values with successive cycles. There was no correlation of changes in nitrate reduction step with temperature or number of cycles.

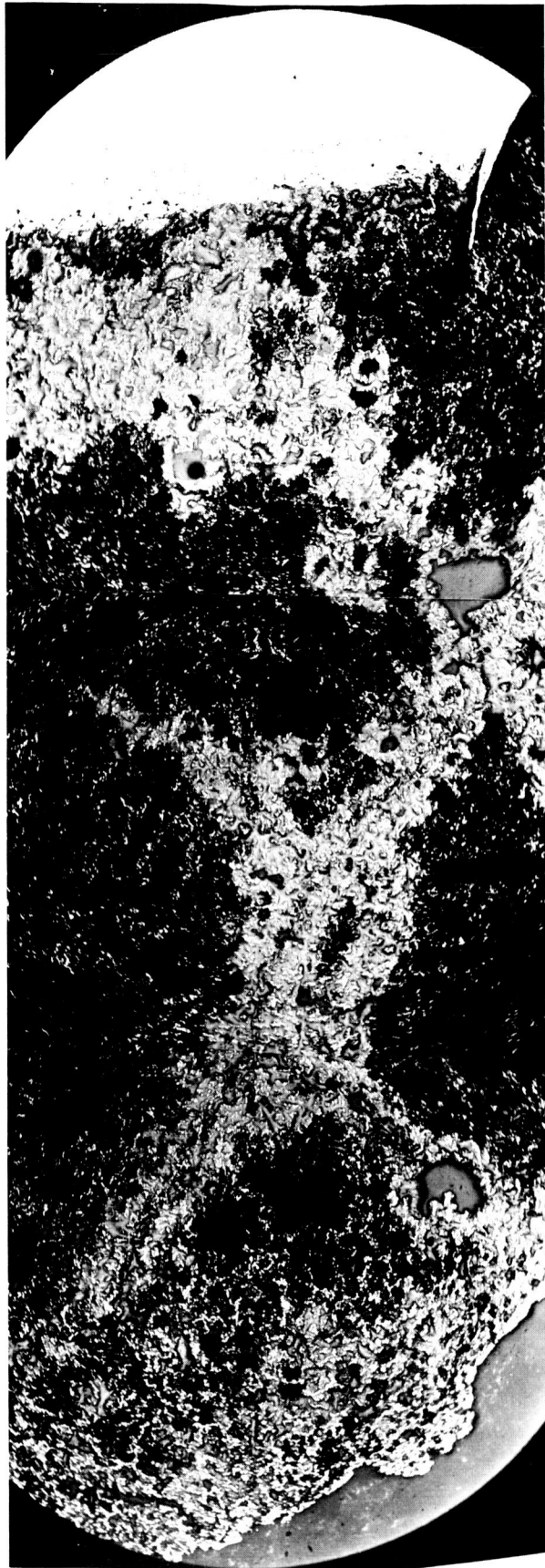


Figure 5. 1. Electrode P₅-29, 40°C, 579 Cycles Photomicrograph

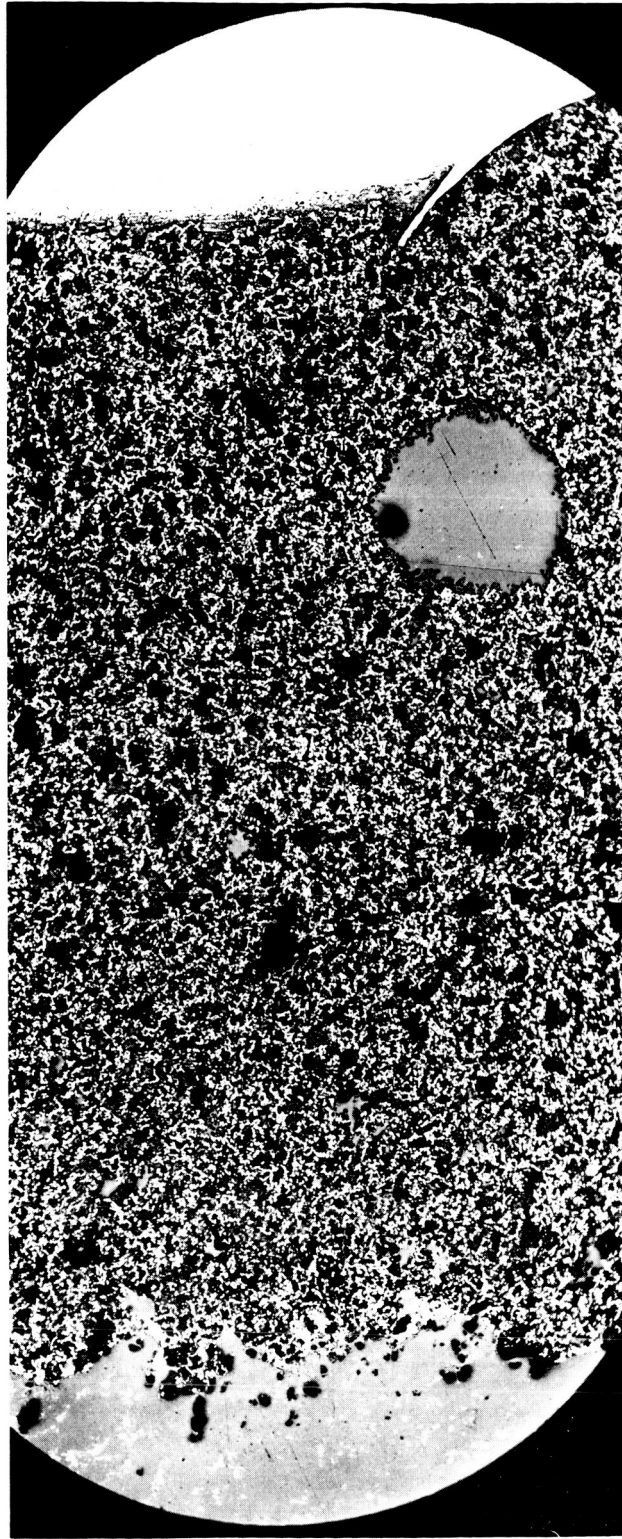


Figure 5.2 Fully Discharged Negative to Gassing - Photomicrograph

TABLE 5.1

CONSTANT VOLTAGE CURRENT LIMITED CHARGING CYCLING ELECTRODES

Cell#	Temp.	Type	Electrode Numbers	Cycles Completed	Electrode Condition
3	0°C	KO KO	P-51, 52, 53, 54* N-91, 92, 93, 94, 95**	100	P-Pimpled N-Good
4	0°C	KO VO	P-95, 96, 97, 98*** N ₅ -15, 16, 17, 18, 20	Pos. 100**** Neg. 579	P-Good N-Good; warped
1	25°C	VO VO	P ₅ -2, 4, 7, 11 N ₅ -3, 4, 6, 9, 10	771	P-Extensively pimpled N-Good
2	25°C	VO	P ₀ -79, 85, 93, 96 N ₁ -81, 83, 85, 96, 97	771****	P-Pimpled; 2 blisters N-Burn Mark
5	40°C	VO	P ₅ -3, 14, 15, 17 N ₅ -10, 11, 12, 14 N ₃ -15	579****	P-Extremely blistered N-Good
6	40°C	VO VO	P ₅ -23, 29; P ₁ -35; P ₀ -63 N ₅ -2, 5, 7, 8; N ₀ -51	579	P-Blister; Spalled after recharacterization N-Good

NOTE: Original VO electrodes replaced at time of refrigerator unit failure were as follows:

*P₀ - 64, 67, 78; P₁ - 79

**N₀ - 53, 54, 55, 56, 57

***P₅ - 18, 24, 27, 28

****Shorted Cells

TABLE 5.2

RESIDUAL CAPACITY MEASUREMENTS OF CONSTANT VOLTAGE CURRENT LIMITED CYCLING TEST CELLS

Positive Electrodes	KO 0°C	VO 25°C	VO 40°C
Constant Current	0*	7.5*	0*
Constant Load	0	26	0
	1103	75	416
	284	40	250

Negative Electrodes	VO	VO	VO
Constant Current	787*	0*	0*
Constant Load	35	0	0
	1170	25	0
	166	14	0

*Shorted Cells

TABLE 5.3

COMPARISON OF CHARACTERIZATION AND RECHARACTERIZATION DATA FOR POSITIVE TEST ELECTRODES

Electrode Number	Cycles	Test Temp.	Cycle No.						Average Charge	Per cent(1) Change
			1	2	3	4	5	6		
P-52	100	0°	*	910	920	940	980	980	974	+12.3
			**	(1190)	1062	1072	1083	1072	1083	
P-97	100	0°		1000	1030	1020	1060	1060	1042	+0.9
				(1050)	1062	1083	1050	1030	1030	
P ₀ -79	771	25°		1190	1170	1170	1180	1190	1183	+10.2
				(1380)	1350	1318	1285	1255	1245	
P ₅ -11	771	25°		1150	1200	1190	1220	1210	1194	+9.0
				(1380)	1310	1310	1285	1265	1255	
P ₅ -17	579	40°		1370	1295	1340	1210	1230	1377	-22.6
				(1155)	1000	1190	1020	1010	1020	
P ₅ -29	579	40°		1370	1305	1330	1200	1230	1274	+12.6
				(1520)	1443	1433	1425	1403	1380	

(1) % Change is the difference between the average characterization and recharacterization capacities expressed as a percentage of the characterization value.

* Characterization capacity.

** Recharacterization capacity.

TABLE 5.4

COMPARISON OF CHARACTERIZATION AND RECHARACTERIZATION DATA FOR NEGATIVE TEST ELECTRODES

Electrode Number	Cycles	Test Temp.	Cycle No.						Average Charge	Per cent(1) Change	
			1	2	3	4	5	6			
N-92	100	0°C	*	1330	1270	1240	1210	1180	1180	1235	+15.0
			**	(1530)	1480	1430	1390	1350	1340	1420)	
N ₅ -15	579	0°C		1520	1455	1475	1320	1340	1340	1408	-3.5
				(1500)	1412	1380	1320	1275	1265	1359)	
N ₁ -97	771	25°C		1570	1570	1570	1570	1570	1630	1580	-9.2
				(1655)	1500	1440	1380	1320	1310	1434)	
N ₅ -3	771	25°C		1380	1420	1380	1420	1350	1380	1388	-5.3
				(1410)	1340	1320	1285	1265	1265	1314)	
N ₃ -15	579	40°C		1360	1335	1435	1370	1320	1380	1367	-1.2
				(1510)	1380	1350	1318	1275	1275	1351)	
N ₅ -2	579	40°C		1390	1440	1400	1450	1400	1420	1417	-3.7
				(1485)	1405	1370	1340	1300	1290	1365)	

(1) % Change is the difference between average characterization and recharacterization and recharacterization capacities expressed as a percentage of the characterization value.

*Characterization capacity.

**Recharacterization capacity.

TABLE 5.5

COMPARISON OF GRAPHITIC AND NITRATE STEPS ON POSITIVE TEST ELECTRODES

Electrode Number	Cycles	Test Temp.	Graphitic Step - Ma. Hrs.						Nitrate Reduction Step-Ma.Hrs.					
			1	2	3	4	5	6	1	2	3	4	5	6
P-52	100	0°C	*277	271	271	277	271	252	-	18	18	19	13	13
			** (158)	160	210	160	193	193	-	13	14	15	18	18
P-97	100	0°C	252	214	233	246	239	246	25	19	19	13	13	19
			(25	158	189	208	208	208	-	6	6	6	6	6
P ₀ -79	771	25°C	107	107	107	107	113	113	13	13	13	13	13	13
			(57	82	95	120	126	139	6	6	6	13	13	6
P ₅ -11	771	25°C	113	113	126	145	139	145	-	13	19	13	19	19
			(13	50	69	76	95	107	6	6	6	13	6	6
P ₅ -17	579	40°C	107	164	183	164	164	158	-	13	13	13	6	6
			(6	25	69	88	101	120	-	6	6	6	6	6
P ₅ -29	579	40°C	82	113	139	132	132	120	-	13	13	13	13	13
			(145	145	158	158	158	164	6	6	6	6	6	6

* Characterization Capacity

** Recharacterization Capacity

*** "-" Visible but not measurable indication.

6.0 SUMMARY AND CONCLUSIONS

6.1 Analytical Techniques

The measurement of individual electrode potential versus reference electrodes prior to and after cyclic testing of the electrodes has been shown to be a valuable tool for showing variations in electrode capacities and changes in graphitic and nitrate steps of positive electrodes before and after cycling tests.

The gassing rate measurements of the positive electrodes show considerable variation in the start and rate of gassing as a function stage of charge, charge rate, and charge rate sequence for presumably similar electrodes. Further studies of this type in conjunction with more detailed knowledge of individual electrode with respect to porosity and pore size distribution, extent of impregnation, and impurity levels appear promising to determine how these affect the charge acceptance of the electrodes.

The photomicrographic examinations provided valuable qualitative information with respect to uniformity of distribution of active material in the sinter structure and identifying the extent of corrosion of the core plating and sinter structure.

The X-ray diffraction measurements were not particularly useful in the present study other than providing a qualitative tool for corroborating the presence of the major known components in the plates in both the charged and discharged state.

6.2 Correlation of Electrode Characterization and Recharacterization Data

There were no correlations detectable between the initial positive electrode capacities and the nitrate reduction step or graphitic capacities. Similarly these characteristics were essentially independent of the total plate weights in the discharged state. The initial capacities of the negative electrodes were essentially independent of total plate weight in the discharged state. The spread in original electrode capacities for this particular lot of V0 electrodes was quite large.

The ratio of maximum to minimum capacity for the positive electrodes was 1.4 and for the negatives 1.6. To eliminate the confounding of this variable with the other test parameters requires either a larger sample of electrodes for testing than was used in the present program or the selection of electrodes of matched capacities prior to conducting the various cycling tests.

It was not possible to develop a statistically valid correlation between the individual electrode characteristics such as capacity; graphitic capacity, or nitrate capacities before and after cycling for any of the three cyclic modes tested. In large measure, this was caused by the loss of a number of cells from all cycling tests by shorting which reduced the number of good cells available for analysis. The order of magnitude changes in capacities before and after cycling were approximately 10% or less for the majority of the electrodes with occasional changes in the order of 25%. The overall trends were that the majority of positive electrodes showed a slight decrease in capacity and the majority of the negative electrodes showed a slight increase in capacity. Both the graphitic and nitrate reduction capacity in general showed decreases for all the cycling tests regimes.

6.3 Effects of Cycling Modes on Residual Capacity

There was insufficient data to quantitatively determine which cycling regime contributed to a greater loss of capacity or so called "memory effects" or to positively identify which electrode was more adversely affected in terms of loss of capacity. Several factors contributed to this result. The principal one was the loss of cells by shorting during the cycling tests which reduce the number of available cells for analysis. The trends from the limited data available indicate that the shallow cycling mode at 21% depth of discharge and to a more limited extent the random depth of discharge cycling mode with average depths of 25 to 75% tend to show a greater decrease in residual capacities than any of the conditions tested. The decrease in residual capacity on the average was greater for the positive electrodes than the negatives. The evidence for this conclusion is shown in Figure 6.0 which summarizes the residual capacity data of all electrodes from cells free of complications due to shorts. No quantitative statements can be made with respect to the effect of temperature. The residual capacity at any given temperature level generally decreases with increasing number of cycles.

6.4 Other Significant Observations

The positive electrodes showed a greater tendency to structural degradation than the negative electrodes. The degradation included the loss of sintered structure integrity presumably by oxidation on overcharge as well as a variable tendency to develop blisters or pimples which developed more frequently at the higher charge rates of C/5 to C/1. These results coupled with the observed variability of gassing rates for the positives suggest that these phenomena are inter-related and should receive more attention in future programs.

The factors which caused many of the cells to short during the cyclic testing were not specifically identified during the program. These cells showed no potential on removal from the tests after the last charge interval. Subsequent capacity measurements on individual electrodes showed in some cases that the positives had the zero capacities and in others the negatives with the other electrode having a measurable capacity. Monitoring the internal cell resistance of cells and individual cell voltages on a periodic basis would have provided more insight to detecting the start of shorting as well as allowing more fruitful failure analysis.

RESIDUAL CAPACITIES @ CONSTANT CURRENT

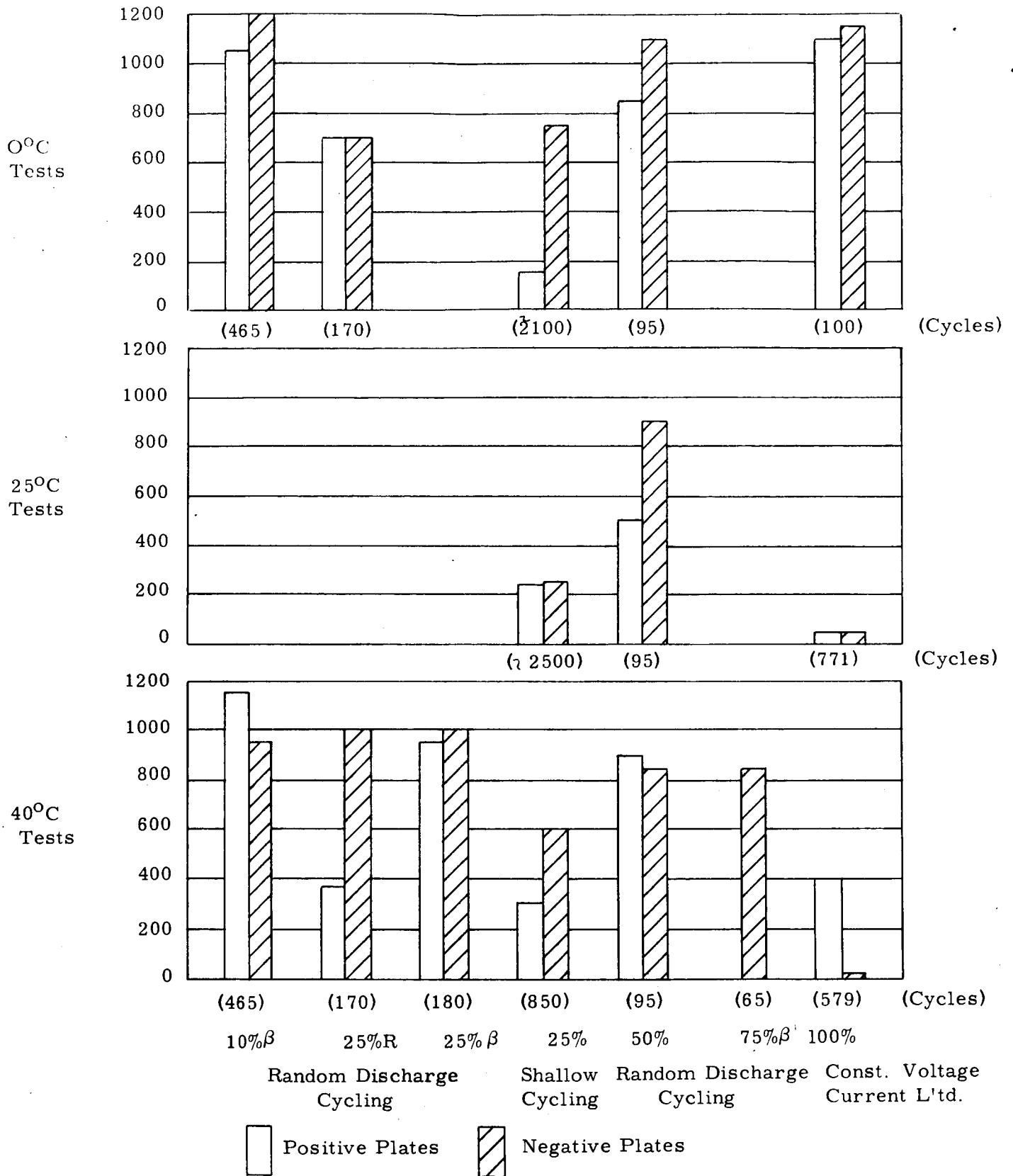


Figure 6.0

7.0 RECOMMENDATIONS FOR FUTURE WORK

1. Conduct a more detailed study of the memory effect to establish the role of the positive electrode self-discharge in causing the memory phenomena.
2. Conduct a detailed study of the onset, magnitude and effects of oxygen evolution on nickel hydroxide electrodes at various charge rates and states of charge.
3. Conduct studies on the effect of overcharge rate, total amount of overcharge, and electrolyte variables on the mechanical integrity of the positive electrode.
4. Determine the specific effect of nitrate ion on positive electrode behavior with respect to gassing, charge acceptance, and self-discharge in the absence of the cadmium electrode.
5. Conduct studies on the origin and significance of the graphitic capacity in relation to attack on the nickel sinter and electroplated parts of the electrode.
6. Conduct studies on the nature and significance of the graphite capacity changes with respect to normal capacity gain or loss.
7. Examine the effects of electrolyte impurities, electrode history, and charging variables on the gassing behavior of positive electrodes.
8. Determine the nature and the source of impurities in cell electrolytes such as the impurities extracted from the plates (e.g. nitrate), the impurities arising from degradation of the separators and other materials used in cell fabrication, and impurities introduced during the cell fabrication.
9. Determine the effect of carbonate level on the migration of cadmium from the negative electrode.

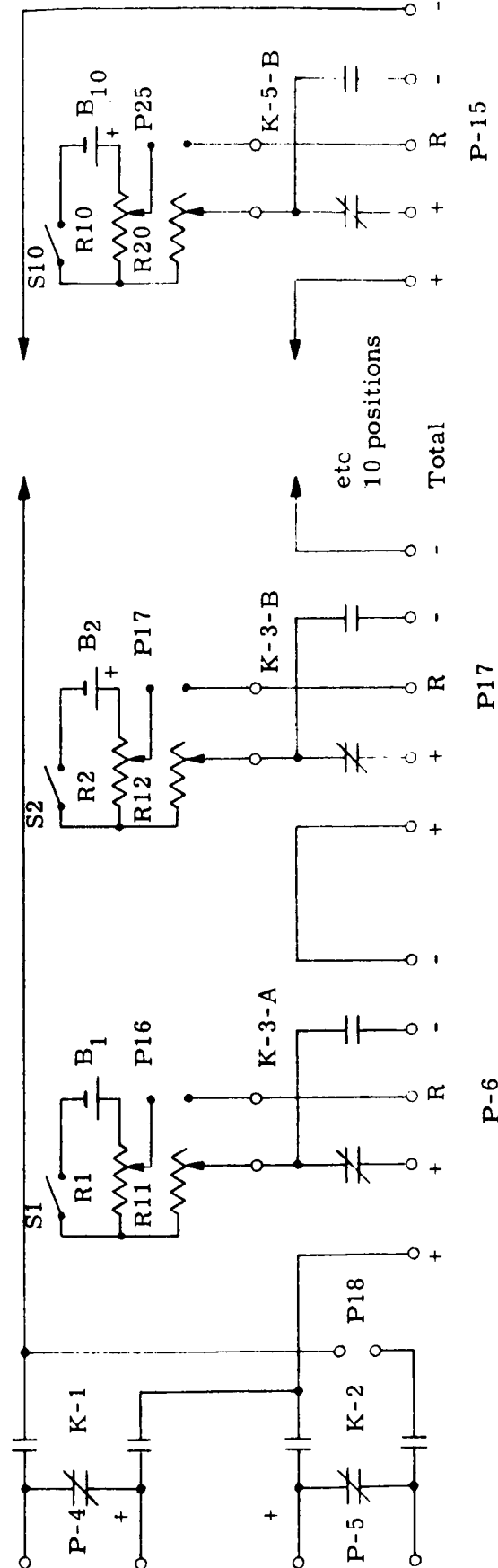
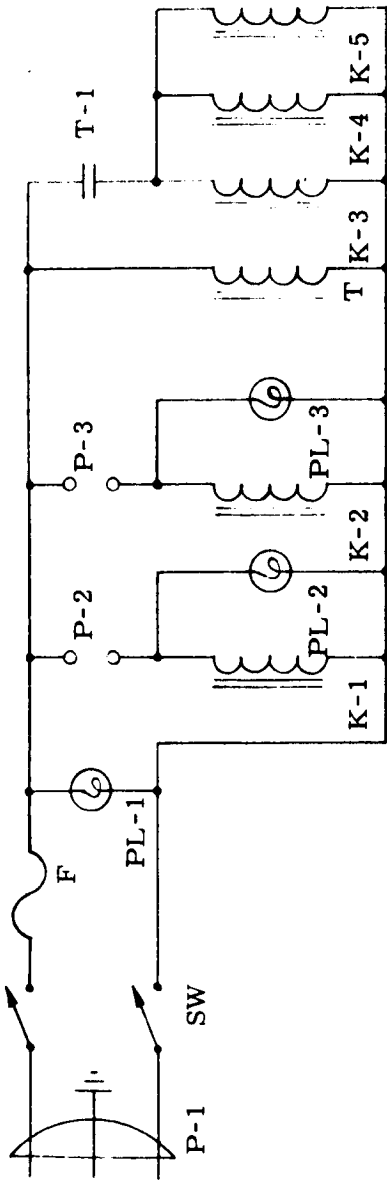
APPENDIX I

Control Equipment Schematics

Ni-Cd Characterization

Characterization Cycle Control

Part 1 of 2 Parts



Note: RL changed with variation in load

C/10	500	12.5 Watts	Ohmite 0117
C/2	100	25	Ohmite 0151
C	50	50	Ohmite 0318

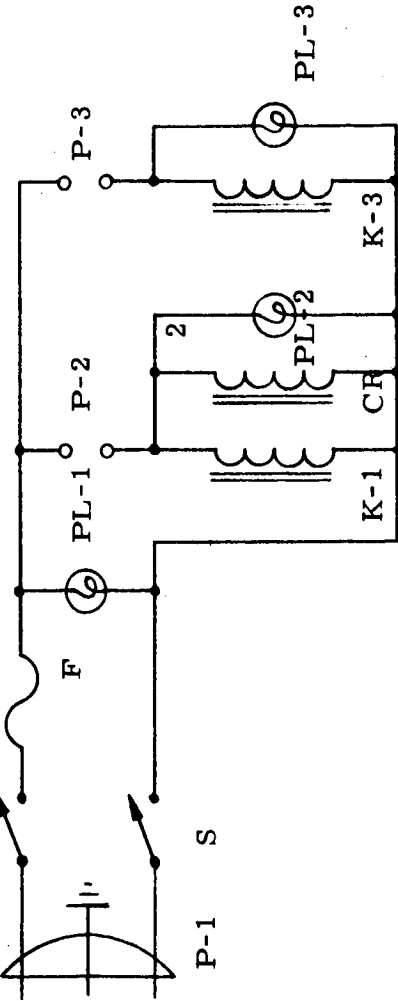
PARTS LIST

Part 2 of 2 Parts

- P-1 Line Cord, CA-CB Controller
- P-2 Control, Charge, Pin Jacks, Yellow
- P-3 Control, Discharge, Pin Jacks, Red
- P-4 Input Charge, CCS, Terminal
- P-5 Input Discharge, CCS Terminal
- P-6 thru P-15 Pin Jacks, Cell Input Red +, Green +, White R, Blue -, Black -
- P-16 thru P-17 Pin Jacks Recorder, Red +, Black -
- P-18 Pin Jacks, G. R. for RL
- SW Switch, Toggle SPDT
- F Fuse, 3A
- PL-1 Pilot, Master, Green
- PL-2 Pilot, Charge, Yellow
- PL-3 Pilot, Discharge, Red
- T Timer, CM, 2 Min
- RL Load Resistance (See Drawing)
- K-1, K-2 Mercury Relay, 3PST 2NO, 1NC, Ebert EM7, 110 VAC Coil
- K-3, K-4 Leach 329-7 4PDT, 110 VAC Coil
- K-5 Leach 337 2PDT, 110 VAC Coil
- S-1 thru S-10 Switch SPST Toggle "Bias"
- B-1 thru B-10 Battery Mercury O Cell
- R-1 thru R-10, 50,000 Ω 2 Watt
- R-11 thru R-20, 3 Meg

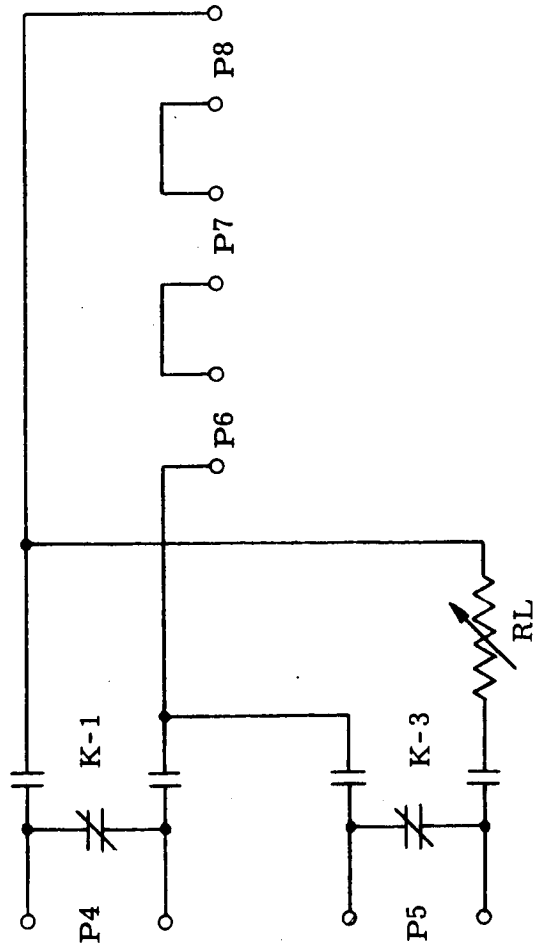
Ni-Cd Characterization

Shallow Cycling Test Controller



- P-1 Line Cord
- P-2 Charge Control Yellow
- P-3 Discharge Control Blue
- P-4 Charge Input Term Strip, 30 Amps
- P-5 Discharge Input Term Strip, 30 Amps
- P-6, P-7, P-8 Cell, 30 Amp Term Strip
- S Switch Master
- F Fuse 5 Amp
- PL-1 Master Green
- PL-2 Charge Yellow
- PL-3 Discharge Red
- K-1, K-3 Mercury 3PST 2NO, Ebert INC.
- EM-7

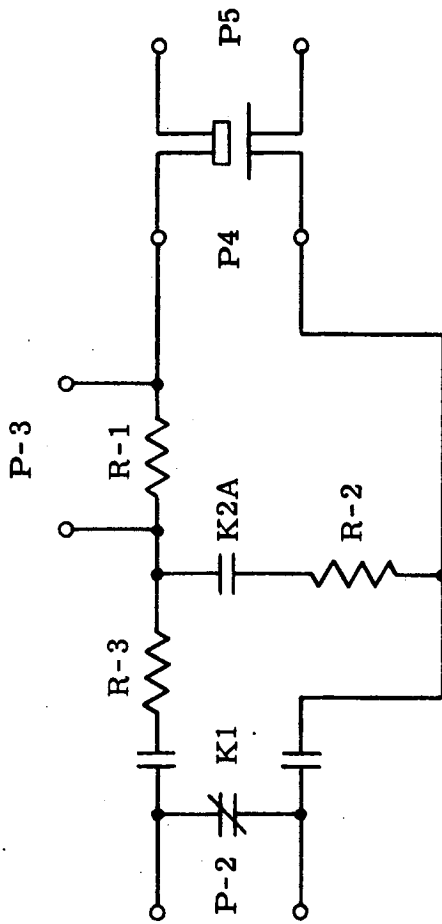
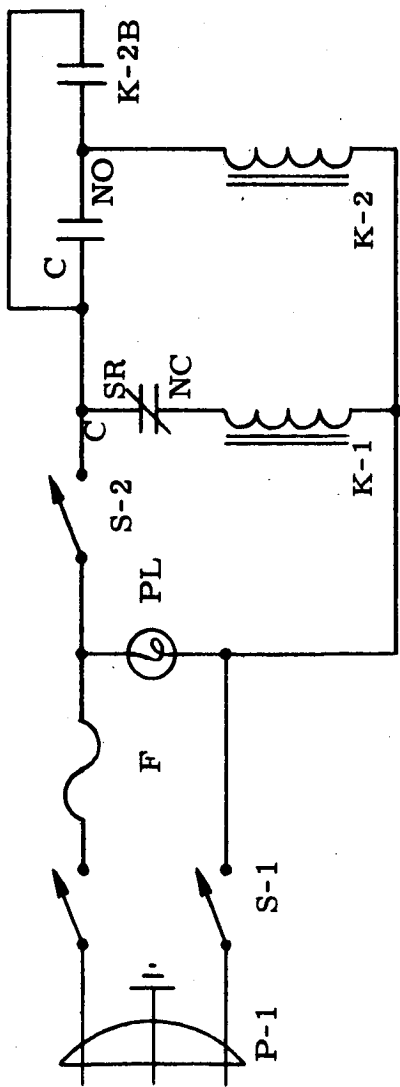
- CR Counter, General Controls CE600BS602
- RL 1 Ohm 50 Watts, Ohmite 0309



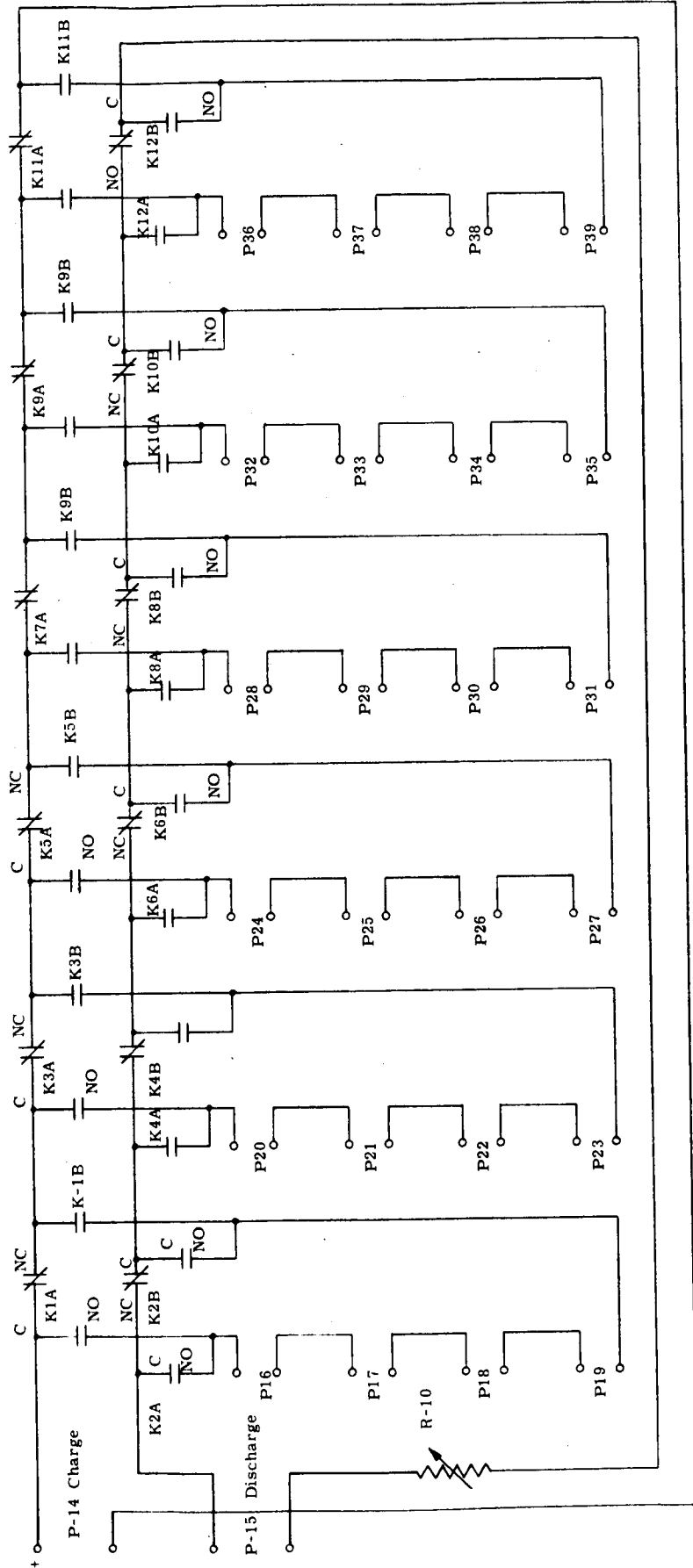
Ni-Cd Characterization

Residual Capacity Test Control

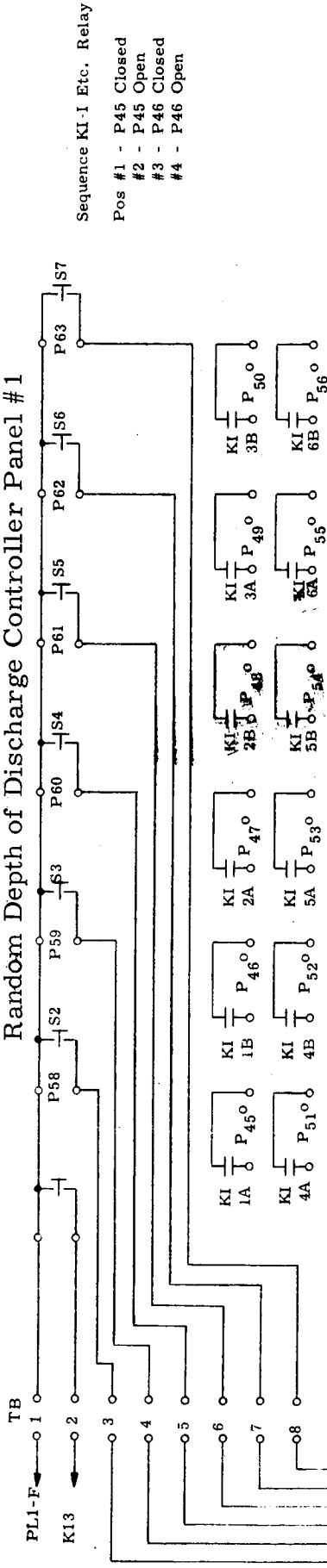
- P-1 Line Cord
- P-2 CC Input Pin Jacks Red + Black -
- P-3 Current Recorder Pin Jacks Red + Black -
- P-4 Cell Current Terminals
- P-5 Voltage Recorder Pin Jacks Red + Black -
- S-1 Master Switch
- S-2 Start-Reset Discharge Fuse SA
- F Fuse SA
- PL Pilot Green
- K-1 Mercury 3PST, 2NO, Ebert, INC EM-7
- K-2 Mercury DPST, 2NO, Ebert, INC MR-14
- SR Microswitch (Recorder)
- R-1 Ampere Shunt, 10 Ohm 10 Watts Low Range
- R-2 Load Resistance
- R-3 Load Resistance, 2 Ohm, 10 Watts High Range



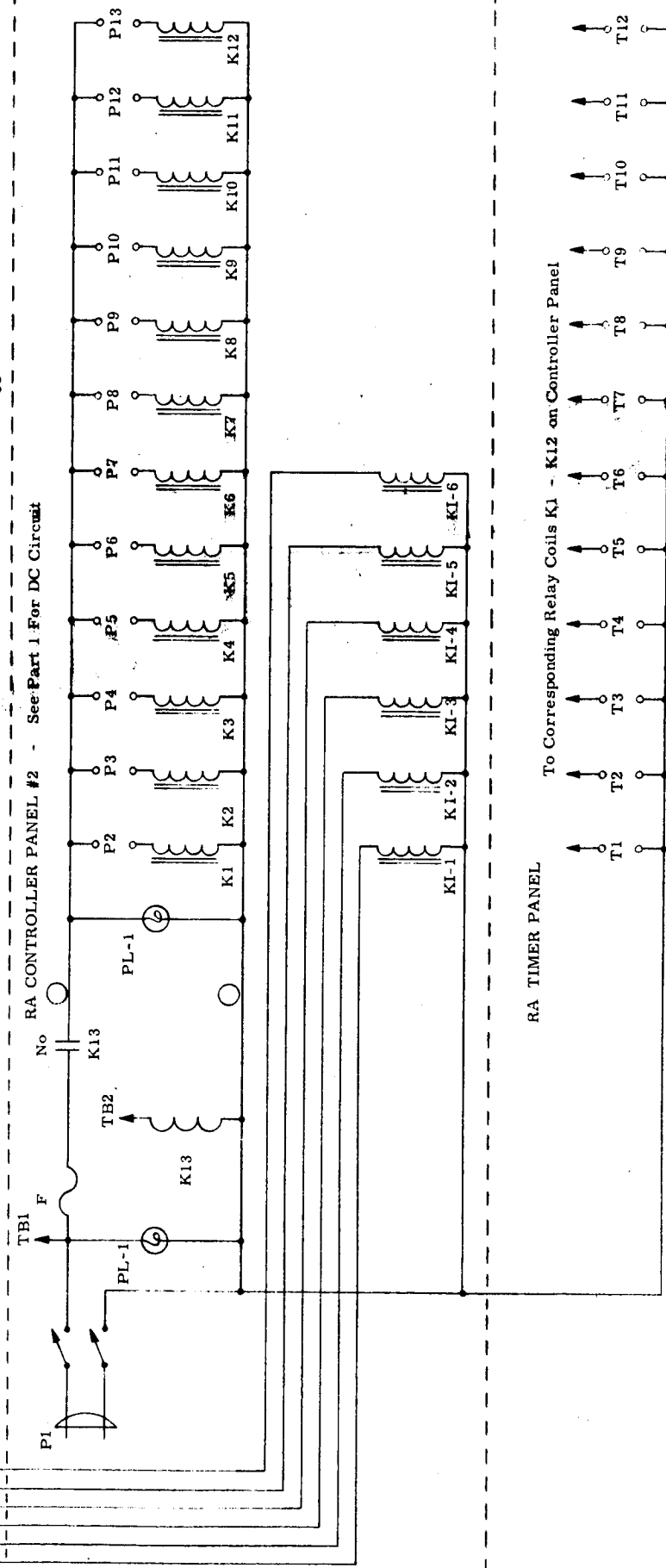
AC Circuit on PT2 Sketch
 Random Depth of Discharge
 Controller Panel Center Section



Random Depth of Discharge Controller Panel #1



RA CONTROLLER PANEL #2 - See Part 1 For DC Circuit

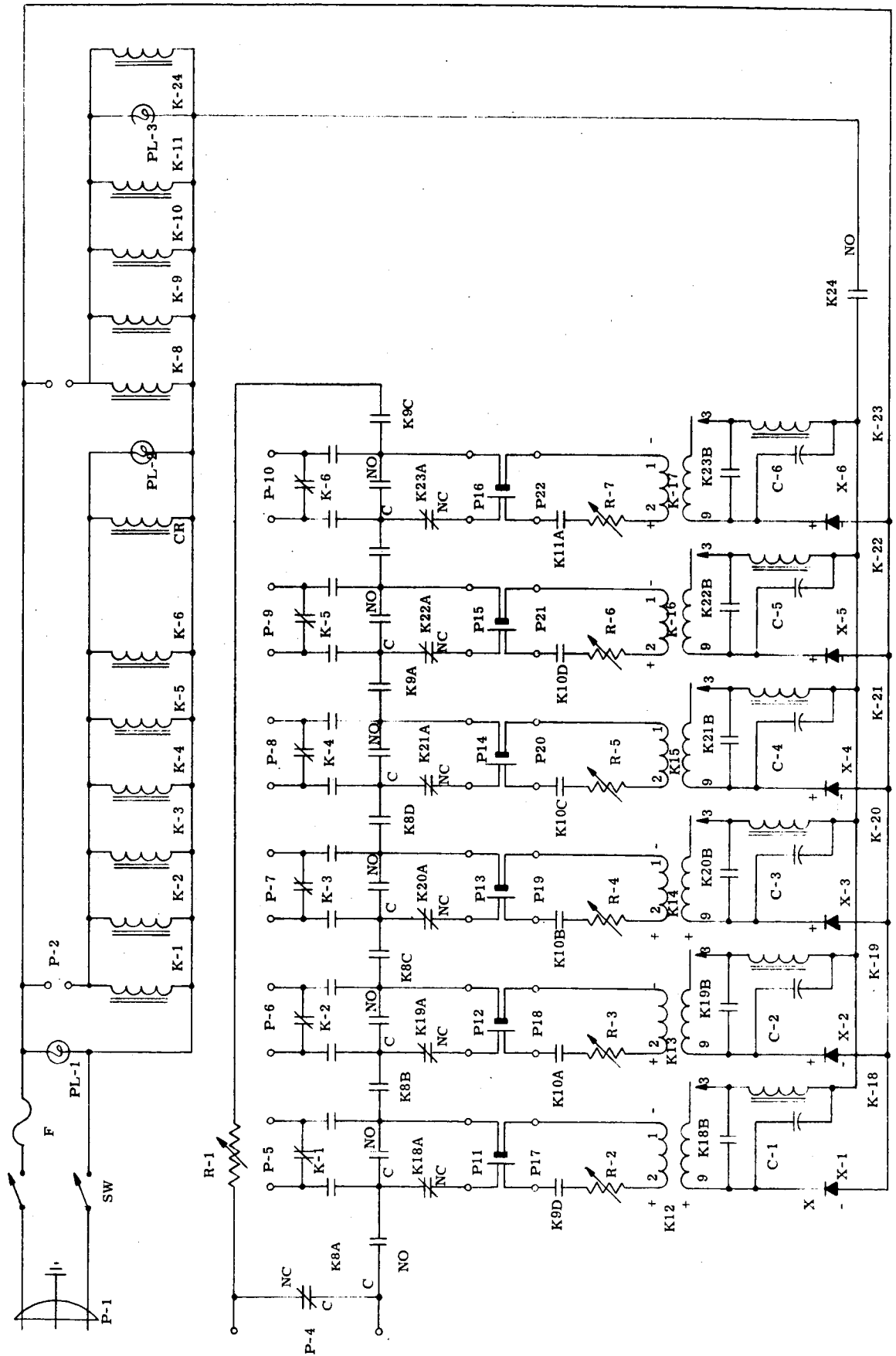


PARTS LIST
RANDOM DEPTH OF DISCHARGE CONTROLLER

Part 3 of 3 Parts

- P-1 Plug, Line Cord Male, 110 Volt Input
- P-2, P-4, P-6, P-8, P-10, P-12 Charge Inputs, Yellow Jacks
- P-3, P-5, P-7, P-9, P-11, P-13, Discharge Inputs, Red Jacks
- P-14 Charge Power, Yellow Jacks
- P-15 Discharge Power, Red Jacks
- P-16 thru P-39 Cell Inputs, Red + Black -
- P-45, P-47, P-49, P-51, P-53, P-55 Charge Outputs, Yellow Jacks
- P-46, P-48, P-50, P-52, P-54, P-56 Discharge Outputs, Red Jacks
- P-57 Lamp Input, Line Cord
- S-1 Master Switch, DPST Toggle
- S-2 thru S-7 Push Button, No Relay Synchronization
- PL-1 Pilot, Master, Green
- PL-2 Pilot, Relay Power Amber
- F Fuse, 5 Amp.
- T-1 thru T-12 Timer, Elapsed Time, Cramed 640E Reset Meter, 115 VAC Coil,
9999.9 Minutes
- K-1 thru K-12 Relays, DPOT, 115 AC Coil Leach 337
- K-13 Lamp Relay (Safety) 12UAC Coil Ebert MR10-SPST-No
- KI-1 thru KI6 Ratchet Relay Guardian 1R-M-120-115, DPDT 3 Positions Sequence
Ratchet
- R-10 Resistor, Load (25 Ohms, 12.5 Watts, Ohmite 0113

Ni-Cd Characterization
 Constant Voltage Controller
 Current Limited
 Part 1 of 2 Parts



PARTS LIST
CONSTANT VOLTAGE - CURRENT LIMITED CONTROLLER

Part 2 of 2 Parts

- P-1 Line Cord 110V AC Power Input
- P-2 Control, Charge Pin Jacks, Yellow
- P-3 Control, Discharge Pin Jacks, Red
- P-4 Input Terminal, Discharge CCS Terminals
- P-5 thru P-10 Input Terminal Charge CCS'S Terminals
- P-11 thru P-16 Cell Input, Power, Pin Jacks; Red +, Black -
- P-17 thru P-22 Cell Input, Control, Pin Jacks, Red +, Black -
- SW Switch DPST Toggle Master
- F Fuse 3A
- PL-1 Pilot, Green, Power On
- PL-2 Pilot, Yellow, Charge On
- PL-3 Pilot, Red, Discharge On
- CR Counter General Controls CE 600B5602
- K-1 thru K-6 Mercury Relay 3PST 2NO, INC Ebert EM7 KOVAC Coil
- K-7 Deleted
- K-8 thru K-10 Leach 329-7 4PDT 110 VAC Coil
- K-11 Leach 337 2PDT 110 VAC Coil
- K-12 thru K-17 VHS Meter Relay, Low Limit Contacts, 100 Microamperes
137 (Assembly Prod).
- K-18 thru K-23 P&B LM 11, 5000V DPDT
- K-24 GE - Time Delay Switch - 1 min. - No
- R-1 Load Resistance, 6 Ohm, 25 Watts, Ohmite O143
- R-2 thru R-7 10,000 Ω Pot WW
- C-1 thru C-6 Condenser SMFD, 200 Volt
- X-1 thru X-6 Rectifier I-10

APPENDIX II

Weights of Electrochemically Cleaned Electrodes

WEIGHT TABULATION OF ELECTROCHEMICALLY CLEANED ELECTRODES

Prefix Number	Positive Electrodes Weight - grams				Negative Electrodes Weight - grams			
	PI	P3	P5	P7	NI	N3	N5	N7
1	11.412	10.870	11.255*	11.041	9.450	9.884	10.544	9.923
2	11.389	11.094	11.509	11.185	10.546	10.391	9.852	10.062
3	10.911	10.932*	11.445	11.013	10.547	9.975	10.202	9.683
4	11.262	11.329	11.231	10.749	9.943	9.969	10.045	10.552
5	11.251	11.506*	11.198	11.730	9.806	10.472	9.971	10.00
6	11.517	10.928	11.497	10.851	10.318	9.912	10.436	9.80
7	11.112	11.564	10.931	10.721	9.853	9.851	9.824	10.23
8	10.838	10.749	10.821	10.853	9.655	10.474	10.344	10.50
9	10.759	10.905	10.973*	10.733	10.197	10.059	9.999	9.50
10	10.758	10.905	10.803	11.551	9.868	10.499	9.953	10.50
11	11.032	11.454	10.830	11.176	10.199	9.852	10.200	10.00
12	10.890	11.109	10.786*	10.86	9.672	9.940	10.280	10.60
13	11.326	10.985	11.532	11.13	10.506	10.628	10.107	"none"
14	10.725	11.094	11.200	11.44	9.975	9.978	9.923	
15	11.010	11.406	11.146	11.23	9.939	10.391	10.062	
16	11.343	11.406	10.751	11.13	10.200	9.653	10.561	
17	11.542	11.046	11.139	11.00	10.349	10.087	9.967	
18	11.090	11.093	11.140	11.13	9.966	10.586	10.053	

H-2

* Defective

WEIGHT TABULATION CONT'D

Prefix Number	Positive Electrodes Weight - grams				Negative Electrodes Weight - grams			
	PI	P3	P5	P7	NI	N3	N5	N7
19	11.048	11.025	11.937	"none"	10.410	10.294	10.660	"none"
20	10.850	10.840	10.753*		10.263	9.954	9.822	
21	11.206	11.424	10.824*		10.322	10.136	10.512	
22	11.152	10.829*	11.088*		10.278	10.143	9.795	
23	11.081	11.283	11.324		10.290*	10.363	9.937	
24	10.699	11.392	10.996		9.959	10.236	9.671	
25	10.906	10.760	11.039		10.254	10.357	10.131	
26	10.699	"none"	11.002		10.634	10.549	9.830	
27	10.908		10.842		9.805	9.889	10.523	
28	12.099		11.393		10.589	10.088	9.972	
29	11.036		11.142		10.383	10.054	10.503	
30	11.290		11.383		10.134	10.585	10.158	
31	10.796		"none"		10.005	10.241	10.217	
32	10.799				10.498	10.598	10.205	
33	11.797				10.514	10.426	10.364	
34	11.540				10.618	9.986	9.895	
35	10.703				9.782	9.997	10.015	
36	10.929				10.036	10.391	"none"	

*Defective

WEIGHT TABULATION CONT'D

Prefix Number <u>Electrode</u> <u>Serial Number</u>	Positive Electrodes Weight - grams			Negative Electrodes Weight - grams				
	PI	P3	P5	P7	NI	N3	N5	N7
37	11.067	"none"	"none"	"none"	10.557	10.441	"none"	"none"
38	11.582				10.71	10.170		
39	11.322				9.987	10.079		
40	10.866				10.318	10.123		
41	11.598				10.406	10.143		
42	10.837				10.227	10.109		
43	10.886				9.838	10.110		
44	11.896				10.436	9.946		
45	11.415				9.876	10.108		
46	11.175				10.309	10.031		
47	11.291				10.109	10.305		
48	11.455				10.192	10.220		
49	11.175				10.137	10.461		
50	11.493				10.121	10.497		
51	10.721				10.189	"none"		
52	11.411				10.465			
53	11.244				9.927			
54	11.527				10.503			

WEIGHT TABULATION CONT'D

Prefix Number	Positive Electrodes Weight - grams			Negative Electrodes Weight - grams				
	PI	P3	P5	P7	NI	N3	N5	N7
<u>Electrode</u> Serial Number								
55	10.889	"none"	"none"	"none"	10.002	"none"	"none"	"none"
56	11.221				9.860			
57	11.240				10.222			
58	11.128				10.461			
59	10.977				9.898			
60	11.235				10.322			
61	11.442				10.372			
62	11.492				10.215			
63	11.270				9.916			
64	11.521				10.251			
65	11.284				9.895			
66	11.315				9.876			
67	11.086				10.289			
68	11.274				10.106			
69	11.098				10.237			
70	11.055				10.006			
71	11.532				9.877			
72	10.987				10.380			

WEIGHT TABULATION CONT'D

Prefix Number	Positive Electrodes Weight - grams			Negative Electrodes Weight - grams				
	PI	P3	P5	P7	NI	N3	N5	N7
Electrode Serial Number								
73	11.019	"none"	"none"	"none"	9.812	"none"	"none"	"none"
74	10.902				10.204			
75	10.892				10.396			
76	10.943				9.559			
77	10.911				10.252			
78	10.703				9.960			
79	10.960				10.131			
80	11.227				9.934			
81	10.697				10.370			
82	10.779				10.320			
83	11.387				10.011			
84	11.466				10.380			
85	11.349				10.326			
86	11.512				10.175			
87	11.943				9.914			
88	11.324				10.013			
89	10.891				10.032			
90	11.219				10.504			

WEIGHT TABULATION CONT'D

Prefix Number	PI	P3	P5	P7	NI	N3	N5	N7
	Positive Electrodes Weight - grams				Negative Electrodes Weight - grams			
91	11.606	"none"	"none"	"none"	10.156	"none"	"none"	"none"
92	11.576				10.311			
93	10.819				10.064			
94	11.411				10.159			
95	11.182				10.035			
96	11.486				10.400			
97	11.421				10.416			
98	11.032				9.755			
99	11.132				10.227			

KO-15 Electrodes
Weight - grams

	P
51	10.1479
52	9.9466
53	10.1534
54	9.7817
55	10.0238
56	10.1717
57	9.8506
58	10.1587
59	10.0025
60	10.2908
61	10.4028
62	10.3051
63	10.3990

WEIGHT TABULATION CONT'd

Prefix Number	P	KO-15 Electrodes
<u>Electrode</u>		Weight - grams
Serial Number		
64	10.2175	
65	10.4377	
66	10.2463	
67	10.1728	
68	10.2017	
69	10.0336	
70	9.8206	
71	10.2273	
72	9.8206	
73	9.8904	
74	10.1136	
75	10.2673	
76	9.8601	
77	10.2031	
78	10.7125	
79	10.0041	
80	10.3164	

APPENDIX III

Generation of Beta Variables

APPENDIX III

Generation of Beta Variables

The Beta distribution defined by

$$\frac{\Gamma(p+q)}{\Gamma(p)\Gamma(q)} (1-x)^{p-1} x^{q-1} \quad 0 \leq x \leq 1$$

is a limited range distribution whose shape is determined by its two parameters p and q and whose mean and variance are given by

$$\frac{q}{p+q} \text{ and } \frac{pq}{(p+q+1)(p+q)^2}$$

Since integrals of the form

$$\int_0^a (1-x)^{p-1} x^{q-1} dx \quad 0 < a < 1$$

cannot be directly evaluated it is not possible to simply generate random variables from the Beta distribution. Neither do there exist tables of random variates from this family of distributions.

However it is possible, using normally distributed variables to generate Beta variables as follows.

Let w_i be a random variate from a normal distribution with mean zero and variance one for $i = 1, 2, \dots, m+n$ such that the w_i 's are independent.

Then $v_n = \sum_{i=1}^n w_i^2$ is distributed as a chi-square variable with parameter

n , i. e.,

$$f(v_n) = \frac{1}{2^{n/2}} \frac{1}{\Gamma(\frac{n}{2})} v_n^{n/2-1} e^{-\frac{1}{2} v_n} \quad 0 \leq v_n < \infty$$

We now obtain the distribution of

$$y = \frac{v_m}{v_n}$$

where v_n and v_m are independent chi-square variables with parameters n and m .

$$f(v_n, v_m) = \frac{1}{2^{\frac{n+m}{2}}} \frac{1}{\Gamma(\frac{n}{2})\Gamma(\frac{m}{2})} v_n^{\frac{n}{2}-1} v_m^{\frac{m}{2}-1} e^{-\frac{1}{2}(v_n+v_m)}$$

Changing variables we

$$\text{let } y = \frac{v_m}{v_n}$$

$$v_n = v_n$$

The Jacobian of the transformation,

$$J = v_n$$

$$f(y, v_n) = \frac{1}{2^{\frac{n+m}{2}}} \frac{1}{\Gamma(\frac{n}{2})\Gamma(\frac{m}{2})} v_n (y v_n)^{\frac{m}{2}-1} v_n^{\frac{n}{2}-1} e^{-\frac{1}{2}(y v_n + v_n)}$$

$$= \frac{1}{2^{\frac{n+m}{2}}} \frac{1}{\Gamma(\frac{n}{2})\Gamma(\frac{m}{2})} y^{\frac{m}{2}-1} v_n^{\frac{n}{2} + \frac{m}{2} - 1} e^{-\frac{1}{2} v_n (y+1)}$$

$$f(y) = \frac{1}{2^{\frac{n+m}{2}}} \frac{1}{\Gamma(\frac{n}{2})\Gamma(\frac{m}{2})} y^{\frac{m}{2}-1} \int_0^{\infty} v_n^{\frac{n}{2} + \frac{m}{2} - 1} e^{-\frac{1}{2} v_n (y+1)} dv_n$$

$$= \frac{1}{2^{\frac{n+m}{2}}} \frac{1}{\Gamma(\frac{n}{2})\Gamma(\frac{m}{2})} y^{\frac{m}{2}-1} \frac{\Gamma(\frac{n}{2} + \frac{m}{2})}{\left[\frac{1}{2}(y+1)\right]^{\left(\frac{n}{2} + \frac{m}{2}\right)}}$$

$$= \frac{\Gamma(\frac{n+m}{2})}{\Gamma(\frac{n}{2})\Gamma(\frac{m}{2})} y^{\frac{m}{2}-1} (y+1)^{-\left(\frac{n+m}{2}\right)}$$

Changing variables again

$$\text{we let } z = \frac{\sum_{i=1}^n w_i^2}{\sum_{i=1}^n w_i^2 + \sum_{i=n+1}^{n+m} w_i^2} = \frac{v_n}{v_n + v_m} = \frac{1}{1 + \frac{v_m}{v_n}}$$

$$\text{or } z = \frac{1}{1+y} \quad \therefore y = \frac{1-z}{z}$$

The Jacobian of the transformation is $-\frac{1}{z^2}$

$$f(z) = \frac{\Gamma(\frac{n+m}{2})}{\Gamma(\frac{n}{2}) \Gamma(\frac{m}{2})} (1-z)^{\frac{m}{2}-1} z^{\frac{n+m}{2}-1} \frac{1}{z^2}$$

$$f(z) = \frac{\Gamma(\frac{n+m}{2})}{\Gamma(\frac{n}{2}) \Gamma(\frac{m}{2})} (1-z)^{\frac{m}{2}-1} z^{\frac{n}{2}-1}$$

which is a Beta distribution with $p = \frac{m}{2}$ and $q = \frac{n}{2}$.

Thus if we take m and n independent variables from a normal distribution with mean zero and variance one and form the statistic

$$z = \frac{\sum_{i=1}^n w_i^2}{\sum_{i=1}^n w_i^2 + \sum_{i=n+1}^{n+m} w_i^2}$$

the z 's so generated will follow a Beta distribution with $p = \frac{m}{2}$ and $q = \frac{n}{2}$.